1. Report No.	2. Government Accession No.	3. Recipient's Catalog No.
FHWA/TX-09/0-5530-1		

4. Title and Subtitle	5. Report Date
PREDICTION OF EMBANKMENT SETTLEMENT OVER SOFT SOILS	December 2008 Published: June 2009
	6. Performing Organization Code

7. Author(s)	8. Performing Organization Report No.
Vipulanandan, C., Bilgin, Ö., Y Jeannot Ahossin Guezo, Vembu, K. and Erten, M. B.	Report 0-5530-1

9. Performing Organization Name and Address	10. Work Unit No. (TRAIS)
University of Houston Department of Civil and Environmental Engineering Houston, Texas 77204-4003	11. Contract or Grant No. Project 0-5530

12. Sponsoring Agency Name and Address	13. Type of Report and Period Covered
Texas Department of Transportation Research and Technology Implementation Office P. O. Box 5080 Austin, Texas 78763-5080	Technical Report: September 2005 - October 2008
	14. Sponsoring Agency Code

15. Supplementary Notes

Research performed in cooperation with the Texas Department of Transportation and the Federal Highway Administration.
Research Project Title: Prediction of Embankment Settlement Over Soft Soils
URL: http://tti.tamu.edu/documents/0-5530-1.pdf

16. Abstract

The objective of this project was to review and verify the current design procedures used by TxDOT to estimate the total and rate of consolidation settlement in embankments constructed on soft soils. Methods to improve the settlement predictions were identified and verified by monitoring the settlements in two highway embankments over a period of 20 months. Over 40 consolidation tests were performed to quantify the parameters that influenced the consolidation properties of the soft clay soils. Since there is a hysteresis loop during the unloading and reloading of the soft CH clays during the consolidation test, three recompression indices (C_{r1}, C_{r2}, C_{r3}) have been identified with a recommendation to use the recompression index C_{r1} (based on stress level) to determine the settlement up to the preconsolidation pressure. Based on the laboratory tests and analyses of the results, the consolidation parameters for soft soils were all stress dependent. Hence, when selecting representative parameters for determining the total and rate of settlement, expected stress increases in the ground should be considered. Also the 1-D consolidation theory predicted continuous consolidation settlement in both of the embankments investigated. The predicted consolidation settlements were comparable to the consolidation settlement measured in the field. Constant Rate of Strain test can be used to determine the consolidation parameters of the soft clay soils. The effect of Active Zone must be considered in designing the edges of the embankments and the retaining walls.

17. Key Words	18. Distribution Statement
Active Zone, Consolidation, Embankment, Field Tests, Recompression Indices, Settlement, Soft Soils	No restrictions. This document is available to the public through NTIS: National Technical Information Service 5285 Port Royal Road Springfield, Virginia 22161

19. Security Classif.(of this report)	20. Security Classif.(of this page)	21. No. of Pages	22. Price
Unclassified	Unclassified	210	

Prediction of Embankment Settlement Over Soft Soils

Project Report No. TxDOT 0-5530-1

Final Report
by

C. Vipulanandan Ph.D., P.E.
Ö. Bilgin, Ph.D., P.E.
Y. Jeannot Ahossin Guezo
Kalaiarasi Vembu
and
Mustafa Bahadir Erten

Performed in cooperation with the
Texas Department of Transportation
and the
Federal Highway Administration

June 2009

Center for Innovative Grouting Materials and Technology (CIGMAT)
Department of Civil and Environmental Engineering
University of Houston
Houston, Texas 77204-4003

Report No. CIGMAT/UH 2009-6-1

ENGINEERING DISCLAIMER

The contents of this report reflect the views of the authors, who are responsible for the facts and the accuracy of the data presented herein. The contents do not necessarily reflect the official views or policies of the Texas Department of Transportation or the Federal Highway Administration. This report does not constitute a standard or a regulation.

There was no art, method, process, or design that may be patentable under the patent laws of the United States of America or any foreign country.

ACKNOWLEDGMENTS

This project was conducted in cooperation with Texas Department of Transportation (TxDOT) and Federal Highway Administration (FHWA).

The researchers thank the TxDOT for sponsoring this project. Also thanks are extended to the Project Coordinator K. Ozuna (Houston District), Project Director S. Yin (Houston District) and Project Committee Members R. Willammee (Fort worth District), M. Khan (Houston District), D. Dewane (Austin District) R. Bravo (Pharr District) and P. Chang (FHWA).

PREFACE

Settlement of highway embankments over soft soils is a major problem encountered in maintaining highway facilities. The challenges to accurately predict the total and rate of consolidation settlements are partly due to the uncertainties in field conditions, laboratory testing, interpretations of laboratory test data, and assumptions made in the development of the 1-D consolidation theory. Hence, there is a need to investigate methods to better predict the settlement of embankments on soft soils.

The objective of this project was to review and verify the current design procedures used in TxDOT projects to estimate the total and rate of consolidation settlements in embankments constructed on soft soils. Methods to improve the settlement predictions were identified and verified by monitoring the settlements in two highway embankments over a period of 20 months. Over 40 consolidation tests were performed to quantify the parameters that influence the consolidation properties of the soft clay soils. Based on the laboratory tests and analyses of the results, the consolidation parameters for soft soils were all stress dependent. Hence, when selecting representative parameters for determining the total and rate of settlement, expected stress increases in the ground should be considered. Also the 1-D consolidation theory predicted continuous consolidation settlement in both of the embankments investigated. The predicted consolidation settlements were comparable to the consolidation settlement measured in the field.

This report reviewed the current TxDOT project approach to predict the total and rate of consolidation settlements of embankments over soft soils. Based on the laboratory and field investigations, methods to further improve the embankment settlement predictions have been recommended.

ABSTRACT

The prediction of embankment settlement over soft soils (defined by the undrained shear strength and/or Texas Cone Penetrometer value) has been investigated for many decades. The challenges mainly come from the uncertainties about the geology, subsurface conditions, extent of the soil mass affected by the new construction, soil disturbances during sampling and laboratory testing, interpretations of laboratory test data, and assumptions made in the development of the one-dimensional consolidation theory. Since the soft soil shear strength is low, the structures on the soft soils are generally designed so that the increase in the stress is relatively small and the total stress in the ground will be close to the preconsolidation pressure. Hence there is a need to investigate methods to better predict the settlement of embankments on soft soils.

The objective of this project was to review and verify the current design procedures used by TxDOT to estimate the total and rate of consolidation settlement in embankments constructed on soft soils. Methods to improve the settlement predictions were identified and verified by monitoring the settlements in two highway embankments over a period of 20 months. Over 40 consolidation tests were performed to quantify the parameters that influenced the consolidation properties of the soft clay soils. Since there is a large hysteresis loop during the unloading and reloading of the soft CH clays during the consolidation test, three recompression indices (C_{r1}, C_{r2}, C_{r3}) have been identified with the recommendation to use the recompression index C_{r1} (based on stress level) to determine the settlement up to the preconsolidation pressure. Based on the laboratory tests and analyses of the results, the consolidation parameters for soft soils were all stress depended. Hence, when selecting representative parameters for determining the total and rate of settlement, expected stress increases in the ground should be considered. Linear and nonlinear relationships between compression indices of soft soils and moisture content and unit weight of soils have been developed. Also the 1-D consolidation theory predicted continuing consolidation settlement in both of the embankments investigated. The predicted consolidation settlements were comparable to the consolidation settlement measured in the field. The Constant Strain Rate test can be used to determine the

consolidation parameters of the soft clay soils. The effect of Active Zone must be considered in designing the edges of the embankments and the retaining walls.

SUMMARY

The prediction of consolidation settlement magnitudes and settlement rates in soft soils (defined by the undrained shear strength and/or Texas Cone Penetrometer value) is a challenge and has been investigated by numerous researchers since the inception of consolidation theory by Terzaghi in the early 1920s. The challenges mainly come from the uncertainties about the geology, subsurface conditions, extent of the soft soil mass affected by the new construction, soil disturbances during sampling and preparation of samples for laboratory testing, interpretations of laboratory test data, and assumptions made in the development of the one-dimensional consolidation theory. Since the soft soil shear strength is low, the structures on the soft soils are generally designed such that the increase in the stress is relatively small and the total stress in the ground will be close to the preconsolidation pressure. Hence, there is a need to further investigate methods to better predict the settlement of embankments on soft soils.

The objective of this project was to review and verify the current design procedures used by TxDOT to estimate the total and rate of consolidation settlements in embankments constructed on soft soils. The review of the design procedures indicated that the methods used to determine the increase in in-situ stresses and the preconsolidation pressure, and the testing method used to determine the consolidation properties were appropriate except for the approach used for determining the rate of settlement. Also the practice of using the recompression index was not clearly defined.

In order to verify the prediction methods, two highway embankments on soft clay with settlement problems were selected for detailed field investigation. Soil samples were collected from nine boreholes for laboratory testing. The embankments were instrumented and monitored for 20 months to measure the vertical settlement, lateral movement, and changes in the pore water pressure. Over 40 consolidation tests were performed to investigate the important parameters that influenced the consolidation settlements of the soft soils.

Based on this study, it was determined that the increase in in-situ stresses due to the embankment are relatively small (generally less than the preconsolidation pressure),

and hence using the proper recompression index became more important to estimate the settlement. Since there is a large hysteresis loop during the unloading and reloading of the soft CH clays during the consolidation test, three recompression indices (C_{r1}, C_{r2}, C_{r3}) have been identified and with the recommendation to use the recompression index C_{r1} (based on stress level) to determine the settlement up to the preconsolidation pressure. Based on the laboratory tests and analyses of the results, the consolidation parameters such as compression index (C_c), recompression indices (C_r), and coefficient of consolidation (C_v) for soft soils were all stress dependent. Hence, when selecting representative parameters for determining the total and rate of settlements, expected stress increases in the ground should be considered. Linear and nonlinear relationships between compression indices of soft soils and moisture content and unit weight of soils have been developed. Also the 1-D consolidation theory predicted continuous consolidation settlement in both the embankments investigated. The predicted consolidation settlements were comparable to the consolidation settlement measured in the field. The pore water pressure measurements in some cases did not indicate consolidation because they may have been located close to the bottom drainage. In one case excess pore water pressures were measured, indicting consolidation was in progress.

The Active Zone influenced the movements at the edge of the embankments. Movements in the Active Zone influenced the crack movements in the retaining wall panels. The Constant Rate of Strain (CRS) test can be used to determine the consolidation properties of soft clay soils. The strain rate used during the test influenced the coefficient of consolidation.

RESEARCH STATEMENT

This research project was to review the current design procedures and verify the applicability of conventional consolidation theory to predict the total and rate of settlements of embankments over soft clays. The study included field sampling, laboratory testing, and monitoring the settlement of two embankments for a period of up to 20 months. Based on this study, further improvements have been suggested to better predict the rate and total settlements of embankment over soft clay soils.

The report will be a guidance document for TxDOT engineers on instrumenting embankments for measuring consolidation settlement and monitoring changes in the Active Zone. Also the Constant Rate Strain (CRS) test has been recommended as an alternative test to determine the consolidation properties of soft soils.

TABLE OF CONTENTS

Page

LIST OF FIGURES xvii

LIST OF TABLES xxiii

1. INTRODUCTION 1

1.1. General 1

1.2. Objectives 3

1.3. Organization 3

2. SOFT SOILS AND HIGHWAY EMBANKMENT 5

2.1. General 5

2.2. Soft Clay Soil Definition 5

2.3. Embankment Settlement 6

2.4. Behavior of Marine and Deltaic Soft Clays 23

3. DESIGN AND ANALYSIS OF HIGHWAY EMBANKMENTS 43

3.1. Highway Embankments 43

3.2. Summary and Discussion 100

4. LABORATORY TESTS AND ANALYSIS 103

4.1. Introduction 103

4.2. Tests Results 104

4.3. Soil Characterization 119

4.4. Preconsolidation Pressure (σ_p) 120

4.5. Compression Index (C_c) 124

4.6. Recompression Index (C_r) 132

4.7. Coefficient of Consolidation (C_v) 137

4.8. Constant Rate of Strain (CRS) Test (ASTM D 4186-86) 141

4.9. Summary 145
5. FIELD STUDY 147
5.1. Introduction 147
5.2. Site History and Previous Site Investigation 148
5.3. Instrumentation 150
5.4. NASA Road 1 Embankment Instrumentation 154
5.5. SH3 Embankment Instrumentation and Results 154
5.6. NASA Road 1 (Project 4) 171
5.7. Summary and Discussion 173
6. CONCLUSIONS AND RECOMMENDATIONS 177
7. REFERENCES 181

LIST OF FIGURES

Page

Fig. 2.1. Typical Configuration of Soil Layers under an Embankment. 7

Fig. 2.2. Field Condition Simulation in Laboratory Consolidation Test. 12

Fig. 2.3. Typical e – log σ_v Relationship for Overconsolidated Clay. 13

Fig. 2.4. Constant Rate of Strain (CRS) Consolidation Cell Used at the University of Houston (GEOTAC Company 2006). 17

Fig. 2.5. Schematic of CRS Test Frame Used at the University of Houston (GEOTAC Company 2006). 17

Fig. 2.6. Commercially Available CRS Test System (GEOTAC Company 2006). 18

Fig. 2.7. 2:1 Method for Vertical Stress Distribution (Holtz and Kovacs 1981). 20

Fig. 2.8. Vertical Stress Due to a Flexible Strip Load (Das 2006). 21

Fig. 2.9. Embankment Loading Using Osterberg's Method (Das 2006). 22

Fig. 2.10. Locations of Soft Clay Soils Used for the Analysis. 26

Fig. 2.11. Rate of Sedimentation of Different Types of Clay Deposits (Leroueil 1990). 27

Fig. 2.12. Probability Distribution Function for the Undrained Shear Strength (a) Marine Clay and (b) Deltaic Clay. 34

Fig. 2.13. Liquid Limit versus Natural Water Content for the Soft Clays (a) Marine Clay and (b) Deltaic Clay. 35

Fig. 2.14. Plasticity Index chart of Deltaic (42 Data Sets) and Marine Soft Clay Soils 36

Fig. 2.15. Predicted and Measured Relationships for Marine and Deltaic Clays. 37

Fig. 2.16. Relationship between Undrained Shear Strength (S_u) and Preconsolidation Pressure (σ_p). 39

Fig. 3.1. Houston Area with the Selected Four Embankments. 44

Fig. 3.2. Variation of TCP Blow Counts with Depth (Borehole 99-1a.). 47

Fig. 3.3. (a) Variation of Moisture Content (MC) with Depth (z) and (b) Change of Moisture Content with Change in Depth ($\Delta MC/\Delta z$). 48

Fig. 3.4. Variation of Undrained Shear Strength with Depth (Borehole 99-1a). 49

Fig. 3.5. e – log σ' of the Two Consolidation Tests Performed on TxDOT Project for 1A Embankment Design and Their Respective Compression and Recompression Index versus log σ' Curves (Project 1: I-10 @ SH-99). 51

Fig. 3.6. Profile of the Soil Layers for Settlement Calculation (Project 1) 52

Fig. 3.7. Comparison of Stress Increase Obtained Using the Osterberg, 2:1, and TxDOT Methods (Project 1). 53
Fig. 3.8. Comparison of the Rate of Settlement by Various Methods of Estimation. 58
Fig. 3.9. Variation of TCP Blow Counts with Depth (Project 2). 60
Fig. 3.10. (a) Variation of Moisture Content (MC) with Depth (z) and (b) Change of Moisture Content with Change in Depth (ΔMC/Δz) (Project 2). 64
Fig. 3.11. Variation of Undrained Shear Strength with Depth (from the Four Borings) (Project 2)..... 65
Fig. 3.12. Profile of the Soil Layers for Settlement Calculation (Project 2)..... 66
Fig. 3.13. Comparison of Stress Increase Obtained Using Osterberg and 2:1 and TxDOT Methods. 68
Fig. 3.14. Effect of Layering on the Rate of Settlement (Project 2). 73
Fig. 3.15. Profile of the Retaining Wall No. 2E, Not to Scale (Project 3 Drawing 22). 75
Fig. 3.16. Location of the Borings Used in the Field (Drawings 13 and 14)..... 75
Fig. 3.17. Variation of TCP Blow Counts with Depth (Project 3)..... 76
Fig. 3.18. (a) Variation of Moisture Content (MC) with Depth (z) and (b) Change of Moisture Gradient with Depth (ΔMC/Δz) (Project 3). 79
Fig. 3.19. Variation of Undrained Shear Strength with Depth (Project 3). 80
Fig. 3.20. (a) e – log σ' Relationship for the Three Samples and (b) Variation of Compression Index with log σ' (Project 3). 82
Fig. 3.21. Profile of the Soil Layers for Settlement Calculation (Project 3)..... 83
Fig. 3.22. Variation of Stress Increase with Depth at the Center and at the Toe of the Embankment Using the Osterberg Method (Project 3)..... 84
Fig. 3.23. Comparison of TxDOT Rate of Settlement Estimation at the Center of the Embankment with New Estimation Using the Same Data. 87
Fig. 3.24. Comparative Graph Showing the Effect of Layering on the Rate of Settlement at the Center of the Embankment (Project 3). 89
Fig. 3.25. Rate of Settlement at the Toe of the Embankment Using TxDOT Method. 91
Fig. 3.26. Comparative Graph Showing the Effect of Layering on the Rate of Settlement at the Toe of the Embankment. 92
Fig. 3.27. Cross Section of the Bridge and the Embankment at Nasa Road 1 Site. 95
Fig. 3.28. Approximate Borehole Locations Drilled in April 2007 (Not to Scale). 95
Fig. 3.29. Variation of Stress Increase with Depth at the Center and at the Toe of the Embankment Using the Osterberg Method (Project 4)..... 97

Fig. 3.30. Comparison of Rate of Settlement (Project 4)..... 100
Fig. 4.1. Location of the Two Field Sites in Houston, Texas. 103
Fig. 4.2. Variation of Moisture Content with Depth in All the Boreholes (SH3)..... 105
Fig. 4.3. Variation of Liquid Limit with Depth (SH3)..... 106
Fig. 4.4. Variation of Plastic Limit with Depth in Boring B1 (SH3)..... 107
Fig. 4.5. Variation of S_u with Depth in Borings B1, B2, B3, and B4 (SH3). 108
Fig. 4.6. Variation of Overconsolidation Ratio with Depth in Borehole B1 (SH3). 109
Fig. 4.7. Variation of Compression Index with Depth in Boring B1 (SH3). 110
Fig. 4.8. Variation of Coefficient of Consolidation with Depth in Borehole B1 (SH3). 111
Fig. 4.9. Variation of Moisture Content with Depth at NASA Rd. 1. 114
Fig. 4.10. Liquid Limit and Plastic Limit of the Soils along the Depth..... 115
Fig. 4.11. Shear Strength Variation with Depth at NASA Rd. 1. 116
Fig. 4.12. Variation of New and Old (a) C_c and (b) C_{r2} with Depth. 118
Fig. 4.13.Void Ratio versus Vertical Effective Stress Relationship for CH Soil (Sample UH-2 22-24) with Multiple Loops..... 119
Fig. 4.14. Comparing the SH3 and NASA Rd.1 Data on Casagrande Plasticity Chart. 120
Fig. 4.15. e – log σ' Curve Showing Casagrande Graphical Method (Method 1) for σ_p Determination (Clay Sample from SH3 Borehole 1, Depth 18-20 ft, CH Clay). 121
Fig. 4.16. Direct Determination Methods for Preconsolidation Pressure. 122
Fig. 4.17. Graphical Methods of Determining the Preconsolidation Pressure..... 123
Fig. 4.18. Correlation of Compression Index of Houston/Beaumont Clay Soil with In-situ Moisture Content. 126
Fig. 4.19. Correlation of Compression Index of Houston/Beaumont Clay Soil with In-situ Unit Weight. 127
Fig. 4.20. e – log σ' of Different Clay Samples from SH3 at Clear Creek Bridge and Their Respective Compression and Recompression Index versus log σ' Curves. 132
Fig. 4.21. e – log σ' Curve Showing the Three Recompression Indices (C_{r1}, C_{r2}, C_{r3}). Clay Sample from SH3 Borehole 1, Depth 18-20 ft, CH Clay..... 134
Fig. 4.22. Correlation of the Different Types of Recompression Indexes with the Compression Index a) C_{r1} vs. C_c, b) C_{r2} vs. C_c, and c) C_{r3} vs. C_c. 136
Fig. 4.23. Comparison of the Different Recompression Indices of Houston SH3 Samples with New Orleans Clay C_r/C_c Range..... 137

Fig. 4.24. e – log σ' Curve of a Houston Clay from SH3 and Their Respective C_v – σ' Curve. 140

Fig. 4.25. Deformation vs. Time at log Scale Curve of Casagrande T_{50} (a) CH Clay and (b) CL Clay. 141

Fig. 4.26. Three ε- log σ' of CRS Tests Performed on Three Specimens from the Same Shelby Tube Sample at Different Strain Rates. 142

Fig. 4.27. Comparison of CRS Test (ε= *0.025/hr*) and IL Test ε – log σ' Relationship (Test Performed on Two Different Specimens from the Same Shelby Tube Sample Recovered from SH3 at Clear Creek, Borehole B5 at 10 – 12 ft Depth). 143

Fig. 4.28. Three C_v- σ' of CRS Tests Performed on Three Specimens (CH Clay) from the Same Shelby Tube Sample at Different Strain Rates. 144

Fig. 4.29. (a) Comparison of CRS Test (ε= *0.025/hr*) and IL Test C_v– σ' Curve (Test Performed on Two Different Specimens from the Same Shelby Tube Sample Recovered from SH3 at Clear Creek, Borehole 5 at 10 – 12 ft Depth); and (b) Pressure Ratio vs. Vertical Effective Stress Corresponding to the CRS Test. 145

Fig. 5.1. Location of the Instrumented Embankment Sites. 148

Fig. 5.2. Sampling and Instrumenting at the SH3 Site (January 2007). 149

Fig. 5.3. Cross Section of the NASA Road 1 Embankment (Project 4). 150

Fig. 5.4. Schematic of the Extensometer. 151

Fig. 5.5. (a) Inclinometer Probe (Geokon Inc 2007) and (b) Inclinometer Casing. 152

Fig. 5.6. Demec on the Embankment Retaining Wall (Project 3). 153

Fig. 5.7. Plan View of SH3 at Clear Creek with the New Boring Locations. 155

Fig. 5.8. Schematic View of Instruments Used in SH3. 155

Fig. 5.9. Groundwater Table Variation with Time (Reference is the Bottom of the Casing at 30 ft Deep as Reference at Boring B1). 156

Fig. 5.10. Inclinometer Reading at Boring B2 (SH3). 157

Fig. 5.11. Measured Relative Displacement with Time at Boring B1. 158

Fig. 5.12. Measurement of Vertical Displacement with Time at Boring B3. 158

Fig. 5.13. Pore Water Pressure Variation with Time at Boring B1 (Project 3). 159

Fig. 5.14. Pore Water Pressure Variation with Time at Boring B3. 160

Fig. 5.15. Water Table Variation with Time (Bottom of the Casing at 20 ft Deep as Reference in Boring B5) (Project 3). 161

Fig. 5.16. Inclinometer Reading at Boring B4 (SH3). 162

Fig. 5.17. Measured Relative Displacement with Time at Boring B5. 163

Fig. 5.18. Pore Pressure Variation with Time at Boring B5. 164
Fig. 5.19. Change in Suction Pressure. 165
Fig. 5.20. Variation in Settlement in Active Zone. 165
Fig. 5.21. Measured Rainfall and Temperature for the Houston (www.weather.gov)..... 166
Fig. 5.22. Variation of Consolidation Settlement (Project 3). 167
Fig. 5.23. Picture View of Demec Points on the Wall: a) for Wall Panel Displacement Monitoring and b) Crack Opening Monitoring (Project 3)..... 168
Fig. 5.24. Relative Displacements of the Wall Panels along the Embankment. 168
Fig. 5.25. Change in the Crack Opening along the Wall. 169
Fig. 5.26. View of L2 Rotation Monitoring Mark Line on the Retaining Wall..... 170
Fig. 5.27. Change in Wall Rotation Monitoring Mark Readings along the Retaining Wall. 170
Fig. 5.28. Piezometer Readings at (a) Borehole UH-2 and (b) Borehole UH-4. 172
Fig. 5.29. University of Houston's Settlement Measurement Set-Up Readings. 173

LIST OF TABLES

Page

Table 2.1. TxDOT Soil Density and Bedrock Hardness Classification. 6
Table 2.2. Recommended u_h/σ Values (Dobak 2003). 16
Table 2.3. Conditions for 1-D Consolidation Tests (Dobak 2003). 18
Table 2.4. Summary of Soft Soil Data. 27
Table 3.1. Summary Information on the Four Selected Embankments. 45
Table 3.2. Laboratory Test and Field Tests Results (Borehole 99-1a). 47
Table 3.3. Summary of Consolidation Parameters Used for the Settlement Estimation. 50
Table 3.4. Summary Table of the Stress Increase in the Soil Mass (Project 1). 52
Table 3.5. Laboratory and Field Tests Results (Boring O-1) (Project 2). 60
Table 3.6. Laboratory and Field Tests Results (Boring O-4) (Project 2). 61
Table 3.7. Laboratory and Field Tests Results (Boring O-5) (Project 2). 62
Table 3.8. Laboratory and Field Tests Results (Boring O-6) (Project 2). 62
Table 3.9. Summary Table of Consolidation Parameters Used for the Settlement Estimation (Project 2). 65
Table 3.10. Summary Table of the Stress Increase in the Soil Mass. 67
Table 3.11. Field Test Results (Borings CCB-2, CCB-1, CCR-2, CCR-4 and CCR-3). 77
Table 3.12. Variation of Soil Types in Five Borings (Project 3). 78
Table 3.13. Variation of Moisture Content in the Six Borings (Project 3). 78
Table 3.14. Variation of Undrained Shear Strength with Depth in the Six Borings (Project 3) 79
Table 3.15. Consolidation Parameters Used for the Settlement Estimation (Project 3) 80
Table 3.16. Summary Stress Increase in the Soil Mass (Project 3). 83
Table 3.17. Summary of Stress Increase in the Soil Mass. 96
Table 4.1. Summary of the Samples Collected. 104
Table 4.2. Summary of Soil Type Parameters (SH3). 112
Table 4.3. Summary of Strength Parameters (SH3). 112
Table 4.4. Summary of Consolidation Parameters (SH3) 113

Table 4-5. Consolidation Parameters from IL Consolidation Tests for NASA Rd. 1. 117

Table 4-6. Soil Parameters of the Samples Used for Consolidation Tests with Multiple Loops. 118

Table 4.7. Estimated Preconsolidation Pressure. 122

Table 4.8. Summary Table of Compression Indices for Various Clay Soils (Holtz and Kovacs 1981). 125

Table 4.9. Correlations for C_c (Azzouz et al. (1976); Holtz and Kovacs (1981)). 129

Table 4.10. Summary of Compressibility Parameters for the Clay Soils (SH3 Bridge at Clear Creek). 135

1. INTRODUCTION

1.1. General

Embankments are among the most ancient forms of construction but also have the most engineering challenges in design, construction, and maintenance. Economic and social development has brought a considerable increase in the construction of embankments since the middle of the nineteenth century, particularly since the 1950s (Leroueil et al. 1990). Embankments are required in the construction of roads, motorways, and railway networks (elevated embankments, access embankments, and embankments across valleys), in hydroelectric schemes (dams and retention dikes), in irrigations and flood control work (regulation dams), harbor installations (seawalls and breakwaters), and airports (runways) (Leroueil 1994).

Historically, embankments have been placed on sites of good geotechnical properties in order to reduce the costs associated with their construction. However, during the last two decades, the demand for expanding the civil infrastructure has forced the use of sites with soft and compressible soils. It is often found that the regions of densest population are in the coastal or delta regions covered with recent deposits of clays, mud, and compressible silts. Therefore, in the past several decades, embankments have been constructed on compressible soils resulting in a number of problems.

The estimation of total and rate of settlement of an embankment with good serviceability is the main design concern of embankments on soft soils. The Terzaghi

(1925) 1-D classical method is widely used to estimate the total and rate of settlement, but it has limitations. Several two- and three-dimensional numerical methods have been developed to predict embankment behavior on soft soils based on the drainage conditions of the soft soils. All the design methods require laboratory testing and/or field testing to determine the parameters to be used. Each parameter can be determined using different tests, resulting in different values for the consolidation parameters (Wissa et al. 1971). The issues along the Texas Gulf coast are even more complicated by the deltaic nature of the soft soils and large variability of properties (Vipulanandan et al. 2007 and 2008).

Overestimation of settlement on overconsolidated soft clays may require ground improvement before construction with added delay and cost to a project. Since the soft soil shear strength is low, the structures on the soft soils are generally designed so that the increase in the stress is relatively small and the total stress in the ground will be close to the preconsolidation pressure. Hence there is a need to investigate methods to better predict the settlement of embankments on soft soils. Therefore, the recompression index determined from a consolidation test has more importance in estimating the settlement. Although the recompression index has been quantified in the literature, its determination is not clearly defined, especially when there is a hysteretic unloading loop for the soft clay soil. Also the influence of the unloading stress level on the recompression index is not clearly quantified.

Instrumenting the embankment with displacement sensors and piezometers to monitor the field behavior of an embankment on soft soil and comparing the results with the predicted behavior is the way to validate the accuracy and reliability of settlement and

rate of settlement estimation methods or models (Ladd et al. 1994; Vipulanandan et al. 2008).

1.2. Objectives

The overall goal of this study was to review and verify the applicability of conventional methods used to predict the total amount of and rate of settlement of embankments on soft clay soils. The specific objectives were as follows:

1) Investigate the methods used by the Texas Department of Transportation (TxDOT) to estimate the total and rate of settlements of embankments on soft soils.
2) Verify the predicted settlements with field studies by instrumenting selected embankments on soft soils. Critically review the selection of the consolidation parameter to predict the settlement.
3) Analyze the field measurements to verify the applicability of the classical consolidation theory and recommend methods to further improve the predictions.

1.3. Organization

Chapter 2 summarizes the background information on total and rate of settlement estimations of embankment on soft clay soils. It also describes the behavior of the soft soil in the Houston and Galveston areas. Chapter 3 investigates the Texas Department of Transportation (TxDOT) approaches to predict the total and rate of settlement in embankments on soft soils. A total of four projects were reviewed and analyzed. Chapter 4 summarizes the laboratory tests performed and investigates the selection of the

settlement parameters to predict the total and rate of settlement. In Chapter 5, field studies on two instrumented embankments on soft soil are analyzed. Conclusions and recommendations are given in Chapter 6.

2. SOFT SOILS AND HIGHWAY EMBANKMENT

2.1. General

The decades-long challenge of estimating settlement of embankments on soft clay soil using laboratory test data and simple consolidation theory has led to either over predicting or under predicting the total rate of settlement of embankments on soft soils (Leroueil et al. 1990). Terzaghi (1925) introduced the first known complete solution of soft clay soil consolidation. His 1-D consolidation theory for settlement calculation and incremental load (IL) consolidation test (ASTM D 2435) have been widely used because of their simplicity in predicting the total and rate of settlement of embankments on soft clay soils. However, due to the time factor imposed by the IL consolidation test procedure, other consolidation tests such as the constant rate of strain (CRS) consolidation test (ASTM D 4186), and the constant rate of loading (CRL) test, which are much faster, were introduced later (Wissa et al. 1971).

2.2. Soft Clay Soil Definition

As defined by the Unified Soil Classification System (USCS), clays are fine-grained soils, meaning they have more than 50% passing the No. 200 sieve, and they are different from the silt soils based on their liquid limit and plasticity index (Holtz and Kovacs 1981).

Terzaghi and Peck (1967) established that the consistency of a clay can be described by its compressive strength (q_u) or by its undrained shear strength S_u (= $q_u/2$)

and is regarded as very soft if unconfined compressive strength is less than 3.5 psi (25 kPa) and as soft soil when the strength is in the range of 3.5 to 7 psi (25 to 50 kPa).

TxDOT identifies a clay soil as soft when the number of Texas Cone Penetrometer (TCP) blow count is less than or equal to 20 for 1-ft penetration ($N_{TCP} \leq 20$) (Table 2.1).

Table 2.1. TxDOT Soil Density and Bedrock Hardness Classification.

Soil Density or Consistency			
Density (Granular)	**Consistency (Cohesive)**	**THD Penetrometer (blows/ft or blows/300mm)**	**Field Identification**
Very Loose	Very Soft	0 to 8	Core (height twice diameter) sags under own weight
Loose	Soft	8 to 20	Core can be pinched or imprinted easily with finger
Slightly Compact	Stiff	20 to 40	Core can be imprinted with considerable pressure
Compact	Very Stiff	40 to 80	Core can only be imprinted slightly with fingers
Dense	Hard	80 to 5"/100 (125mm/100)	Core cannot be imprinted with fingers but can be penetrated with pencil
Very Dense	Very Hard	5"/100 to 0"/100 (125mm/100 to 0mm/100)	Core cannot be penetrated with pencil

2.3. Embankment Settlement

An embankment increases the stress in the soil layers underneath (Fig. 2.1), and the saturated soft clay soils, being a highly compressible soil, will consolidate (settle).

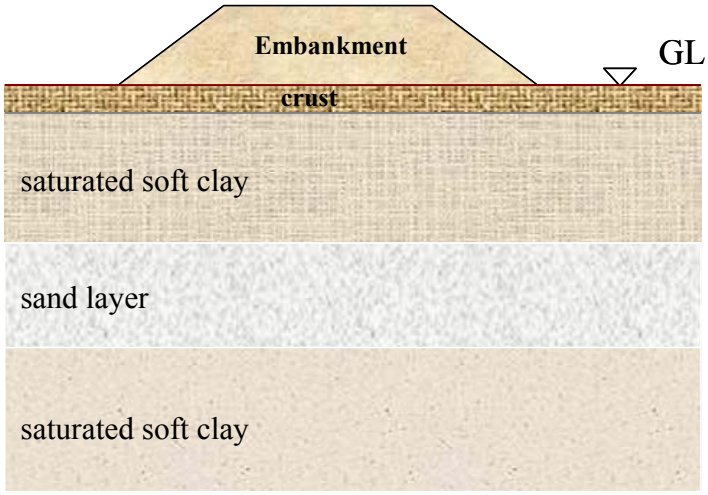

Fig. 2.1. Typical Configuration of Soil Layers under an Embankment.

2.3.1. Terzaghi Classical 1-D consolidation model

Terzaghi's complete solution for one-dimensional consolidation is stated as follows (Leroueil et al. 1990):

Hypotheses:

(1) The strains in the clay layer are 1-D and remain small (ε_z is small).

(2) The soil is homogeneous and saturated.

(3) The particles of the soil and the pore fluid are incompressible.

(4) The flow of the pore fluid is 1-D and obeys Darcy's law.

(5) The permeability is constant (k = constant).

(6) A linear relation exists between the effective vertical stress (σ'_v) and the void ratio

$$de = -a_v d\sigma'_v . \qquad 2\text{-}1$$

(7) The soil has no structural viscosity.

The use of the first hypothesis permits the fundamental equation of consolidation to be written in the form

$$\frac{\partial e}{\partial t} = \frac{k(1+e_o)}{\gamma_w}\frac{\partial^2 u}{\partial z^2} \qquad 2\text{-}2$$

where e is void ratio, e_o is initial void ratio, k is coefficient of permeability, γ_w is unit weight of water, t is time, u is pore water pressure, and z is drainage path.

This equation expresses the fact that the rate of change in void ratio (and, as a result, the rate of deformation) at a given instant depends on the permeability and the form of the excess pore pressure isochrones, but not on the compressibility of the material.

Using hypotheses (6) and (7), Equation 2-2 can be written

$$\frac{\partial u}{\partial t} - \frac{\partial \sigma_v}{\partial t} = \frac{k(1+e_o)}{\gamma_w a_v}\frac{\partial^2 u}{\partial z^2} \qquad 2\text{-}3$$

When the applied stress $\sigma_v^{'}$ is constant ($\frac{\partial \sigma_v}{\partial t} = 0$), Equation 2-3 takes the classical form of the Terzaghi equation

$$\frac{\partial u}{\partial t} = \frac{k(1+e_o)}{\gamma_w a_v}\frac{\partial^2 u}{\partial z^2} \qquad 2\text{-}4$$

The function $k(1+e_o)/\gamma_w a_w$ in this differential equation has been called the coefficient of consolidation (c_v) and is given by

$$c_v = \frac{k}{\gamma_w \left(\frac{a_v}{1+e_o} \right)} = \frac{k}{\gamma_w m_v} \qquad 2\text{-}5$$

and

$$\frac{\partial u}{\partial t} = c_v \frac{\partial^2 u}{\partial z^2} \qquad 2\text{-}6$$

This equation can also be written in terms of excess pore pressures (Schlosser et al. 1985)

$$\frac{\partial (\Delta u)}{\partial t} = c_v \frac{\partial^2 (\Delta u)}{\partial z^2} \qquad 2\text{-}7$$

Equation 2-6 is the basic differential equation of Terzaghi's consolidation theory and is solved with the following boundary conditions:

$$z = 0, \ u = 0$$
$$z = 2H_{dr}, \ u = 0$$
$$t = 0, \ u = u_0$$

giving the time factor T_v as follows

$$T_v = \frac{c_v t}{H_{dr}^2} \qquad 2\text{-}8$$

For the given load increment on a specimen, Casagrande and Fadum (1940) developed the graphical *logarithm-of-time method* to determine c_v at 50% average degree of consolidation with $T_{50} = 0.197$. Taylor (1942) developed *the square-root-of-time graphical method* giving c_v at 90% average of consolidation with $T_{90} = 0.848$. These two graphical methods, Equations 2-9 and 2-10, are commonly used to determine the coefficient of consolidation and are described in ASTM D 2435 – 96.

Using the Casagrande method,

$$c_v = \frac{0.197 H^2_{dr}}{t_{50}} \qquad 2\text{-}9$$

and using the Taylor method,

$$c_v = \frac{0.848 H^2_{dr}}{t_{90}} \qquad 2\text{-}10$$

where H_{dr} is the maximum drainage path.

The primary consolidation settlement (S_p) of the clay is represented as follows:

For normally consolidated clay

$$S_p = \frac{C_c H}{1+e_0} log\left(\frac{\sigma_0^{'} + \Delta\sigma^{'}}{\sigma_0^{'}}\right) \qquad 2\text{-}11$$

and for overconsolidated clay

$$S_p = \frac{C_r H}{1+e_0} log\left(\frac{\sigma_p}{\sigma_0^{'}}\right) + \frac{C_c H}{1+e_0} log\left(\frac{\sigma_0^{'} + \Delta\sigma^{'}}{\sigma_p}\right) \qquad 2\text{-}12$$

where

C_c = compression index

C_r = recompression index

e_o = initial void ratio

H = soil layer height $\Delta\sigma'$

σ'_o = in-situ vertical effective stress at rest

σ_p = preconsolidation pressure

$\Delta\sigma'$ = stress increase in the soil mass due to embankment loading.

(1) **The time rate of consolidation**

From the incremental load (IL) test

$$T_v = \frac{c_v t}{H_{dr}^2} \rightarrow c_v = \frac{T_v H_{dr}^2}{t} \qquad 2\text{-}13$$

and from the Constant rate of strain (CRS) test (Wissa et al. 1971)

$$c_v = -\frac{H^2 log\left[\frac{\sigma_{v2}}{\sigma_{v1}}\right]}{2\Delta t log\left[1 - \frac{u_h}{\sigma_v}\right]} \qquad 2\text{-}14$$

where

c_v = coefficient of consolidation

H_{dr} = longest drainage path

H = average specimen height between t_1 and t_2

T_v = time factor

u_h = average excess pore pressure between t_2 and t_1

Δt = elapsed time between t_1 and t_2

σ_{v1} = applied axial stress at time t_1

σ_{v2} = applied axial stress at time t_2.

The following are the standard definitions and methods of determination for all the parameters used in Equations 2-11, 2-12, 2-13, and 2-14.

2.3.2. Incremental Load (IL) test (ASTM D 2435)

The one-dimensional consolidation test procedure, a simulation of the field condition in the laboratory (Fig. 2.2) first suggested by Terzaghi to determine the compressibility parameters and rate of settlement of clayey soils, is performed in a consolidometer, also called the oedometer. Following the standard test method for 1-D consolidation (American Society of Testing and Material (ASTM) D 2435 – 96), the soil specimen is placed inside a metal ring with two porous stones, one at the top of the specimen and another at the bottom (Fig. 2.2) to comply with the plain strain condition. Load increment ratios of unity are applied, and each increment is left on for 24 hours to obtain characteristic time-settlement relationships, from which consolidation parameters are obtained. From the void ratio (e) versus logarithm of vertical stress ($\log \sigma_{v,}$) (Fig. 2.3) relationship, the preconsolidation pressure σ_p, the compression index C_c, and recompression index C_r are determined. The specimen is kept under water during the test. The test takes several days (typically from 5 to 15 days or more).

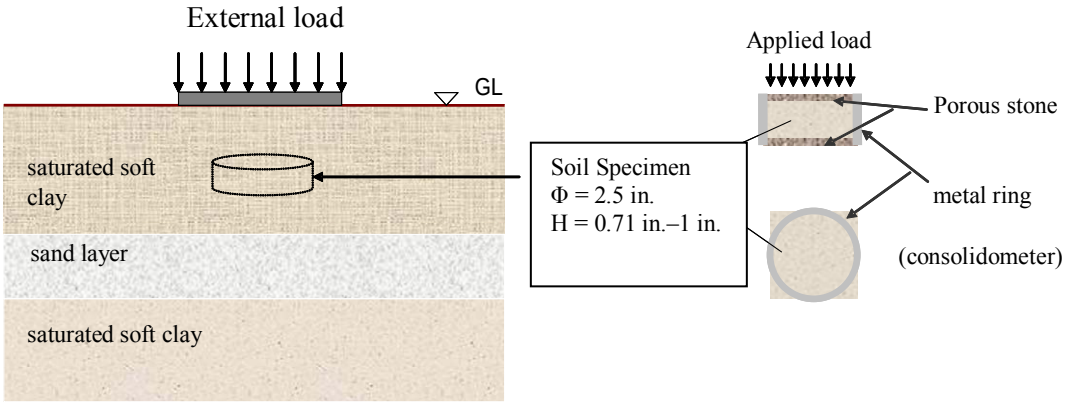

Fig. 2.2. Field Condition Simulation in Laboratory Consolidation Test.

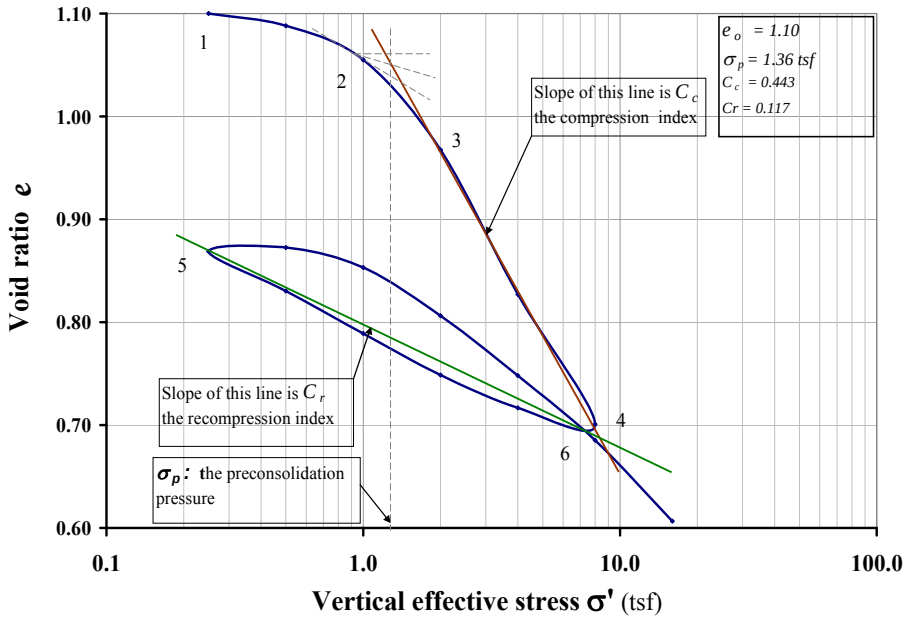

Fig. 2.3. Typical e – log σ_v Relationship for Overconsolidated Clay.

The preconsolidation pressure, σ_p, is the highest stress the clay soil ever felt in its history. There are several methods to determine σ_p, which are discussed in Chapter 4, but the Casagrande graphical method was used in Fig. 2.3.

The compression index, C_c, is the slope of the virgin compression section of the curve (Section 3 – 4 in Fig. 2.3)

$$C_c = \frac{-(e_4 - e_3)}{log\,\frac{\sigma_4}{\sigma_3}}. \qquad 2\text{-}15$$

The recompression index C_r is the average slope of the hysteretic loop, as shown in Fig. 2.3, and it is assumed to be independent of the stress.

2.3.3. Constant rate of strain test

In 1969, after about 40 years of use of the IL test without major modification for clay soil compressibility and rate of settlement parameter determination, two new methods of performing a consolidation test were introduced:

- the Controlled Gradient test (CG test) by Lowe et al. (1969), and
- the Constant Rate of Strain test (CRS test) by Smith and Wahls (1969).

These tests were used to overcome some of the limitations of the conventional test (IL test) in real-time monitoring of pore water pressure (u vs. t) and the total time needed to complete a test.

The Constant Rate of Strain (CRS) 1-D consolidation, also specified as Controlled-Strain Loading by ASTM D 4186-86, is the technique in which a saturated clay sample is consolidated at constant volume under a back pressure and loaded, with no lateral strain, by incremental load, at a constant rate of strain (Wissa et al. 1971). Terzaghi's complete solution for 1-D consolidation and its hypotheses are valid and applied.

The features of the CRS consolidation test are as follows:

- contrary to the oedometer cell, the sample is provided only one drainage surface, the top porous stone; the bottom drainage surface is locked and used to measure the excess pore water pressure at the sample base (u_h) (Fig. 2.4),
- fully computerized because of the need for constant rate of strain ($d\varepsilon = 0$), which requires a control and update of the stress applied at all times (t) (Fig 2.5 and Fig. 2.6),

- faster compared to the IL test. The CRS test can be completed in less than 24 hours.

The parameters governing the CRS consolidation test (Wissa et al. 1971) and ASTM D 4186-86, are as follows:

- consolidation test results are strain rate ($\dot{\varepsilon}$) dependent,
- selection of strain rate is based on the criteria developed by Wissa et al. (1971). The strain rate ($\dot{\varepsilon}$) does not affect as much the $e - log\ \overline{\sigma}_v$ curve as the coefficient of consolidation c_v. Consequently, the optimum rate of strain for a given soil is a trade-off between the speeds best suited for determining the $e - log\ \overline{\sigma}_v$ curve and the coefficient of consolidation c_v

  ($\overline{\sigma}_v$ is the average effective stress), and
- because field strain rates cannot be accurately determined or predicted, it is not feasible to relate the laboratory-test strain rates to the field strain rates. However, it may be feasible to relate field pore pressure ratios (u_h/σ_v) to laboratory pore pressure ratios. After Wissa et al. (1971), all parameters can be accurately determined with the strain rate giving u_h/σ_v values of 2% to 5%, but the ASTM D 4186-86 established a preferable ranging from 3% to 30%.

As summarized by the compiled data of Dobak (2003) (Table 2.2), the range of pore pressure ratios for a representative test providing reliable coefficient of consolidation (c_v) depends on the type of the soil.

Table 2.2. Recommended u_h/σ Values (Dobak 2003).

Recommended u_h/σ values	Soil type	Reference
0.5	Kaolinites, Ca-montmorillonites, Messena clay	Smith and Wahls (1969)
0.05	Boston blue clay (artificially sedimented)	Wissa et al. (1971)
0.1-0.15	Bakebol clay	Sällfors (1975)
0.3-0.5 (u_{hmin} = 7 kPa)	Silts and clays from the coal field of Mississippi Plains (Kentucky)	Gorman et al. (1978)

Note: In the table u_{hmin} is u_h

- the coefficient of consolidation, the only parameter differently determined from the IL parameters, is given by the following relationship:

$$c_v = -\frac{H^2 \log\left[\frac{\sigma_{v2}}{\sigma_{v1}}\right]}{2\Delta t \log\left[1-\frac{u_h}{\sigma_v}\right]} \qquad 2\text{-}16$$

where

σ_{v1} = applied axial stress at time t_1

σ_{v2} = applied axial stress at time t_2

H = average specimen height between t_1 and t_2

Δt = elapsed time between t_1 and t_2

u_h = average excess pore pressure between t_2 and t_1

σ_v = average total applied axial stress between t_2 and t_1.

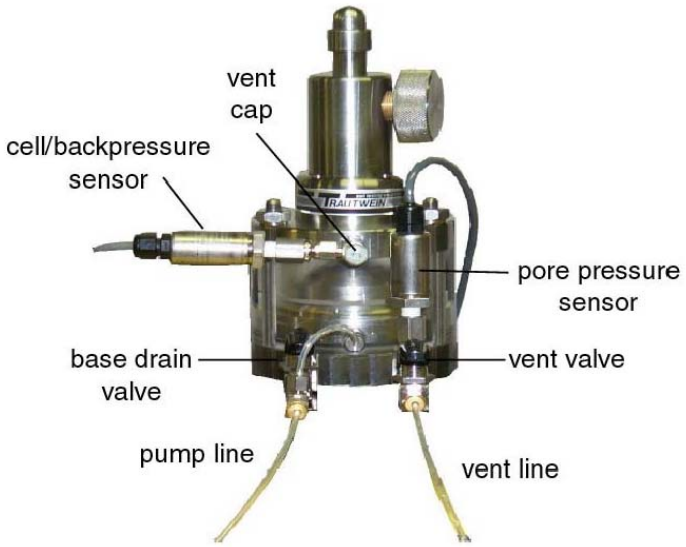

Fig. 2.4. Constant Rate of Strain (CRS) Consolidation Cell Used at the University of Houston (GEOTAC Company 2006).

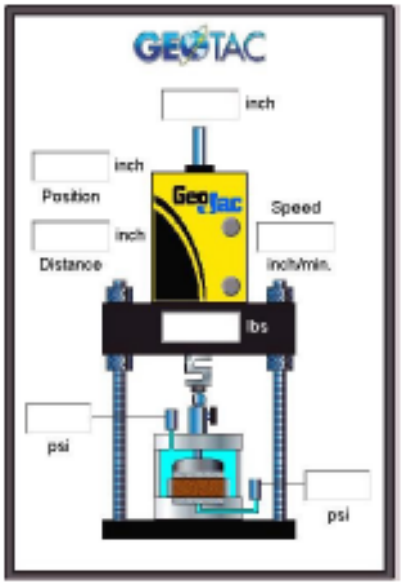

Fig. 2.5. Schematic of CRS Test Frame Used at the University of Houston (GEOTAC Company 2006).

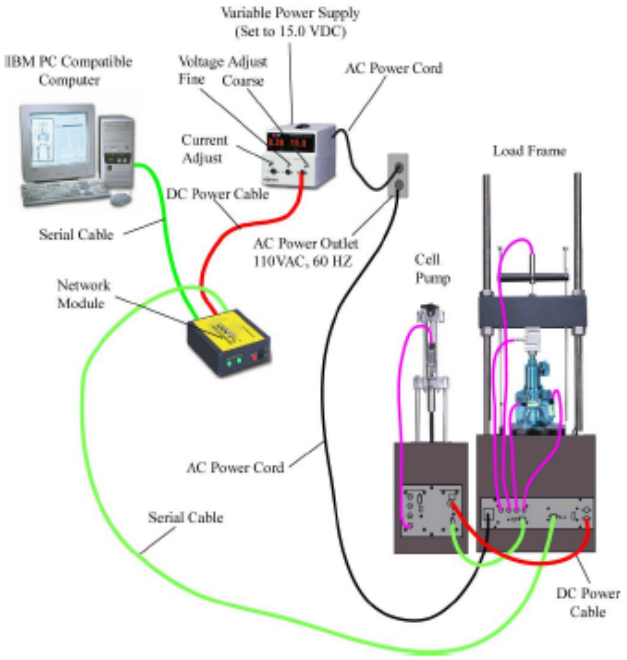

Fig. 2.6. Commercially Available CRS Test System (GEOTAC Company 2006).

Table 2.3. Conditions for 1-D Consolidation Tests (Dobak 2003).

Types of tests		Conditions of loading	Exponential model of stress changes $\sigma = a \cdot t^n$	Governing physical processes
IL		σ = const	n = 0	- creep of soil skeleton - seepage
CL	CRL	$\Delta\sigma/\Delta t$ = const	n = 1	- character and changes in stress increase - seepage - creep of soil skeleton
	CRS CG	$\Delta\sigma/\Delta t$ increasing	n > 1	

CRL is the Constant Rate of Loading test.
CG is the Constant Gradient test, meaning that the pore water pressure at the base of the specimen is kept constant throughout the test.

2.3.4. Two-dimensional consolidation

Consolidation under an embankment is actually two- or three-dimensional. Several theoretical solutions for the two-dimensional consolidation problem were developed as early as 1978 (Leroueil et al. 1990); these have certain deficiencies in their hypotheses upon which they are based:

(1) Isotropic behavior of the clay skeleton.

(2) Constant coefficient of consolidation.

(3) Determination of consolidation parameters in the horizontal direction.

The effect of the second dimension is only important when the width of the base (W) of the embankment is less than twice the thickness ($W < 2d$) of the clay layer (Leroueil et al. 1990).

The use of these 2-D consolidation models was uncommon until the recent development and popularization of finite element (FE) and finite difference (FD) computer programs. In fact, the need to combine stability analysis with settlement analysis resulted in 2-D and 3-D numerical modeling of the problem (FE and FD).

To truly understand and predict soils' behavior, it is necessary to have a complete knowledge of stresses and strains at all compatible loading levels right up to failure. Constitutive relations or stress-strain laws embrace information on both shear stresses and deformations at all stages of loading, from pre-failure states to failure (Nagaraj and Miura 2001).

Consequently, several 2-D constitutive models for soft clay soil behavior have been developed and implemented in FE and FD programs. For example, linearly elastic, perfectly plastic, hyperbolic, and several other academic models were implemented in the

existing numerical frames (Plaxis, FLAC). Most of the models are isotropic, but soft clay soil is an anisotropic material. Models such as MIT-E3 (Whittle and Kavvadas 1994) and the multi-laminate model (Cudny 2003) are two of the advanced models that considered the anisotropic behavior of soft clay soil. All these models require several parameters, leading to more laboratory testing.

2.3.5. Stress increase in the soil mass due to embankment loading ($\Delta\sigma$)

- **2:1 Method**

The 2:1 method is the simplest method to calculate the stress increase with depth, due to embankment loading, in the soil mass. It is an empirical method (Holtz and Kovacs 1981) based on the assumption that the area over which the load acts increases in a systematic way with depth, Fig. 2.7.

$$\Delta\sigma_z = \frac{\sigma_o BL}{(B+z)(L+z)} \qquad 2\text{-}17$$

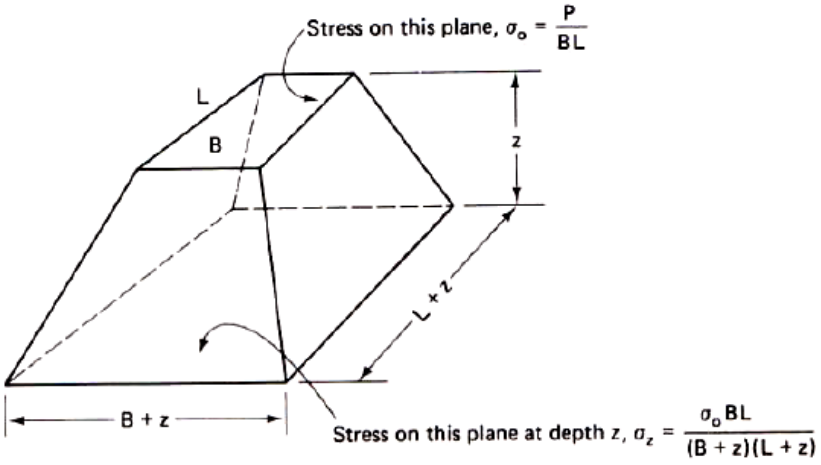

Fig. 2.7. 2:1 Method for Vertical Stress Distribution (Holtz and Kovacs 1981).

- **Modified Boussinessq method**

The vertical stress caused by a vertical strip load (finite width and infinite length) (Fig. 2.8) is given by Equation 2-18, which is derived from the Boussinessq (1883) solution of stresses produced at any point in a homogeneous, elastic, and isotropic medium as the result of a point load applied on the surface of an infinitely large half-space.

$$\Delta\sigma_z = \frac{q}{\pi}\left\{\tan^{-1}\left[\frac{z}{x-(B/2)}\right] - \tan^{-1}\left[\frac{z}{x+(B/2)}\right] - \frac{Bz\left[x^2 - z^2 - (B/4)\right]}{\left[x^2 + z^2 - (B^2/4)\right]^2 + B^2z^2}\right\} \qquad 2\text{-}18$$

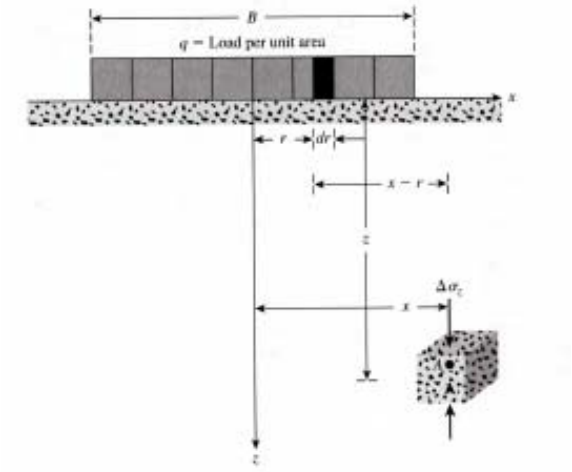

Fig. 2.8. Vertical Stress Due to a Flexible Strip Load (Das 2006).

- **Osterberg method**

Based on Boussinessq's expression, Osterberg derived the vertical stress increase in a soil mass due to an embankment loading, considering its real geometry (crest) (Fig. 2.9), which is given by the following equations:

$$\Delta\sigma_z = \frac{q_o}{\pi}\left[\left(\frac{B_1 + B_2}{B_2}\right)(\alpha_1 + \alpha_2) - \frac{B_1}{B_2}(\alpha_2)\right] \quad \text{2-19}$$

where $q_0 = \gamma H$

$$\alpha_1\,(radian) = tan^{-1}\left(\frac{B_1 + B_2}{z}\right) - tan^{-1}\left(\frac{B_1}{z}\right) \quad \text{2-20}$$

$$\alpha_2 = tan^{-1}\left(\frac{B_1}{z}\right). \quad \text{2-21}$$

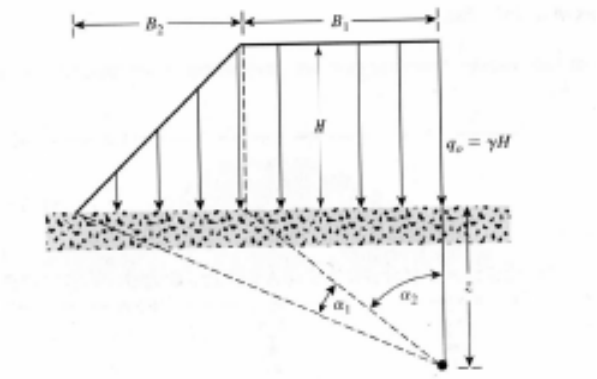

Fig. 2.9. Embankment Loading Using Osterberg's Method (Das 2006).

2.3.6. Summary and discussion

Terzaghi's (1925) 1-D consolidation theory is the basis for consolidation settlement estimation tests. CRS, CRL, and CG tests have been created to account for some of the limitations of the IL test.

2-D and 3-D consolidation models have been developed based on the real behavior of soft soil under embankments. This has resulted in more advanced settlement calculation and avoidance of the oversimplification of the settlement problem.

Settlement issues such as effective stress increase, estimation of soil properties, drainage conditions, and soil layering are considered as critical for more accurate prediction of the total amount of and rate of settlement.

2.4. Behavior of Marine and Deltaic Soft Clays

More and more construction projects are encountering soft clays, and hence, there is a need to better quantify the properties of soft clays. In this study, data from many parts of the world are used to characterize the soft clays based on the type of deposits. Physical, index, and strength properties for marine and deltaic soft clays were determined and investigated using the soft soil database developed from the published data in the literature. Data were analyzed using statistical methods (mean, standard deviation, variance, and probability density function), and the undrained shear strength (S_u) versus preconsolidation (σ_p) was verified. A new strength relationship between undrained shear strength (S_u) and in-situ vertical stress (σ_v) has been developed for the soft clays. Also, constitutive models used for soft soil behavior prediction have been reviewed.

Soft clays are found in marine, lacustrine, deltaic, and coastal regions or as a combination of deposits around the world. They are of relatively recent geological origin, having been formed since the last phase of the Pleistocene, during the past 20,000 years. In addition to the geological factors, salinity, temperature, and the type of clay have a direct effect on the lithology of the soft clays. The behavior of soft soils has been studied for well over four decades, and there are several property relationships in the literature on soft clays.

Bjerrum (1974) evaluated methods to determine the undrained shear strength of soft clay soils. Based on the study, it was concluded that the laboratory triaxial tests on undisturbed samples consolidated to in-situ effective stress better represented the strength of the soft soil in different directions. It was also noted that the field vane test is the best possible practical approach for determining the undrained strength for stability analysis. A number of studies after Bjerrum (1974) have attempted to relate the undrained shear strength of soil to the preconsolidation pressure (σ_p), in-situ vertical stress (σ_v), time-to-failure, and plasticity index (PI). Since the early 1970s, a number of investigators have studied the behavior of soft soils and their properties have been documented in the literature.

2.4.1. Soil correlations

Comprehensive characterization of soft soil at a particular site would require an elaborate and costly testing program generally limited by funding and time. Instead, the design engineer must rely upon more limited soil information and that is when correlations become most useful. However, caution must always be exercised when using broad, generalized correlations of index parameters or in-situ test results with soft soil properties. The source, extent, and limitations of each correlation should be examined carefully before use to ensure that extrapolation is not being done beyond the original boundary conditions. In general, local calibrations, where available, are to be preferred over broad, generalized correlations. In this study, information reported from various locations around the world was used to develop statistical geotechnical properties and correlations. In addition, some of the common correlations in the literature will be

verified with the data available. The correlations in the literature will be helpful in identifying the important variable and in eliminating the others.

Soft soil is a complex engineering material that has been formed by a combination of various geologic, environmental, and chemical processes. Because of these natural processes, all soil properties in-situ will vary vertically and horizontally. Recovering undisturbed soil samples is considered a challenge and various methods are being adopted around the world. Even under the most controlled laboratory test conditions, soil properties will exhibit variability. The property variability is notable in samples recovered from shallow depths considered being in the Active Zone. Although property in-situ condition correlations are important to a better understanding of the factors influencing the behavior of soft clays, adequate precautions must be taken to verify the relationships for more specific applications.

2.4.2. Database on soft soils

Soft clays are encountered around the world (Fig. 2.10), and the information in the literature can be characterized based on the type of deposits. In general, the properties of the soft soils will be influenced by the geology, mineralogy, geochemistry, and the lithology (composition and soil texture) of the deposits. Although a number of physical and chemical factors enter into the classifications of deposits, in the geotechnical literature, classification is made according to the marine, lacustrine, coastal, or deltaic depositional environments. Marine clays are the most investigated group of soft clays and are generally characterized as homogenous deposits with flocculation of particles due to salinity resulting in highly sensitive clays. Soft clay soils data from Japan (Ariake clay), South Korea (Pusan clay), Norway (Drammen, Skoger Spare, Konnerud, and Scheitlies

clays), Canada (Eastern Canada clay), and the USA (Boston blue clay) are classified as marine deposits. Properties of the soft soils collected from the literature are summarized in Table 2.4. A total of 52 data sets were collected on marine clays from around the world. The rate of deposition varied from 30 to 1600 cm/1,000 years and is compared to other deposits in Fig. 2.11.

The soft soils from the Houston-Galveston area in Texas, U.S.A., are characterized as deltaic deposits. The deltas of large rivers form a very active and very complex sedimentation environment. Deltaic deposits are generally stratified in a random manner with the interbedded coarse materials, organic debris, and shells. The combination of a significant amount of solid material, topography, and current, along with the interaction between fresh river water and salt seawater, led to high rates of deltaic deposits (Fig. 2.11).

Fig. 2.10. Locations of Soft Clay Soils Used for the Analysis.

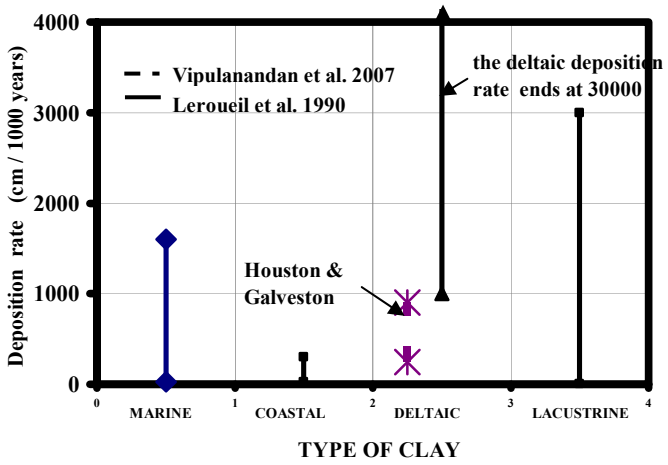

Fig. 2.11. Rate of Sedimentation of Different Types of Clay Deposits (Leroueil 1990).

Table 2.4. Summary of Soft Soil Data.

ANALYSIS	W_n (%)	W_L (%)	PL (%)	PI (%)	S_u (kPa)	σ_p (kPa)	e_o (%)	References
MARINE CLAY (Number of data = 51)								
RANGE	30 - 133	32 -121	19.4 - 33	12 - 50.5	1.8 - 25	7.5 - 248	80 -352	Nagaraj & Miura (2001); Chung et al.(2002); Shibuya & Tamrakar (1999); Nash, Sills, Davison, Powell & Lloyd (1992)
MEAN	73.6	64.2	24.3	35.2	17.5	74.5	195.2	
STANDARD DEVIATION	22.3	22.2	3.4	11.7	6.6	41.8	58.9	
COV (%)	30.3	34.6	13.8	33.2	37.9	56.1	30.2	
DELTAIC CLAY : Houston_Galveston (Number of data sets = 97)								
RANGE	13 - 59	24 - 93	8 - 35	8 - 61	7 - 25	-	34 - 156	Vipulanandan et al (2006)
MEAN	28.9	53.6	21.8	32.4	19.5	-	76.7	
STANDARD DEVIATION	9.5	22.7	6.9	16.9	5.1	-	25.1	
COV (%)	32.8	42.4	31.6	52.2	26.2	-	32.7	

Houston and Galveston, Texas, are on two Pleistocene terrace formations found along the Gulf Coast, west of the Mississippi River and north of the Rio Grande River, exposed at the surface to about 100 km inland from the present coastline. The lower formation, termed the upper Lissie formation or the Montgomery formation (the latter designation will be used here), was deposited on a gentle slope on an older Pleistocene formation during the Sangamon Interglacial Stage by streams and rivers near the existing coast where numerous large and small rivers deltas developed. After deposition, the nearby sea level was lowered during the first Wisconsin Glacial Stage, producing desiccation and consolidation of the Montgomery soils, which consisted primarily of clays and silts. At the beginning of the Peorian Interglacial Stage as the glaciers were retreating, the sea level returned to its previous level, producing a preconsolidation effect within the Montgomery formation. At the same time, rivers and streams produced sedimentary deposits on top of the slightly seaward-sloping Montgomery formation from the existing coastline to about 60 km inland. The resulting new formation, primarily a fresh-water deposit sloping toward the Gulf of Mexico, has characteristics typical of deltaic environments, including point bar, natural levee, backswamp, and pro-delta deposits within, beside, and at the termination of distributary channels. This formation is known as the Beaumont formation in Texas. After deposition, the nearby Gulf of Mexico receded by about 125 m once more during the late Wisconsin Glacial Stage, inducing desiccation in the Beaumont and redesiccating the underlying Montgomery. Finally, with the recession of the late Wisconsin glaciers, the sea level returned to its present level, leaving both formations preconsolidated through desiccation. The rate of deposit was

estimated to be between 250-900 cm/1,000 years (Vipulanandan et al. 2007). A total of 97 data sets have been collected from Houston and Galveston area deltaic soil, and the range of values is summarized in Table 2.4.

2.4.3. Statistical Properties

(a) Marine Clay

(i) Natural Moisture Content (W_n): The moisture content varied from 30% to 133% with a mean of 73.6%, standard deviation of 22.3%, and coefficient of variation of 30.3%. This coefficient of variation was the second lowest observed for the marine clay properties being investigated in this study. This COV was in the typical range of values observed for other marine clay properties. Of the probability distribution functions considered (Beta, Erlang, Exponential, Gamma, Lognormal, Normal, Triangular, Uniform, and Weibull), the Beta distribution has the least error based on the 51 data sets.

(ii) Liquid Limit (LL): The liquid limit varied from 32% to 121% with a mean of 64.2%, standard deviation of 22.2%, and coefficient of variation of 34.6%. The variability observed in the LL, based on the COV, was similar to the moisture content. Of the probability distribution functions considered (Beta, Erlang, Exponential, Gamma, Lognormal, Normal, Triangular, Uniform, and Weibull), the Triangular distribution has the least error, based on the 51 data sets.

(iii) Plasticity Limit (PL): The plastic limit varied from 19.4% to 33% with a mean of 24.3%, standard deviation of 3.4% and coefficient of variation of 13.8%. The variability observed in the PL, based on the COV, was the lowest, indicating that it had the lowest variability of all the other marine clay properties being investigated in this study. Of the

probability distribution functions considered (Beta, Erlang, Exponential, Gamma, Lognormal, Normal, Triangular, Uniform, and Weibull), the Normal distribution has the least error based on the 13 data sets.

(iv) Plasticity Index (PI): The plasticity index varied from 12% to 50.5%, with a mean of 35.2%, a standard deviation of 11.7%, and a coefficient of variation of 33.2%. Of the probability distribution functions considered (Beta, Erlang, Exponential, Gamma, Lognormal, Normal, Triangular, Uniform, and Weibull), the Beta distribution has the least error, based on the 13 data sets.

(v) Undrained Shear Strength (S_u): The undrained shear strength varied from 1.8 kPa to 25 kPa, with a mean of 17.5 kPa, a standard deviation of 6.6 kPa, and a coefficient of variation of 37.9%. The COV was in the same range as the LL, typical for the marine clay. Of the probability distribution functions considered (Beta, Erlang, Exponential, Gamma, Lognormal, Normal, Triangular, Uniform, and Weibull), the Beta distribution (Fig. 2.12) has the least error, based on the 51 data sets.

(vi) Undrained Shear Strength-to-In situ Stress Ratio (S_u/σ_v): The undrained shear strength-to-in situ stress ratio varied from 0.08 to 1.39, with a mean of 0.52, a standard deviation of 0.27, and a coefficient of variation of 51.9%. Of the probability distribution functions considered (Beta, Erlang, Exponential, Gamma, Lognormal, Normal, Triangular, Uniform, and Weibull), lognormal distribution has the least error, based on the 49 data sets.

(vii) Preconsolidation Pressure (σ_p): The preconsolidaton pressure varied from 7.5 kPa to 248 kPa with a mean of 74.5 kPa, a standard deviation of 41.8 kPa, and a coefficient of variation of 56.1 kPa. Of the probability distribution functions considered (Beta, Erlang,

Exponential, Gamma, Lognormal, Normal, Triangular, Uniform, and Weibull), the Weibull distribution has the least error, based on the 51 data sets.

(viii) Undrained Shear Strength-to-Preconsolidation Pressure Ratio (S_u/σ_p): The Undrained Shear Strength-to-Preconsolidation Pressure Ratio varied from 0.06 to 0.47, with a mean of 0.26, a standard deviation of 0.08, and a coefficient of variation of 30.8. Of the probability distribution functions considered (Beta, Erlang, Exponential, Gamma, Lognormal, Normal, Triangular, Uniform, and Weibull), the Beta distribution has the least error, based on the 51 data sets.

(ix) Overconsolidation Ratio (OCR): The overconsolidation ratio varied from 1 to 4, with a mean of 2.01, a standard deviation of 0.89, and a coefficient of variation of 44.3. Of the probability distribution functions considered (Beta, Erlang, Exponential, Gamma, Lognormal, Normal, Triangular, Uniform, and Weibull), the Beta distribution has the least error, based on the 49 data sets.

(x) Void ratio (e_o): The void ratio varied from 80% to 352%, with a mean of 195.2%, a standard deviation of 58.9%, and a coefficient of variation of 30.2%. The COV was in the same range of several other parameters for the marine clay. Of the probability distribution functions considered (Beta, Erlang, Exponential, Gamma, Lognormal, Normal, Triangular, Uniform, and Weibull), the Normal distribution has the least error, based on the 51 data sets.

(xi) Undrained Shear Strength-to-Void ratio (S_u/e_o): Undrained shear strength-to-void ratio varied from 0.68 to 24.51, with a mean of 10.10, a standard deviation of 5.20, and a coefficient of variation of 51.5. Of the probability distribution functions considered (Beta,

Erlang, Exponential, Gamma, Lognormal, Normal, Triangular, Uniform, and Weibull), the Normal distribution has the least error based on the 51 data sets.

(b) Deltaic Clay

(i) Natural Moisture Content (W_n). The moisture content varied from 13% to 59%, with a mean of 28.9%, a standard deviation of 9.5%, and a coefficient of variation of 32.8%. The probability distribution function was normal based on 97 data. Based on the mean and range of moisture contents, the moisture content in the deltaic soils were less than half that of marine clays. Based on variance, the marine clay had a more than 600% higher variance than did deltaic clay. This large variance could partly be due to the fact that the marine clay data was gathered from three continents, as compared to the deltaic, which was from one location. Of the probability distribution functions considered (Beta, Erlang, Exponential, Gamma, Lognormal, Normal, Triangular, Uniform, and Weibull), Beta distribution has the least error, based on 97 data.

(ii) Liquid Limit (LL). The liquid limit varied from 24% to 93%, with a mean of 53.6%, a standard deviation of 22.7%, and a coefficient of variation of 2.36%. Of the probability distribution functions considered, (Beta, Erlang, Exponential, Gamma, Lognormal, Normal, Triangular, Uniform, and Weibull), Beta distribution has the least error based on 97 data.

(iii) Plastic Limit (PL). The plastic limit varied from 8 to 35, with a mean of 21.8, a standard deviation of 6.9, and a coefficient of variation of 31.6%. Of the probability distribution functions considered (Beta, Erlang, Exponential, Gamma, Lognormal,

Normal, Triangular, Uniform, and Weibull), Weibull distribution has the least error, based on 97 data.

(iv) Plasticity Index (PI). The plasticity index varied from 8 to 61, with a mean of 32.4, a standard deviation of 16.9, and a coefficient of variation of 52.2%. Of the probability distribution functions considered (Beta, Erlang, Exponential, Gamma, Lognormal, Normal, Triangular, Uniform, and Weibull), Beta distribution has the least error, based on 97 data.

(v) Undrained Shear Strength (S_u). The undrained shear strength varied from 7 kPa to 25 kPa, with a mean of 19.5, a standard deviation of 5.1, and a coefficient of variation of 326.2%. Of the probability distribution functions considered (Beta, Erlang, Exponential, Gamma, Lognormal, Normal, Triangular, Uniform, and Weibull), Beta distribution (Fig. 2.12) has the least error, based on 97 data.

(vi) Undrained Shear Strength-to-In situ Stress Ratio (S_u/σ_v): The Undrained Shear Strength-to-In situ Stress Ratio varied from 0.05 to 3.12, with a mean of 0.42, a standard deviation of 0.65, and a coefficient of variation of 154.8%. Of the probability distribution functions considered, (Beta, Erlang, Exponential, Gamma, Lognormal, Normal, Triangular, Uniform, and Weibull). Beta distribution has the least error, based on 97 data.

(vii) Void ratio (e_o): The moisture content varied from 34% to 156%, with a mean of 76.7, a standard deviation of 25.1, and a coefficient of variation of 32.7%. Of the probability distribution functions considered (Beta, Erlang, Exponential, Gamma, Lognormal, Normal, Triangular, Uniform, and Weibull), Beta distribution has the least error, based on 97 data.

(viii) Undrained Shear Strength-to-Void ratio (S_u/e_o): The Undrained Shear Strength-to-Void ratio varied from 4.41 to 56.91, with a mean of 28.63, a standard deviation of 11.80, and a coefficient of variation of 41.2%. Of the probability distribution functions considered (Beta, Erlang, Exponential, Gamma, Lognormal, Normal, Triangular, Uniform, and Weibull), Beta distribution has the least error, based on 97 data.

Based on the variance, marine clay showed greater variation in natural moisture content (w_n), undrained shear strength (S_u), and void ratio (e_o), compared to the deltaic deposit. Similarly, deltaic deposit showed greater variation in plasticity limit and plasticity index, compared to the marine clay.

Based on COV, the deltaic clay properties had higher values than marine clay, except for the undrained shear strength. It is of interest to note that the natural moisture content and void ratio had similar values for marine and deltaic deposits.

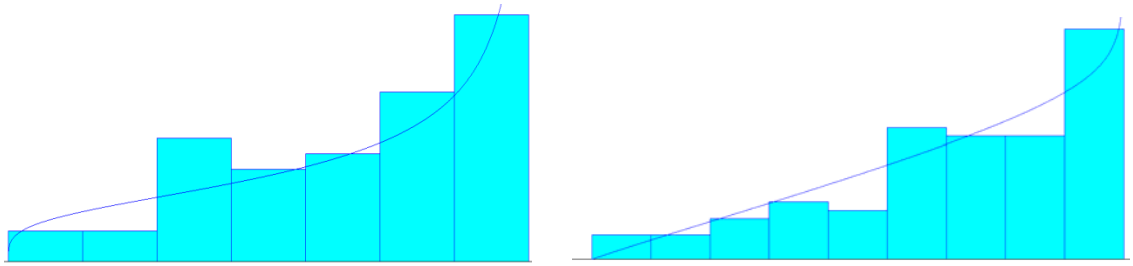

a.) Marine: Beta distribution **b.) Deltaic: Beta distribution**

Fig. 2.12. Probability Distribution Function for the Undrained Shear Strength (a) Marine Clay and (b) Deltaic Clay.

2.4.4. Property Correlations (from Table 2.4)

(i) LL versus Natural Moisture Content

Marine Clay: For 52.9% of the marine clays, the natural moisture content was higher than the liquid limit indicating the sensitive nature of the clay (Fig. 2.13 (a)). The mean of the moisture content was 73.6% compared to the mean of the liquid limit of 64.2%. The coefficient of variations for the moisture content and liquid limits was 30.3% and 34.6%, respectively, indicating similar variability in the two measured parameters.

Deltaic Clay: For 97.9% of the deltaic clays, the natural moisture content was lower than the liquid limit, opposite of what was observed for the marine clay (Fig. 2.13 (b)). The mean of the moisture content was 28.9%, compared to the mean of the liquid limit of 53.6%. The coefficient of variations for the moisture content and liquid limits was 32.8% and 42.4%, respectively. Based on the COV and the standard deviation, the variability in the liquid limit was higher than the moisture content.

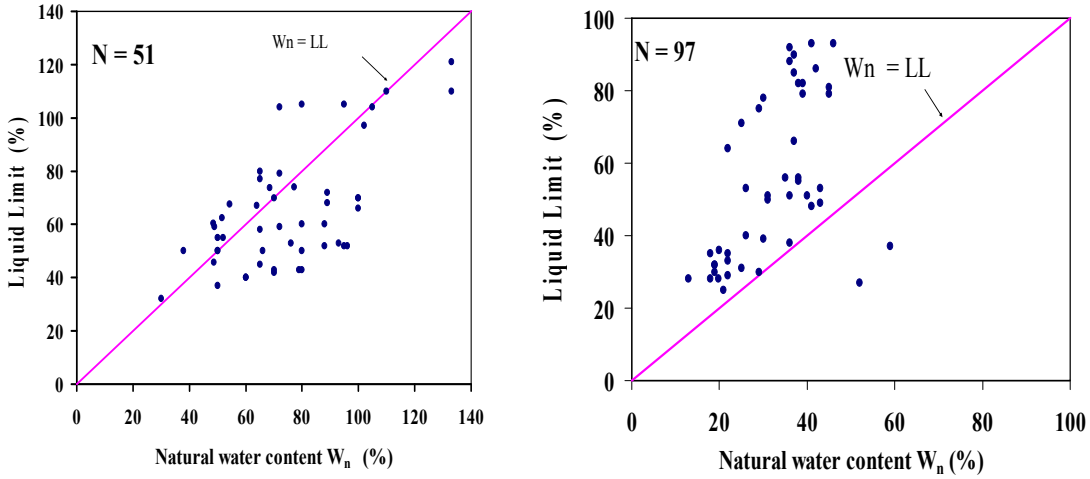

(a) Marine clay **(b) Deltaic clay**

Fig. 2.13. Liquid Limit versus Natural Water Content for the Soft Clays (a) Marine Clay and (b) Deltaic Clay.

(ii) Plasticity Index Chart

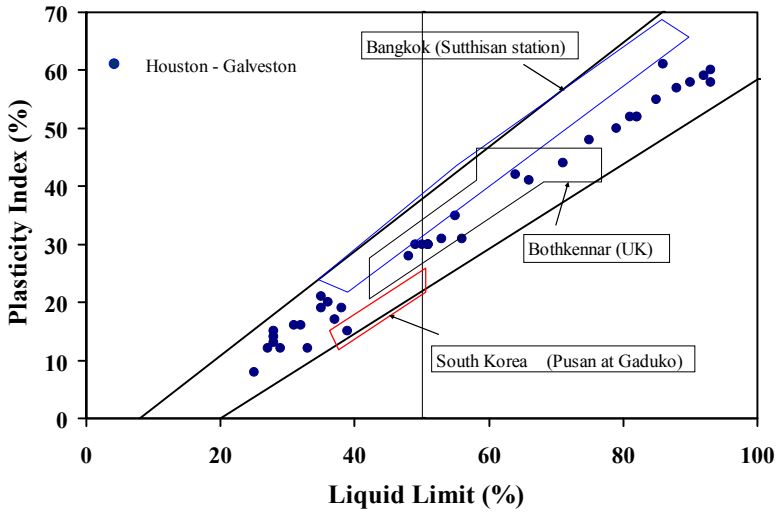

Fig. 2.14. Plasticity Index chart of Deltaic (42 Data Sets) and Marine Soft Clay Soils.

Marine Clay: The Bangkok and Bothkennar (UK) clays were predominantly CH soils, as shown in Fig. 2.14. The Bangkok clay showed greater variation in the index properties than the Bothkennar (UK) clay. The South Korean clay was CL.

Deltaic Clay: Both CH and CL clays are present in the deltaic deposits in the Houston-Galveston area. Compared to the marine clay, the deltaic clays showed the greatest variation in the index properties.

(iii) Undrained Shear Strength versus In-situ Stress

Based on the inspection of the undrained shear strength (S_u) and in-situ vertical stress (σ_v) relationships for the marine clays and deltaic clays (Fig. 2.15 a and b), the

following conditions must be satisfied in developing the mathematical relationship. When

$\sigma_v \geq 0$

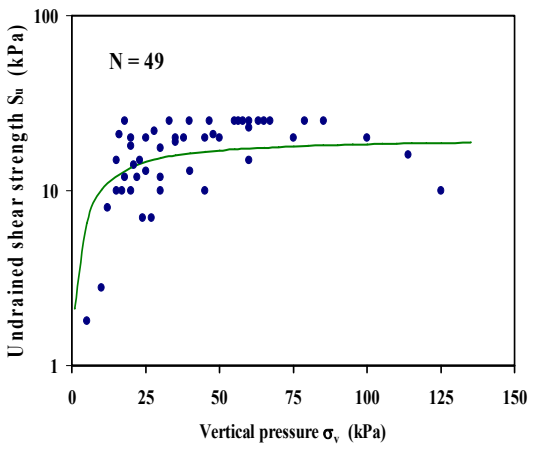

$$\log S_u = \frac{\sigma_v}{2.293 + 0.7677\sigma_v}$$

(a) Marine clay

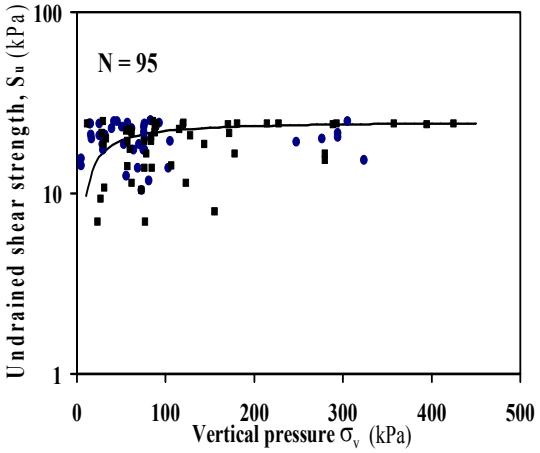

$$\log S_u = \frac{\sigma_v}{2 + 0.7153\sigma_v}$$

(b) Deltaic clay

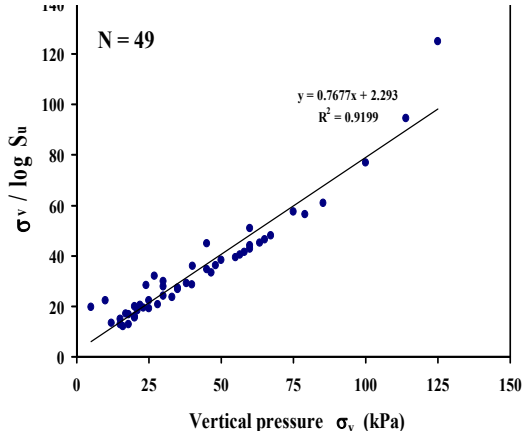

(c) Marine clay

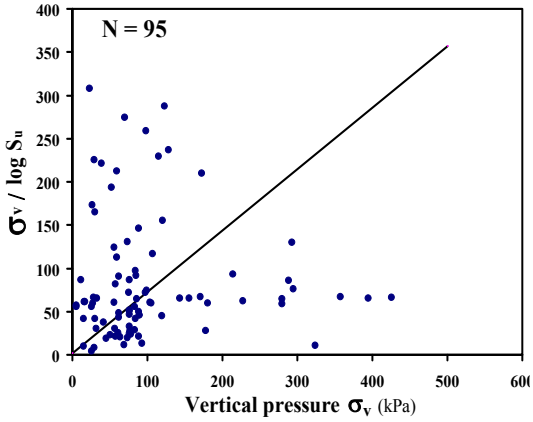

(d) Deltaic clay

Fig. 2.15. Predicted and Measured Relationships for Marine and Deltaic Clays.

$$\frac{d\ log\ S_u}{d\sigma_v} > 0 \qquad \text{2-22a}$$

$$\frac{d^2\ log\ S_u}{d\sigma_v^{\ 2}} < 0 \qquad \text{2-22b}$$

In this study, the soft clay undrained shear strength was limited to 25 kPa even if the vertical stress increased indefinitely.

When $\sigma_v \longrightarrow \infty$, $\dfrac{d\ log\ S_u}{d\sigma_v} = 0$. 2-23

Also, when $\sigma_v \longrightarrow \infty$, $S_u \longrightarrow 25\,kPa.$

One mathematical relationship that will satisfy these conditions is the two-parameter hyperbolic equation, which can be represented as follows

$$log S_u = \frac{\sigma_v}{A + B\sigma_v} \quad . \qquad 2\text{-}24$$

When the vertical overburden stress (σ_v) tends to infinity, the undrained shear stress reaches its theoretical maximum ($\log S_{u\ ult}$), and it will be related to parameter B as follows:

$$logS_{u\ ult} = 1/B \quad \text{with} \quad S_{u\ ult} = 25\ kPa.$$

One way to verify the applicability of Equation 3-4 to the log S_u-vertical stress (σ_v) data is to rearrange the equation to represent a linear relationship as follows:

$$\sigma_v / \log S_u = A + B\ \sigma_v. \qquad 2\text{-}25$$

If the data can be represented by a linear relationship (Equation 2-25) within an acceptable limit (high coefficient of correlation), then it can be stated that the load-displacement relationship is hyperbolic. Parameters A and B can be obtained from the linear relationship. Fig. 2-15 (c) and (d) show the typical plot of $\sigma_v / logS_u$ versus σ_v for the marine and deltaic clays.

Marine Clay: Of the two types of deposits investigated, the hyperbolic relationship better represented the marine clay. The parameters A_M and B_M for the marine clay were 2.293 and 0.7677, respectively, with a coefficient of correlation (R^2) of 0.9199.

Deltaic Clay: The parameters A_D and B_D for the deltaic clay were 2 and 0.7153, respectively.

(iii) Undrained Shear Strength versus Preconsolidation pressure (σ_p)

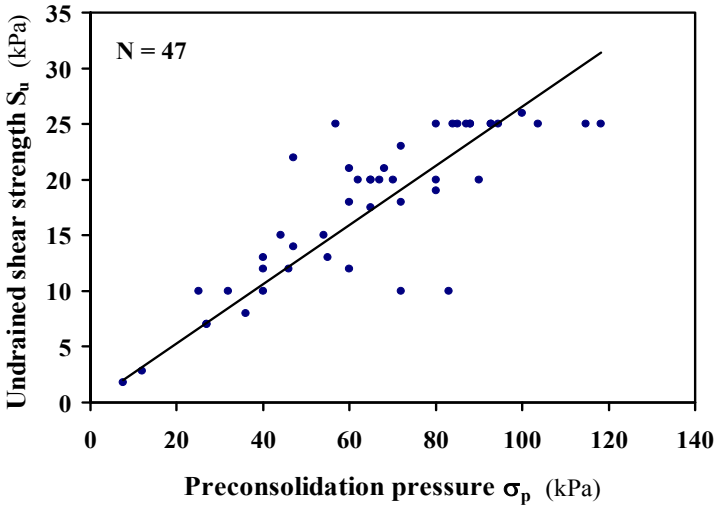

Fig. 2.16. Relationship between Undrained Shear Strength (S_u) and Preconsolidation Pressure (σ_p).

Marine Clay: Based on over 50 data sets collected from the literature, the relation between S_u and σ_p was linear, as presented in the literature. The S_u/σ_p ratio was 0.27, with a coefficient of correlation (R) of 0.82. The S_u/σ_p ratio proposed by Mesri (1988) was 0.22.

2.4.5. Summary and discussion

Based on the literature review and data available in the literature on soft marine and deltaic clays, properties and correlations were investigated. Houston-Galveston area soils are deltaic deposits. Based on the review and analyses of the data collected, the following conclusions can be advanced:

(1) Several analytical methods are available to determine the increase in the in-situ stresses due to the construction of an embankment. In most cases, 1-D consolidation theory was used to predict the total and rate of settlement.

(2) Several test methods are available to determine the consolidation properties of soft clays.

(3) Several mean properties of the marine and deltaic clays have been quantified. The mean physical (moisture content, void ratio) and geotechnical properties (liquid limit, plastic limit) of marine clays were higher than those of the deltaic clays. The mean undrained shear strength of the two deposits was comparable. The natural moisture content of over 52% in the marine clays was higher than the liquid limit, but the trend was reversed for the deltaic clays.

(4) Based on the COV, the marine clay showed greater variation in the natural moisture content (w_n), undrained shear strength (S_u), and void ratio (e_o), compared to the deltaic clay deposit. Similarly, deltaic clay showed greater variation in plasticity limit and plasticity index (limited data), compared to the marine clay.

(5) Based on the COV, the deltaic clay properties had higher values than the marine clay properties, except for the undrained shear strength. It is of interest to note that the natural moisture content and void ratio had similar values for marine and

deltaic deposits. Variation in the properties of the deltaic clays was higher than the marine clays. Also, the probability distribution functions (pdf) for the various properties have been determined. The pdf for the marine and deltaic clays were similar.

3. DESIGN AND ANALYSIS OF HIGHWAY EMBANKMENTS

3.1. Highway Embankments

In the greater Houston area, embankments are used by TxDOT in road construction. As a coastal city, the Houston-Galveston soil formation is deltaic (O'Neill and Yoon 1995): an alternation of clay, silty clay (very soft, soft, medium, and stiff), silt, and sand layers in the top 100 ft, leading to a big scatter in the soil parameters with depth (Vipulanandan et al. 2007). The soft soil below the ground water is considered to be the cause of settlement of heavy structures. Hence four embankments on soft soils were selected for detailed analyses.

Current practice used to estimate the consolidation settlement magnitudes and settlement rates in TxDOT Projects are as follows:

- subsurface investigations to recover undisturbed samples using Shelby tubes
- incremental load (IL) consolidation test in the laboratory
- estimation of the settlements using 1-D consolidation theory, using the soil parameters from the IL consolidation tests.

3.1.1. Locations and clay soil types

All four highway embankments were located in the Houston area, with its deltaic soil formation (Fig. 3.1 and Table 3.1).

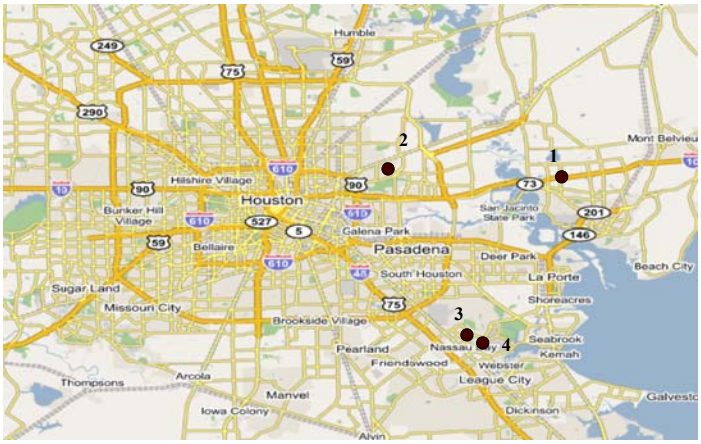

Fig. 3.1. Houston Area with the Selected Four Embankments.

Table 3.1. Summary Information on the Four Selected Embankments.

Sl No	Reference	Status	Location	Average soft clay layer thickness (ft)	S_u (psi)	Embankment Size HxB (ftxft)	Instrumentation	Settlement estimation (in)
1A	TxDOT Project No. 0508-02-101 (2002)	New	IH10 at SH99 Eastside Borings 99-1a & 99-8a	20 to 35	2.85 to 15.15	12 x 120	None	3.19
1B	TxDOT Project No. 0508-02-101 (2002)	New	IH10 at SH99 Westside Boring 99-1a	35	6.15 to 9.05	9 to 24 x 120	None	5.27 to 8.99
2	TxDOT Project No. 0028-02-081 (2006)	New	US 90 at Oates Rd	47.5 to 58.25	-	27.5 to 28 x 220 to 234	None	7.37 to 9.42
3	TxDOT Project No. 0051-03-069 (1993)	Completed in 1993	SH3 Clear Creek	30	3 to 13.8	10.5 x 108	Proposed instrumentation: demec points, inclinometer, piezometer, tensiometer and extensometer	8.50
4	TxDOT Project No. 0981-01-104 (2000)	Completed in 2000	NASA Rd 1: from Annapolis to Taylor Lake	65	2 to 14.5	20 x 60	Proposed instrumentation: piezometer and extensometer	37.87

3.1.2. Objective and analysis

The objective was to review the approaches used in Texas Department of Transportation (TxDOT) projects for embankment settlements and rate of settlement estimation.

3.1.3. Project No 1A (I-10 @ SH99)

At the time of review of the data (August 2006), the project was still not under construction. The designed embankment height was 12 ft, and the base width (W) was 120 ft. The ratio $\frac{H}{W}$ was 0.10. Several borings were done on site to collect the geotechnical information. Two soil samples from one boring (99-1a) were used for the consolidation tests.

- **Field tests**

The Texas Cone Penetrometer (TCP) test was performed at several locations, and the information was used to determine the consistency of the soils. Since TCP tests are performed at 5-ft intervals, the soil consistency thickness can be determined to an accuracy of 5 ft. The variation of blow counts in Boring 99-1a up to 55 ft is shown in Fig. 3.2. Based on Boring 99-1a, the soft clay (CH) layer thickness was about 35 ft deep ($N_{TCP} \leq 20$). The water table was at a depth of 6.5 ft.

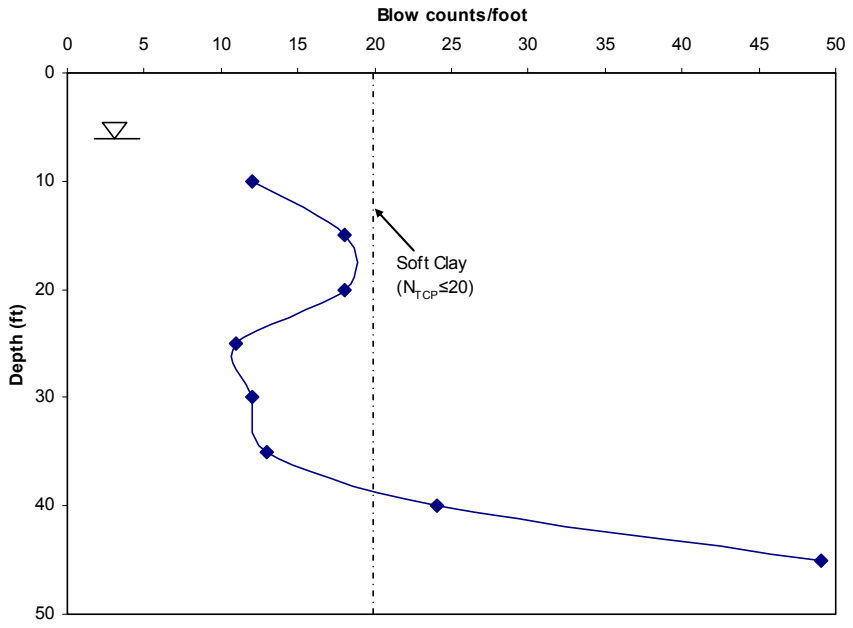

Fig. 3.2. Variation of TCP Blow Counts with Depth (Borehole 99-1a.).

Table 3.2. Laboratory Test and Field Tests Results (Borehole 99-1a).

Depth (ft)	TCP	Soil type	S_u (psi)	LL (%)	PI (%)	MC (%)
5		CH	7.65	53	36	20
10	12	CH	6.15	58	38	25
15	18	CH	3.75	78	54	29
20	18			82		28
25	11	CH	5.35	71	50	27
30	12		9.05	76		26
35	13	CH		63	39	31
40	24			29		25
45	49	CL		44	26	25
50			11.7	54		21
55						21

- **Laboratory tests (Project 1)**

Consolidation (IL), moisture content, Atterberg's limits, and triaxial unconfined compression tests were performed with the soil samples from Boring 99-1a. The test results are summarized in Table 3.2 and Table 3.3.

Soil type: Based on the index property tests (Table 3.2) up to 35 ft was CH clay soil, and below it was CL soil. Also, the moisture content varied from 20% to 30%, as shown in Fig. 3.3(a). The largest change in moisture content was observed at a depth of 35 ft. The change of moisture content with change in depth ($\Delta MC/\Delta z$) versus depth (z) is shown in Fig. 3.3(b), and the values varied from -1.2 to 1. The highest change was observed between 35 and 40 ft (representing a change in moisture content of 6%), and also represented the transition from soft CH to CL clay soil.

The undrained shear strength obtained from the unconfined compression test varied between 3.75 and 9.05 psi in the top 30 ft of soft CH clay, as shown in Fig. 3.4.

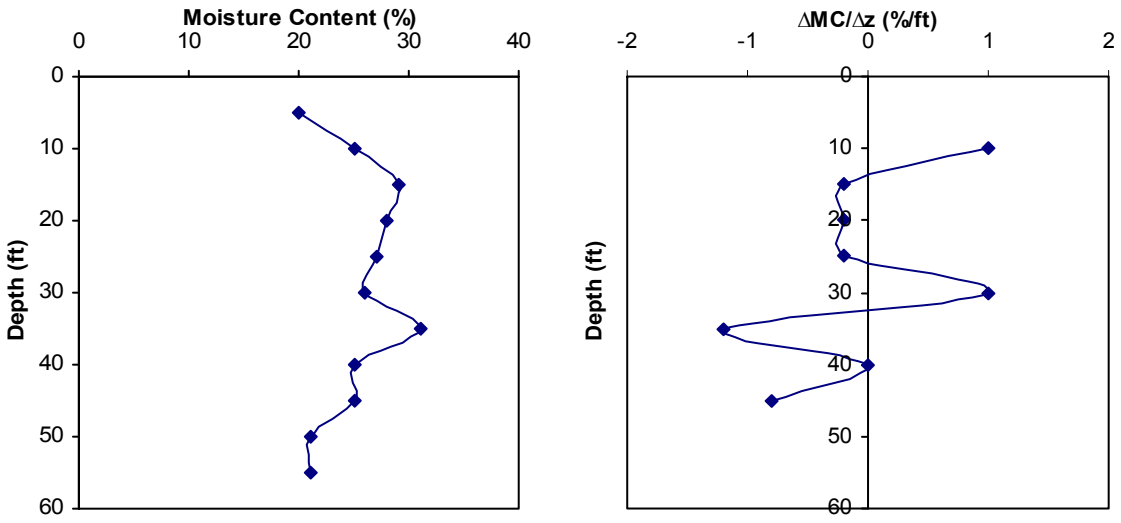

a.) Variation of Moisture Content b.) Change of Moisture Content

Fig. 3.3. (a) Variation of Moisture Content (MC) with Depth (z) and (b) Change of Moisture Content with Change in Depth ($\Delta MC/\Delta z$).

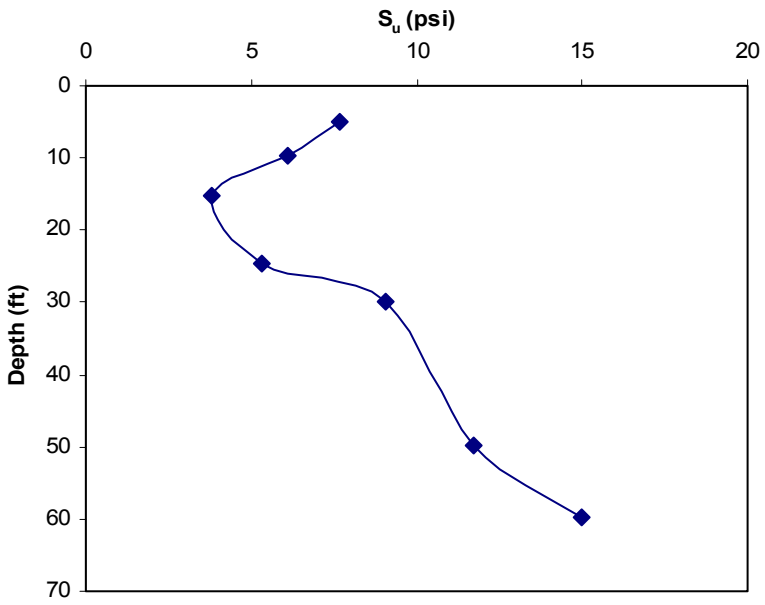

Fig. 3.4. Variation of Undrained Shear Strength with Depth (Borehole 99-1a).

- **Consolidation properties (Project 1)**

The consolidation parameters, summarized in Table 3.3, were obtained from the standard incremental load consolidation test using samples from Boring 99-1a. Two consolidation tests were done on samples collected from depths of 5 ft and 25 ft. Consolidation data obtained from a sample collected at 5 ft depth was used to represent soil to a depth of 19 ft. The data obtained from a sample collected at the 25 ft depth was used to represent soil to a depth of 37 ft.

Table 3.3. Summary of Consolidation Parameters Used for the Settlement Estimation.

Settlement parameters										
TxDOT										
Depth (ft)	Layers height (ft)	C_c	C_r	e_o	$C_{v\ Av}$ (in^2/day)	σ_p (psf)	σ_o (psf)	OCR	$\Delta\sigma$ (psf)	$\sigma_o+\Delta\sigma$ (psf)
1.50	3	0.174	0.06	0.57	1.06	3800	200	19.0	1672	1872
6.50	7	0.174	0.06	0.57	1.06	3800	607	6.3	1650	2257
14.50	9	0.174	0.06	0.57	1.02	3800	1107	3.4	1613	2720
23.50	9	0.180	0.04	0.70	1.02	5000	1671	3.0	1562	3233
32.50	9	0.180	0.04	0.70	1.02	5000	2234	2.2	1597	3831

- **Stress Dependency of Consolidation Parameters (C_c, C_r)**

The stress dependency of the compression and recompression indices was investigated based on the data available. The samples were loaded to 16 tsf and unloaded to 0.25 tsf. The slope (-d*e* /d*log*σ') was determined for each load increment (Fig. 3.5).

For the sample collected at 5 ft (above the ground water table), the compression index, along the loading path, varied from 0.010 to 0.083 when the applied load was increased from 0.25 tsf to 2 tsf and from 0.083 to 0.166 when the applied stress was increased from 2 tsf to 16 tsf. When unloading, the recompression index (C_r) varied from 0.048 to 0.058 when the applied load varied from 4 tsf to 0.25 tsf. The C_r increased with the reduction of the stress (Fig. 3.5(a)). Hence, C_c and C_r are stress dependent parameters.

For the sample collected at 25 ft (below the ground water table), the compression index, along the loading path, varied from 0.0233 to 0.075 when the applied load was increased from 0.25 tsf to 2.5 tsf and from 0.075 to 0.179 when the applied stress was increased from 2.5 tsf to 16 tsf. When unloading, the recompression index (C_r) varied from 0.0068 to 0.045 when the applied load varied from 4 tsf to 0.25 tsf. The C_r

decreased with the reduction of the stress after reaching a peak value of 0.08 (Fig. 3.5(a)). Hence, C_c and C_r are stress dependent parameters.

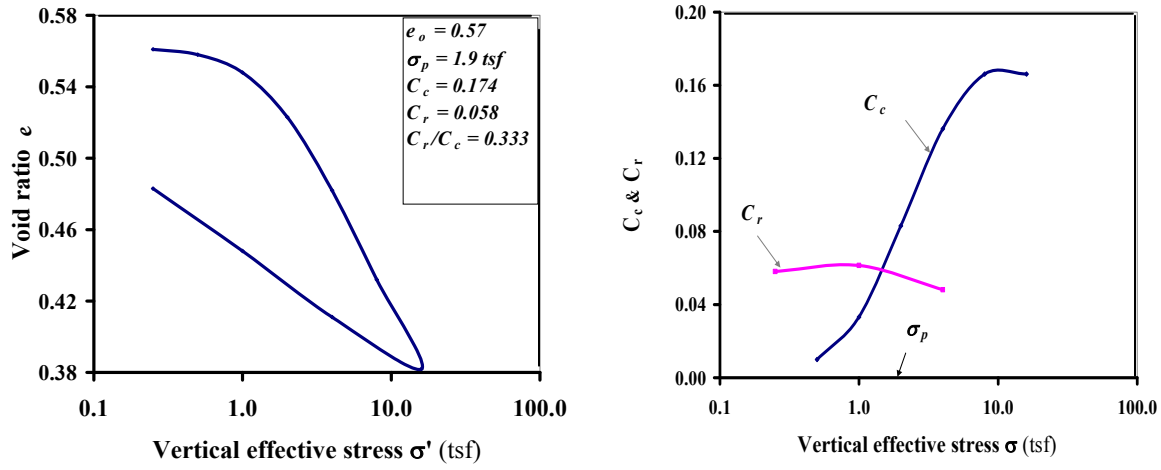

a.) IH10 at SH99 Boring 99-1a at 5ft

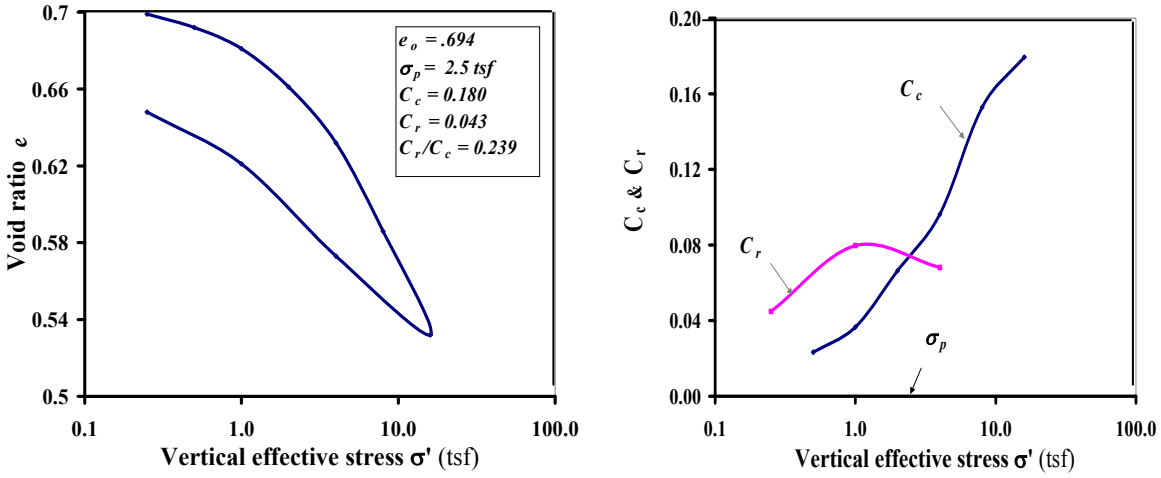

d.) IH10 at SH99 Boring 99-1a at 25ft

Fig. 3.5. e – log σ' of the Two Consolidation Tests Performed on TxDOT Project for 1A Embankment Design and Their Respective Compression and Recompression Index versus log σ' Curves (Project 1: I-10 @ SH-99).

- **Stress Increase due to embankment loading**

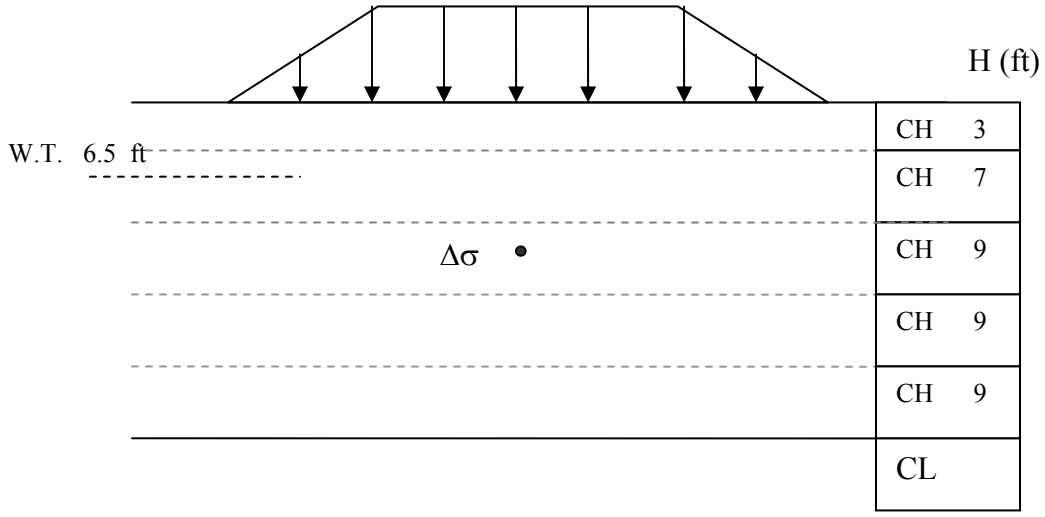

Fig. 3.6. Profile of the Soil Layers for Settlement Calculation (Project 1).

The stress increase in the soil mass due to the embankment loading ($\Delta\sigma$), (Fig. 3.6), calculated in the TxDOT project, is compared with values obtained using the Osterberg method and 2:1 method, in Table 3.4 and Fig. 3.7.

Table 3.4. Summary Table of the Stress Increase in the Soil Mass (Project 1).

TxDOT								Osterberg method		2 : 1 method	
Depth (ft)	Depth (ft)	Layers height (ft)	σ_p (psf)	σ_o (psf)	OCR	$\Delta\sigma$ (psf)	$\sigma_o+\Delta\sigma$ (psf)	$\Delta\sigma$ (psf)	$\sigma_o+\Delta\sigma$ (psf)	$\Delta\sigma$ (psf)	$\sigma_o+\Delta\sigma$ (psf)
1.50	1.50	3	3800	200	19.0	1672	1872	1680	1880	1659	1859
6.50	6.50	7	3800	607	6.3	1650	2257	1680	2287	1594	2201
14.50	14.50	9	3800	1107	3.4	1613	2720	1667	2774	1499	2606
23.50	23.50	9	5000	1671	3.0	1562	3233	1631	3302	1405	3076
32.50	32.50	9	5000	2234	2.2	1597	3831	1573	3807	1322	3556

As shown in Fig. 3.7, the stress increase ratio based on TxDOT project approach to the Osterberg method ranged from 1 to 0.96. But the ratio obtained using the 2:1 method ranged from 1.01 to 1.21. The method used in the TxDOT project, which was

specified as Modified Boussinessq method, was very similar to the Osterberg stress increase calculation method.

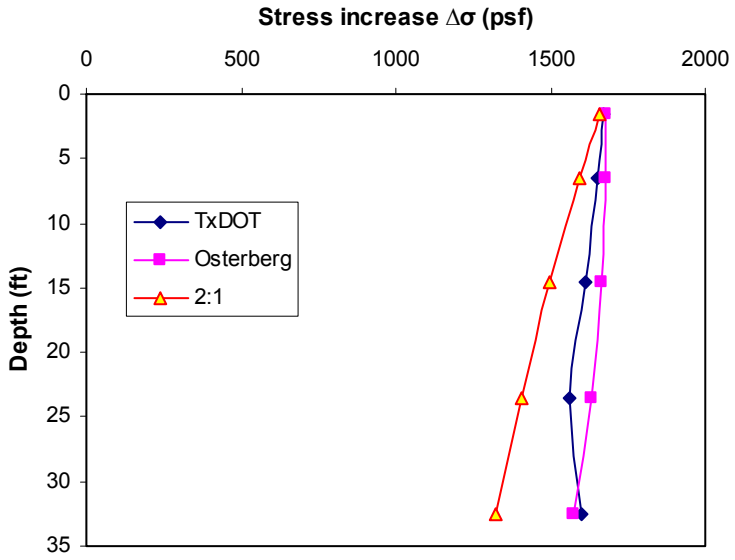

Fig. 3.7. Comparison of Stress Increase Obtained Using the Osterberg, 2:1, and TxDOT Methods (Project 1).

- **Total settlement (Project 1)**

Based on the information provided, the settlement estimation by the TxDOT project approach was 6.10 in. for the total primary settlement.

UH Check: In all the layers, the total stress ($\Delta\sigma$' + σ'_o) was less than the preconsolidation pressure (σ_p). Therefore, the recompression index (C_r) was the governing parameter for the total primary settlement S_p:

$$S_p = \frac{CrH}{1+e_0} log\left(\frac{\sigma_0' + \Delta\sigma'}{\sigma_0}\right).$$

Using Osterberg's stress increase results (Table 3.4), the following result was obtained:

Layer 1: $S_p = \frac{0.06x3}{1+0.57} log\left(\frac{1880}{200}\right) = 0.1116\ ft$

Layer 2: $S_p = \frac{0.06x7}{1+0.57} log\left(\frac{2287}{607}\right) = 0.1541\ ft$

Layer 3: $S_p = \frac{0.06x9}{1+0.57} log\left(\frac{2774}{1107}\right) = 0.1372\ ft$

Layer 4: $S_p = \frac{0.04x9}{1+0.70} log\left(\frac{3302}{1671}\right) = 0.0626\ ft$

Layer 5: $S_p = \frac{0.04x9}{1+0.70} log\left(\frac{3807}{2234}\right) = 0.0490\ ft$.

Hence the total primary settlement was

Sp = 0.1116 + 0.1541+ 0.1372 + 0.0626 + 0.0490 = 0.5145 ft = 6.17 in.

The difference between the UH and TxDOT project estimations was 0.07 in. It must be noted that for the consolidation parameters defined in Chapter 4 (C_{r1}, C_{r2}, and C_{r3}), C_{r3} was used in the calculation instead of C_{r1} since no other data were available.

- **Rate of settlement (Project 1)**

  TxDOT Project Approach

The TxDOT rate of settlement estimation in the TxDOT project, using C_v values in Table 3.3, predicted a settlement of 4.24 in. after 48 months, which represented 69.47% of the total primary settlement (6.10 in.). This result was obtained by considering the following drainage condition for each layer:

- Layer 1 had two drainage surfaces: top and bottom boundaries
- Layer 2 had two drainage surfaces: top and bottom boundaries

- Layer 3 had one drainage surface: top or bottom boundaries
- Layer 4 had one drainage surface: top or bottom boundaries
- Layer 5 had two drainage surfaces: top and bottom boundaries.

The rate of settlement was then calculated for each layer, and for a specific time (48 months in this case) the total settlement was the sum of the settlements of all layers.

(a) Calculations

48 months = 48 x 30 days

The time factor as defined in Chapter 2 is given by

$$T_v = \frac{c_v t}{H_{dr}^2} \quad . \qquad 2\text{-}13$$

The average degree of consolidation is given by the following equation (Das 2006)

$$\frac{U\%}{100} = \frac{(4T_v/\pi)^{0.5}}{\left[1+(4T_v/\pi)^{2.8}\right]^{0.179}} \quad . \qquad 3\text{-}1$$

Hence if T_v is determined, the degree of consolidation (U%) can be calculated using Equation (3-1)

Layer 1; $T_v = \frac{1.06(48x30)}{(1.5x12)^2} = 4.71 \longrightarrow$ U% = 99.67

Layer 2; $T_v = \frac{1.06(48x30)}{(3.5x12)^2} = 0.865 \longrightarrow$ U% = 90.34

Layer 3; $T_v = \frac{1.02(48x30)}{(9x12)^2} = 0.126 \longrightarrow$ U% = 40.01

Layer 4; $T_v = \frac{1.02(48x30)}{(9x12)^2} = 0.126 \longrightarrow$ U% = 40.01

Layer 5; $T_v = \frac{1.02(48x30)}{(4.5x12)^2} = 0.504 \longrightarrow$ U% = 76.55

Consequently the total settlement S_{p48} after 48 months was

S_{p48} = (0.9967 x 0.1116) + (0.9034 x 0.1541) + (0.1372 x 0.4001) + (0.0626 x 0.4001) + (0.0490 x 0.7655)

= 0.3677 ft

= 4.41 in.

The difference of 0.17 in. as compared to the TxDOT result (4.24 in.) could be due to the approximation of the average degree of consolidation (U%).

One layer consideration

Method 1

Considering two drainages surfaces (top and bottom), the primary settlement reached after 48 months was calculated using the following procedure:

Weighted average of the coefficient of consolidation

$$C_v = \frac{\sum C_{vi} H_i}{\sum H_i} = \frac{(12x10x1.06) + (12x27x1.02)}{12x37} = 1.031\ in^2 / day$$

$$T_v = \frac{c_v t}{H_{dr}^2} = \frac{1.031(48x30)}{(18.5x12)^2} = 0.0301 \longrightarrow U\% = 19.58.$$

S_{p48} = 0.1958 x 6.17 = 1.21 in.

Based on this approach, the settlement after 48 months will be 1.21 in., representing 20% of the total primary settlement.

Method 2

Considering two drainages surfaces (top and bottom), the necessary time to reach 69.47% of primary settlement was calculated using the following procedure.

Weighted average of the coefficient of consolidation

$$C_v = \frac{\sum C_{vi} H_i}{\sum H_i} = \frac{(12x10x1.06)+(12x27x1.02)}{12x37} = 1.031\ in^2\ /\ day$$

$$T_v = \frac{(\pi/4)(U\%/100)^2}{\left[1-(U\%/100)^{5.6}\right]^{0.357}} \qquad 3\text{-}2$$

With U% = 69.47%, Tv = 0.398

$$t = \frac{T_v H_{dr}^2}{C_v} = \frac{0.398(18.5x12)^2}{1.031} = 19{,}025\ day$$

= 634 months = 53 years.

Hence the time taken for consolidation of 69.47% was 634 months, which was more than 13 times the 48 months estimated by the TxDOT project approach and the results are compared in Fig. 3.8.

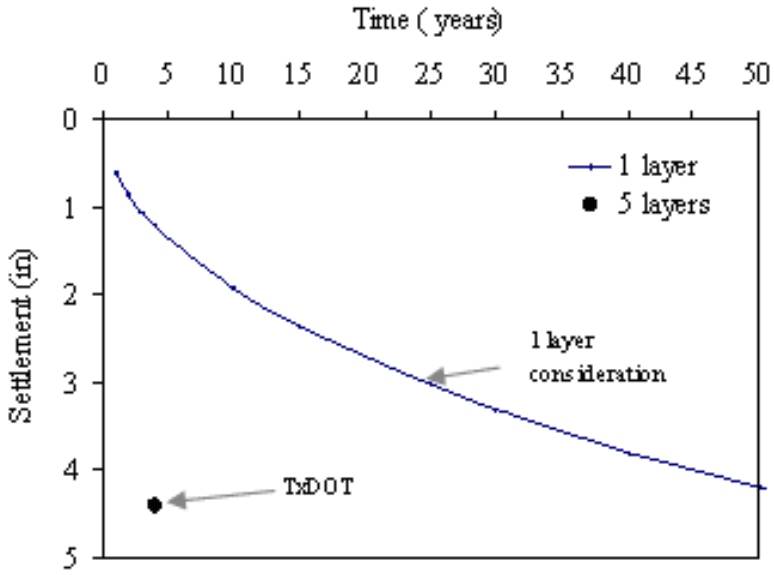

Fig. 3.8. Comparison of the Rate of Settlement by Various Methods of Estimation.

Comments on the settlement prediction (Project 1)

- All the predictions are based on two consolidation tests. These two tests are representing 37 ft of soil. The number of tests is not representative of the variability in deltaic soil deposits. At least one consolidation test should be done every 6 ft of depth to better estimate the consolidation properties.
- The method used to estimate the stress increase was similar to the Osterberg method.
- Since the applied load on the soft soil was less than the preconsolidation pressure, the slope of the unloading section of the e –logσ' curve (C_r) was used for estimating the settlement. It must be noted that the recompression index varied with the applied stress.
- The method used in the TxDOT project had layers of soft soils to estimate the time of settlement. This approach underestimated the time of settlement and is

not correct (based on theory) because of the assumed drainage condition for each layer.

3.1.4. Project No 2 (US 90 @ Oates Road)

At the time of review of the data (August 2006), the project was still not under construction. The designed embankment height (H) was 22.7 ft and the base width (W) was 220 ft. The ratio $\frac{H}{W}$ was 0.125. Four borings were taken up to a depth of 80 ft to collect the geotechnical information. Four samples were used for the consolidation tests.

- **Field tests (Project 2)**

The Texas Cone Penetrometer (TCP) test was performed at several locations to determine the soil layers' strength and to identify the soft soil (Tables 3.5 through 3.8). TCP tests were performed at 5-ft intervals; consequently, the soil consistency thickness was determined to an accuracy of 5 ft. The variations of blow counts in these borings (O-1, O-4, O-5 and O-6) are shown in Fig. 3.9. Based on the TCP blow count, the soft clay layer thickness was about 30 ft deep (TCP $\leq$ 20). The water table was located at a depth of 15 ft (Fig. 3.9).

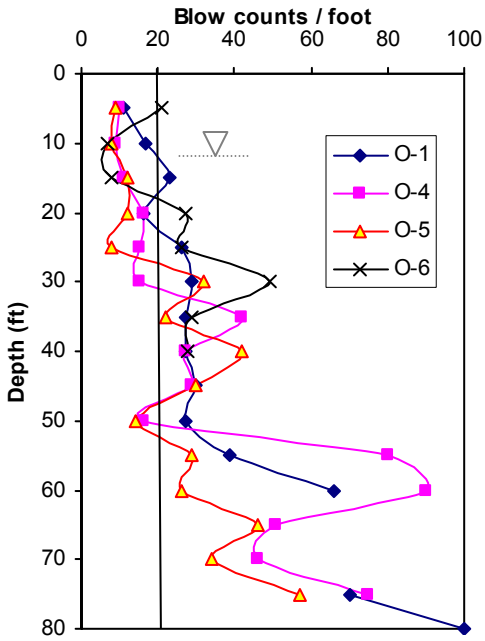

Fig. 3.9. Variation of TCP Blow Counts with Depth (Project 2).

Table 3.5. Laboratory and Field Tests Results (Boring O-1) (Project 2).

Depth (ft)	TCP	Type	S_u (psi)	LL (%)	PI (%)	MC (%)
5	11	CH	12.30	60	42	18
10	17	CL	6.15			21
15	23	CL	3.75	32		22
20	16	CL	14.88			23
25	26	CL	18.95	45	31	17
30	29	CH	10.90	67	42	28
35	27	CH	12.30			26
40	27	CH	17.05			27
45	30	CH	9.75			35
50	27	CH		83		34
55	39	CL	11.00	33		21
60	66	CL				16
65		CL	34.10			16
70		SAND				
75	70	SAND				
80	100					

Table 3.6. Laboratory and Field Tests Results (Boring O-4) (Project 2).

Depth (ft)	TCP	Type	S_u (psi)	LL (%)	PI (%)	MC (%)
5	10	CH	6.90	69	51	20
10	9	CL	2.90			
15	11	CL		27		19
20	16	CL	8.35			19
25	15	CL	8.20	27		17
30	15	CH	19.85			17
35	42	CH	14.75			25
40	27	CH	10.65	70	47	29
45	29	CH				27
50	16	CL	8.90	33		19
55	80	SC				21
60	90	CL	27.95	45	30	18
65	51	CL	22.90	38		17
70	46	CL		22		19
75	75	CL		19		22
80						

Table 3.7. Laboratory and Field Tests Results (Boring O-5) (Project 2).

Depth (ft)	TCP	Type	S_u (psi)	LL (%)	PI (%)	MC (%)
0		CL				
5	9	CH	7.00			22
10	8	CH	4.10			26
15	12	CL	5.63	45		23
20	12	CL	6.65			19
25	8	CL	9.25	23		19
30	32	CL				14
35	22	CL	11.73			22
40	42	CH	25.70			18
45	30	CH	23.33	75	49	26
50	14	CH		81		31
55	29	CH	14.45	80		31
60	26	CH	18.85	81	54	33
65	46	SC		22	7	21
70	34	SC				18
75	57	CH		60		25
80						

Table 3.8. Laboratory and Field Tests Results (Boring O-6) (Project 2).

Depth (ft)	TCP	Type	S_u (psi)	LL (%)	PI (%)	MC (%)
5	21	CH	7.50	64		23
10	7	CH	2.85			28
15	8	CH	4.65	52		29
20	27	CL	13.30	39	24	24
25	26	CL	12.65	25		28
30	39	CL		40	26	21
35	29	CL	11.00	37		17
40	28	CH	13.30	64		23

- **Laboratory tests**

Incremental load consolidation, moisture content, Atterberg's limits, and triaxial unconfined compression tests were performed with the samples from the four borings. The results are summarized in (Tables 3.5 through 3.9).

Soil type: Based on the index property tests, the top 5 to 25 ft was mainly CL clay over a 25 ft-deep layer of CH clay. Also, the moisture content variation shown in Fig. 3.10(a) fluctuated between 15 and 35%. The largest change in moisture content was observed at a depth of 55 ft in Boring O-1. The change in moisture content with change in depth ($\Delta MC/\Delta z$) versus depth (z), (Fig. 3.10(b)) values ranged from -2.7 to 2.1, with the highest change between 50 and 55 ft in Boring O-1, representing a change in moisture content of -13%, and was the transition from CH to CL clay soil.

The undrained shear strength obtained from the unconfined compression test varied between 2.90 and 25.70 psi in the top 50 ft of clay soil, as shown in Fig. 3.11.

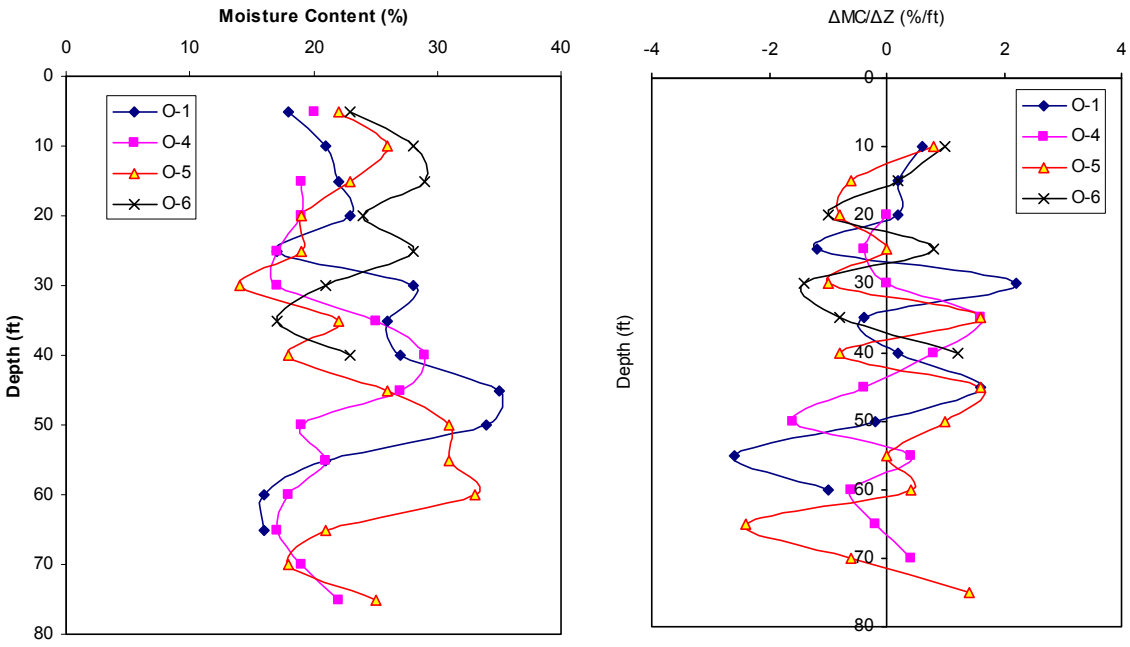

a.) Variation of Moisture Content

b.) Change of Moisture Content

Fig. 3.10. (a) Variation of Moisture Content (MC) with Depth (z) and (b) Change of Moisture Content with Change in Depth (ΔMC/Δz) (Project 2).

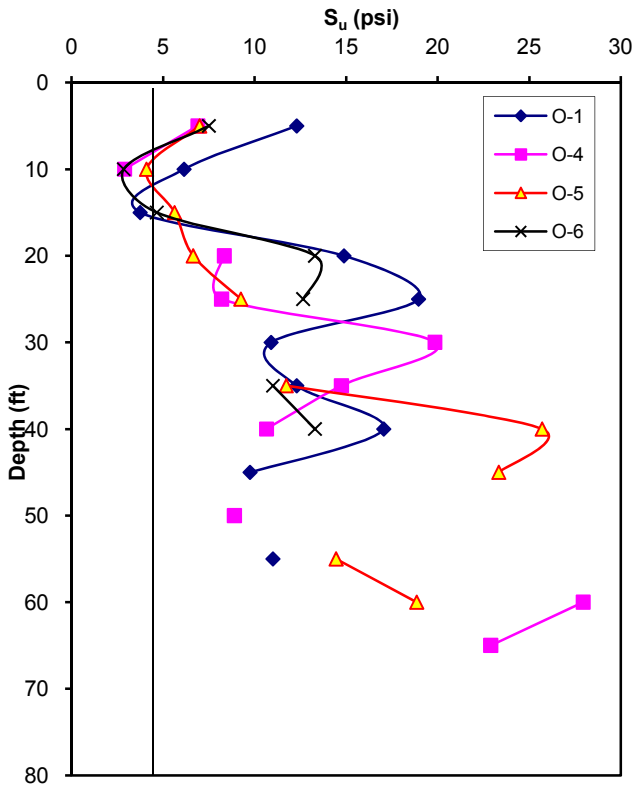

Fig. 3.11. Variation of Undrained Shear Strength with Depth (from the Four Borings) (Project 2).

Table 3.9. Summary Table of Consolidation Parameters Used for the Settlement Estimation (Project 2).

Settlement parameters										
TxDOT										
Depth (ft)	Layers height (ft)	C_c	C_r	e_o	$C_{v\ Av}$ (in^2/day)	σ_p (psf)	σ_o (psf)	OCR	$\Delta\sigma$ (psf)	$\sigma_o + \Delta\sigma$ (psf)
2.5	5.0	0.279	0.021	0.75	0.5	4600	313	14.7	3540	3853
7.5	5.0	0.202	0.021	0.68	1.6	3400	938	3.6	3540	4478
12.5	5.0	0.202	0.021	0.68	1.6	3400	1407	2.4	3538	4945
18.8	7.5	0.138	0.008	0.69	1.0	4400	1798	2.4	3533	5331
26.3	7.5	0.138	0.008	0.69	1.0	4400	2267	1.9	3521	5788
33.5	7.0	0.155	0.036	0.56	0.7	6600	2721	2.4	3502	6223
40.5	7.0	0.155	0.036	0.56	0.7	6600	3159	2.1	3476	6635
47.5	7.0	0.155	0.036	0.56	0.7	6600	3598	1.8	3442	7040

- **Consolidation properties (Project 2)**

The consolidation parameters, summarized in Table 3.9, were determined from the standard incremental load consolidation test using the samples from the borings. A total of four IL consolidation tests were performed.

- **Stress Dependency Phenomena (C_c, C_r)**

The e – log σ' of the four consolidation tests were not available to study the stress dependency of compression (C_c) and recompression (C_r) indices.

- **Stress Increase due to embankment loading (Project 2)**

The stress increase in the soil mass due to the embankment loading (Δσ), calculated by TxDOT project approach, (Fig. 3.12), is compared with values obtained using the Osterberg and 2:1 methods, as shown in Table 3.10 and Fig. 3.13.

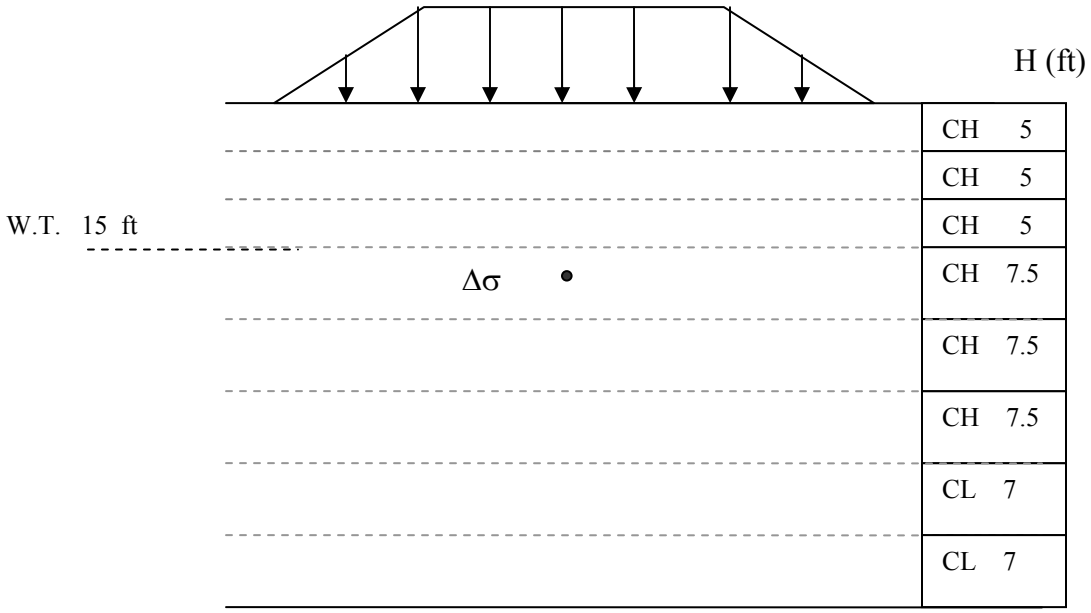

Fig. 3.12. Profile of the Soil Layers for Settlement Calculation (Project 2).

Table 3.10. Summary Table of the Stress Increase in the Soil Mass.

TxDOT							Osterberg method		2 to 1 method	
Depth (ft)	Layers height (ft)	σ_p (psf)	σ_o (psf)	OCR	$\Delta\sigma$ (psf)	$\sigma_o+\Delta\sigma$ (psf)	$\Delta\sigma$ (psf)	$\sigma_o+\Delta\sigma$ (psf)	$\Delta\sigma$ (psf)	$\sigma_o+\Delta\sigma$ (psf)
2.5	5.0	4600	313	14.7	3540	3853	3540	3853	3500	3813
7.5	5.0	3400	938	3.6	3540	4478	3538	4476	3423	4361
12.5	5.0	3400	1407	2.4	3538	4945	3526	4933	3350	4757
18.8	7.5	4400	1798	2.4	3533	5331	3493	5291	3262	5060
26.3	7.5	4400	2267	1.9	3521	5788	3429	5696	3163	5430
33.5	7.0	6600	2721	2.4	3502	6223	3347	6068	3072	5793
40.5	7.0	6600	3159	2.1	3476	6635	3256	6415	2990	6149
47.5	7.0	6600	3598	1.8	3442	7040	3162	6760	2911	6509

As observed in Fig. 3.13, the TxDOT project approach stress increase values were higher than the Osterberg and 2:1 methods. The ratio of the TxDOT project approach values to the Osterberg's values ranged from 1 to 1.09, and the ratio obtained with the 2:1 method ranged from 1.01 to 1.18. The TxDOT project approach, which was specified as the Modified Boussinessq method, was closer to the Osterberg stress increase calculation method.

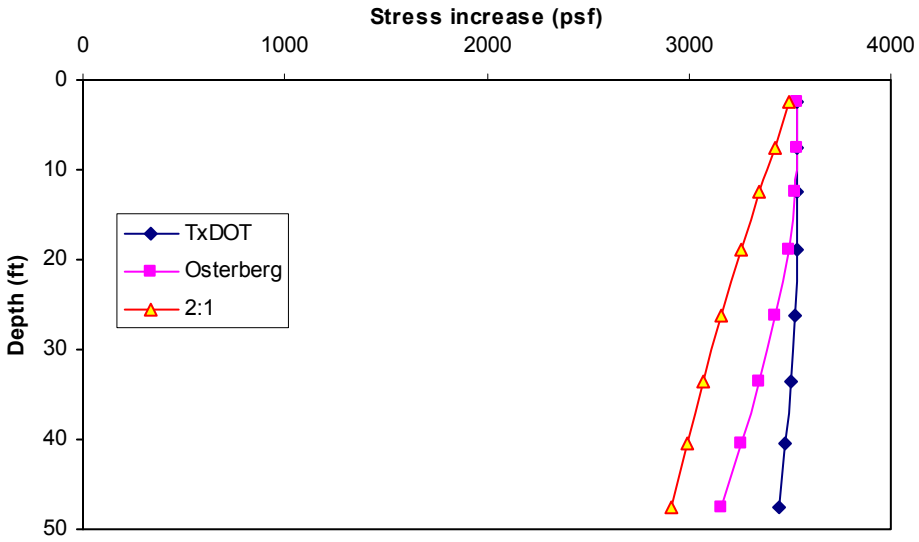

Fig. 3.13. Comparison of Stress Increase Obtained Using Osterberg and 2:1 and TxDOT Methods.

- **Total settlement (Project 2)**

Based on the TxDOT project approach settlement estimation was 7.13 in. for the total primary settlement.

UH Check: In five layers out of eight, the total effective stress ($\Delta\sigma' + \sigma'_o$) was higher than the preconsolidation pressure (Table 3.10). Therefore, the compression (C_c) and recompression index (C_r) were both the governing parameters of the total primary settlement S_p,

$$S_p = \frac{C_r H}{1+e_0} log\left(\frac{\sigma_p}{\sigma_0'}\right) + \frac{C_c H}{1+e_0} log\left(\frac{\sigma_0' + \Delta\sigma'}{\sigma_p}\right).$$

Using Osterberg's stress increase results (Table 3.10), we obtained the following results:

Layer 1: $S_p = \frac{0.021x5}{1+0.75} log\left(\frac{3853}{313}\right) = 0.0654\ ft$

Layer 2: $S_p = \frac{0.021x5}{1+0.68} log\left(\frac{3400}{938}\right) + \frac{0.202x5}{1+0.68} log\left(\frac{4476}{3400}\right) = 0.1067\ ft$

Layer 3: $S_p = \frac{0.021x5}{1+0.68}log\left(\frac{3400}{1407}\right) + \frac{0.202x5}{1+0.68}log\left(\frac{4933}{3400}\right) = 0.1211\,ft$

Layer 4: $S_p = \frac{0.008x7.5}{1+0.69}log\left(\frac{4400}{1798}\right) + \frac{0.138x7.5}{1+0.69}log\left(\frac{5291}{4400}\right) = 0.0628\,ft$

Layer 5: $S_p = \frac{0.008x7.5}{1+0.69}log\left(\frac{4400}{2267}\right) + \frac{0.138x7.5}{1+0.69}log\left(\frac{5696}{4400}\right) = 0.0789\,ft$

Layer 6: $S_p = \frac{0.036x7}{1+0.56}log\left(\frac{6068}{2721}\right) = 0.0563\,ft$

Layer 7: $S_p = \frac{0.036x7}{1+0.56}log\left(\frac{6415}{3159}\right) = 0.0497\,ft$

Layer 8: $S_p = \frac{0.036x7}{1+0.56}\log\left(\frac{6600}{3598}\right) + \frac{0.155x7}{1+0.56}\log\left(\frac{6760}{6600}\right) = 0.0498\,ft$.

Hence the total primary settlement was

Sp = 0.0654 + 0.1067 + 0.1211 + 0.0628 + 0.0789 + 0.0563 + 0.0497 + 0.0498

= 0.5907 ft = 7.09 in.

The difference between the UH and TxDOT project approach estimations was 0.04 in. It must be noted that since the e – log σ' of the consolidation tests were not available, the types of recompression indices (C_{r1}, C_{r2}, C_{r3}) (Refer Section 4.6.1) used were not known.

- **Rate of settlement (Project 2)**

  TxDOT Project Approach

TxDOT project approach rate of settlement estimation, using the C_v values in Table 3.9, predicted a settlement of 6.63 in. after 120 months which represented over

90% of the total primary settlement (7.13 in.). This result was obtained by considering two drainage surfaces (top and bottom) for each layer.

The rate of settlement was then calculated for each layer, and for a specific time (120 months in this case) the total settlement was the sum of the settlements of all layers.

(a) Calculation

120 months = 120 x 30 = 3600 days

$$T_v = \frac{c_v t}{H_{dr}^2} \qquad 2\text{-}13$$

$$\frac{U\%}{100} = \frac{(4T_v/\pi)^{0.5}}{\left[1+(4T_v/\pi)^{2.8}\right]^{0.179}} \qquad 3\text{-}1$$

Layer 1 $T_v = \frac{0.5(3600)}{(2.5x12)^2} = 2.000 \longrightarrow$ U% = 98.64

Layer 2 $T_v = \frac{1.6(3600)}{(2.5x12)^2} = 6.400 \longrightarrow$ U% = 99.70

Layer 3 $T_v = \frac{1.6(3600)}{(2.5x12)^2} = 6.400 \longrightarrow$ U% = 99.70

Layer 4 $T_v = \frac{1.0(3600)}{(3.75x12)^2} = 1.778 \longrightarrow$ U% = 98.19

Layer 5 $T_v = \frac{1.0(3600)}{(3.75x12)^2} = 1.778 \longrightarrow$ U% = 98.19

Layer 6 $T_v = \frac{0.7(3600)}{(3.5x12)^2} = 1.429 \longrightarrow$ U% = 96.90

Layer 7 $T_v = \frac{0.7(3600)}{(3.5x12)^2} = 1.429 \longrightarrow$ U% = 96.90

Layer 8 $T_v = \frac{0.7(3600)}{(3.5x12)^2} = 1.429 \longrightarrow$ U% = 96.90.

Consequently the total settlement S_{p120} after 120 months was

S_{p120} = (0.9864 x 0.0654) + (0.997 x 0.1067) + (0.997 x 0.1211) + (0.9819 x 0.0628) + (0.9819 x 0.0789) + (0.969 x 0.0563) + (0.969 x 0.0497) + (0.969 x 0.0498) = 0.5817 ft = 6.98 in.

There is a difference of 0.35 in. with the TxDOT result of 6.63 in., which could be partly due to the noted difference in the stress increase and to the approximation of the average degree of consolidation U%.

One layer consideration

Method 1

Considering two drainage surfaces (top and bottom), the settlement primary settlement reached after 120 months can be calculated using the following procedure:

Weighted average of the coefficient of consolidation

$$C_v = \frac{\sum C_{vi} H_i}{\sum H_i} = \frac{(5x0.5)+(10x1.6)+(15x1)+(21.5x0.7)}{51.5} = 0.943\, in^2 / day$$

$$T_v = \frac{c_v t}{H_{dr}^2} = \frac{0.953(3600)}{(25.75x12)^2} = 0.0355 \longrightarrow U\% = 21.28$$

S_{p120} = 0.2128 x 7.09 = 1.51 in.

Based on this approach, the settlement after 120 months will be 1.51 in., representing about 21% of the total primary settlement.

Method 2

Considering two drainage surfaces (top and bottom), the necessary time to reach 90% of primary settlement can be calculated using the following procedure:

Weighted average of the coefficient of consolidation

$$C_v = 0.943\ in^2 / day$$

$$T_v = \frac{(\pi / 4)(U\% / 100)^2}{\left[1 - (U\% / 100)^{5.6}\right]^{0.357}}$$

With U% = 90 %, T_v = 0.848

$$t = \frac{T_v H_{dr}^2}{C_v} = \frac{0.848(25.75x12)^2}{0.943} = 85862\,day = 2862 \text{ months} = 238 \text{ years.}$$

This result of 2,862 months was about 24 times more than the TxDOT prediction of 120 months to reach 90% of the primary settlement (Fig. 3.14).

Comment on the settlement prediction (Project 2)

- All the predictions were based on four consolidation tests. These four tests are representing 51 ft of soil. The number of tests is not representative of the variability in deltaic soil deposits. At least one consolidation test should be done every 6 ft of depth to better estimate the consolidation properties.
- The method used to estimate the stress increase was closer to the Osterberg method. The soft clay soil was overconsolidated and in five layers out of eight the total effective stress was higher than the preconsolidation pressure. Therefore, both the compression and recompression indices are governing parameters of the total primary settlement. The e –logσ' curves of the four

consolidation tests were not available. Consequently, the type of the three recompression indexes used was not known.

- The TxDOT project approach used layers of soft soils to estimate the time of settlement. This approach underestimated the time of settlement and is not correct because of the assumed drainage condition for each layer.

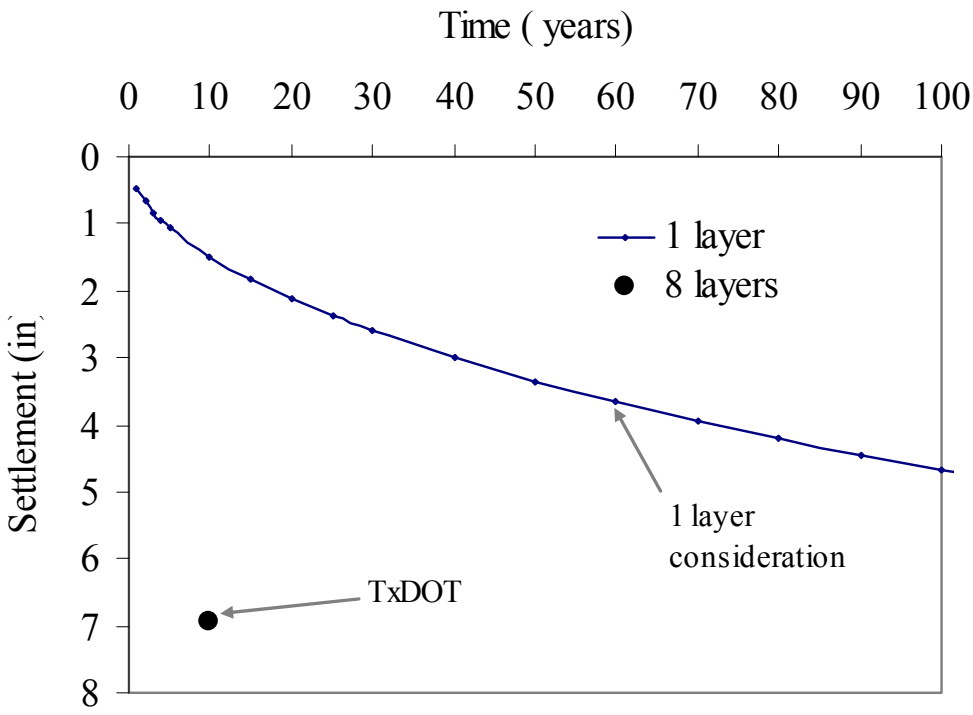

Fig. 3.14. Effect of Layering on the Rate of Settlement (Project 2).

3.1.5. Project No 3 (SH3 @ Clear Creek)

At the time of review of the data (2007), the highway embankment had been in service for 14 years. The designed embankment height varied from 7.81 to 8.92 ft, and the base width (W) was 108 ft (Fig. 3.15). The ratio $\frac{H}{W}$ varied then from 0.07 to 0.08. About 20 borings were taken on site to collect the geotechnical information from 1965 through 1991 for construction, widening, and modification of the road as follows:

- Through September and October 1965, seven borings (M-1, M-2, M-3, R-1, R-2, M-12, and R-13) were completed to a 100 ft depth to widen the roadway and to construct the bridges over Clear Creek and Clear Creek Relief. The construction work was completed in 1971.
- During February, March, and September of 1984, seven new borings (CCB-1, CCB-2, CCB-3, CCR-1, CCR-2, CCR-3 and CCR-4) were completed to a 60 ft depth to widen and elevate the North Bridge (NB) roadway, to remove and replace the NB bridges over Clear Creek and Clear Creek Relief, and to construct the retaining walls at NB roadway and bridge approaches.
- One boring (CCR-5) was completed to a 75 ft depth in November 1991 for the removal and replacement of the South Bridge (SB) and construction of retaining walls at SB Clear Creek Relief bridge approaches. The construction work was completed in December 1993 (Fig. 3.16).
- Finally, in January 2007, five borings (B1, B2, B3, B4 and B5) were drilled to a depth of 20 to 30 ft by the University of Houston to assess the embankment settlement and the retaining wall movement.

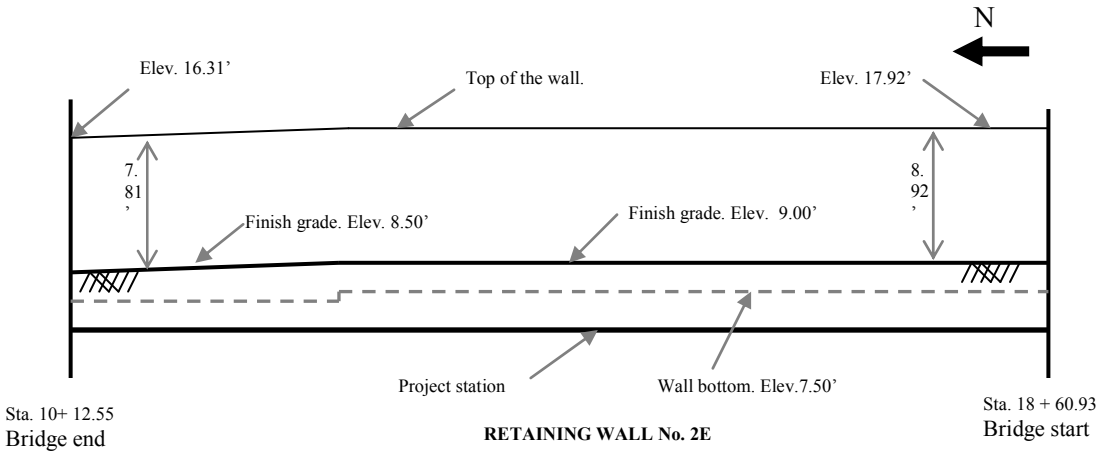

Fig. 3.15. Profile of the Retaining Wall No. 2E, Not to Scale (Project 3 Drawing 22).

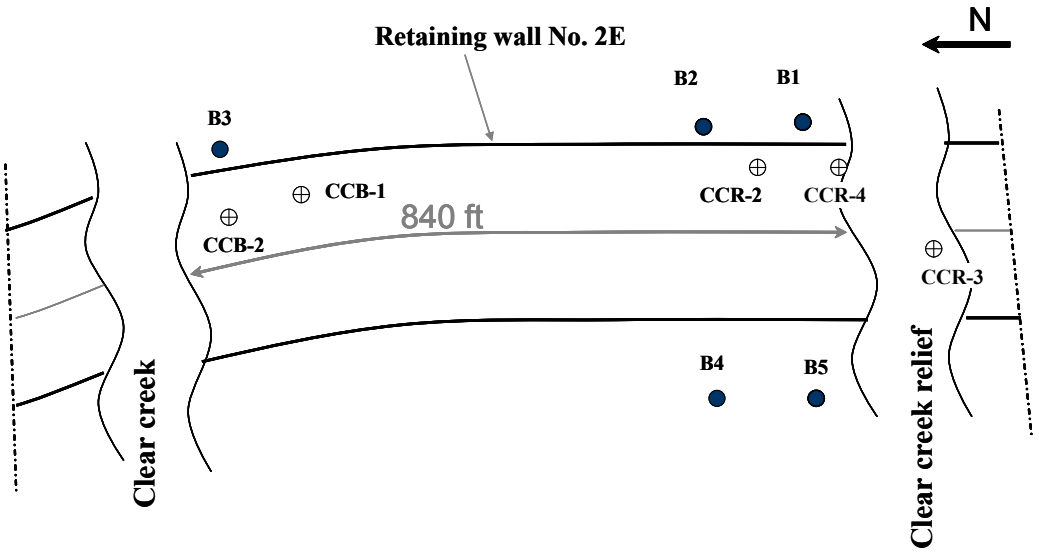

Fig. 3.16. Location of the Borings Used in the Field (Drawings 13 and 14).

- **Field tests (Project 3)**

The Texas Cone Penetrometer (TCP) test was performed at 15 locations, and the information was used to determine the consistency of the soil. Only the Borings CCB-1, CCB-2, CCR-2, CCR-3, and CCR-4 (Fig. 3.16) data were used for the design of the

embankment. Since the TCP tests are performed at 5-ft intervals (Table 3-11), the soil consistency thickness can be determined to an accuracy of 5 ft. The variation of blow counts in the four borings up 40 and 60 ft is shown in Fig. 3.17. Based on the borings, the soft soil layer thickness was about 45 ft deep ($N_{TCP} \leq 20$). In 2007, the average water table was at 6.5 ft below the ground and was fluctuating based on the weather.

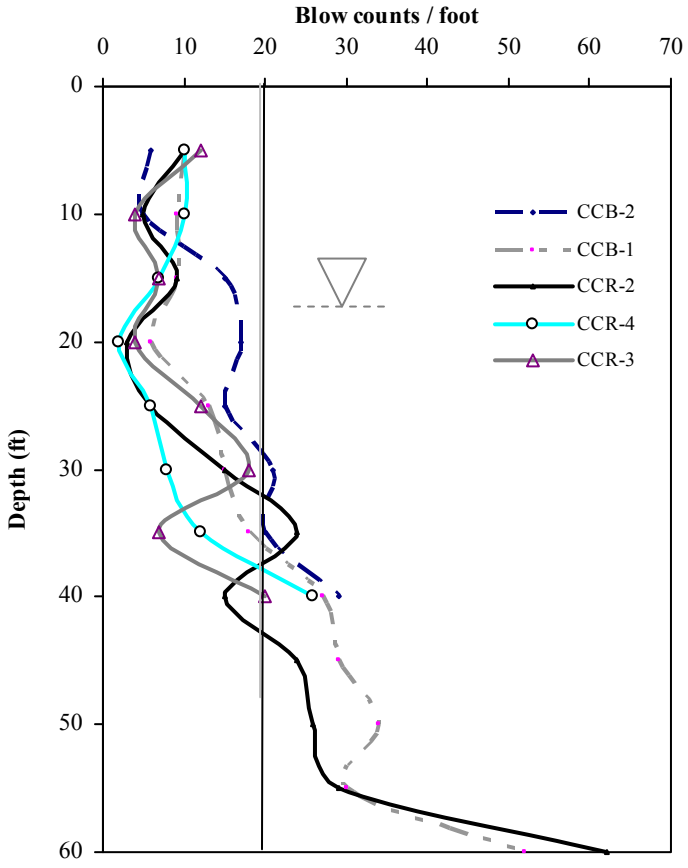

Fig. 3.17. Variation of TCP Blow Counts with Depth (Project 3).

Table 3.11. Field Test Results (Borings CCB-2, CCB-1, CCR-2, CCR-4 and CCR-3).

		TCP blow count				
	Elevation (ft)	12.3	12.2	12.7	11.9	11.8
	Borings	**CCB-2**	**CCB-1**	**CCR-2**	**CCR-4**	**CCR-3**
Boring depth (ft)	5	6	10	10	10	12
	10	5	9	5	10	4
	15	15	9	9	7	7
	20	17	6	3	2	4
	25	15	13	6	6	12
	30	21	15	15	8	18
	35	20	18	24	12	7
	40	29	27	15	26	20
	45		29	24		
	50		34	26		
	55		30	29		
	60		52	62		

- **Laboratory tests (Project 3)**

The Consolidation (IL) tests were performed on three samples from Boring CCR-3 in 1984. The moisture content, Atterberg limits, and triaxial unconfined compression tests were performed with the soil samples from five borings.

Soil type: Based on the index property tests (Table 3.12), the top 5 to 25 ft was CH clay soil and below it was CL soil. Also, the moisture content varied between 18% and 44%, as shown in Fig. 3.18(a). The largest change in moisture content was observed at a depth of 25 ft. The change of moisture content per unit depth ($\Delta MC/\Delta z$) versus depth (z) is shown in Fig. 3.18(b), and the values varied from -11.5 to 6%/ft. The highest change was observed between 25 and 30 ft in boring CCR-4 (representing a total change in moisture content of 23%) and was in the very soft (TCP < 8) CH to CL clay soils.

The undrained shear strength obtained from the unconfined compression test varied between 2 and 6.5 psi in the top 35 ft soft CH clay as shown in Table 3.14 and Fig. 3.19.

Table 3.12. Variation of Soil Types in Five Borings (Project 3).

Soil type				
Depth (ft)	**CCR-1**	**CCR-2**	**CCR-3**	**CCR-4**
5				CH
10			CH	
15	CH	CH		CH
20	CL	CH		CH
25			CH	
30		CL	CL	CH
35				CL
40	CH		CH	SC
45	CH	CL		
50				
55				
60		CH		

Table 3.13. Variation of Moisture Content in the Six Borings (Project 3).

Moisture content						
Depth (ft)	**CCB-2**	**CCB-1**	**CCR-1**	**CCR-2**	**CCR-3**	**CCR-4**
5	22	22		27	25	32
10	27	28		27	30	33
15	29	28.5	28	27	34	33
20		27	20	37	44	33
25	20	23	32	30	23	44
30	21	19	30	24	21	21
35	18	21.5	25	20	22	22
40	29		20	20	32	
45		20	22	23		
50		19	28	23		
55		22.3	18	25		
60		22	24			

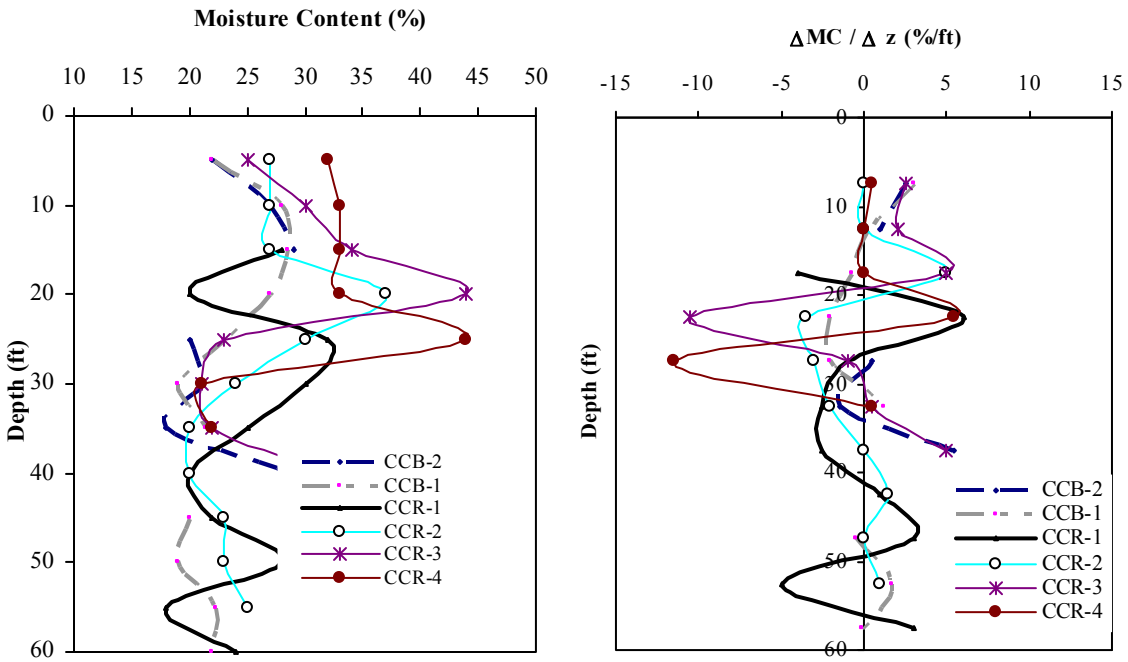

a.) Variation of Moisture Content b.) Change of Moisture gradient

Fig. 3.18. (a) Variation of Moisture Content (MC) with Depth (z) and (b) Change of Moisture Gradient with Depth (ΔMC/Δz) (Project 3).

Table 3.14. Variation of Undrained Shear Strength with Depth in the Six Borings (Project 3).

Undrained shear strength S_u (psi)						
Depth (ft)	**CCB-1**	**CCB-2**	**CCR-1**	**CCR-2**	**CCR-3**	**CCR-4**
5	7	8.5				
10	8.5	2			5	
15	5.8	2.5	7.5	9		5
20	7		7	6		5
25	7.5	3			4	
30	7.7	7.5		3	7	3
35	5.5	6.5				5
40		17.5	12		12	3
45	6.5		15	10		
50	18					
55						
60				17		

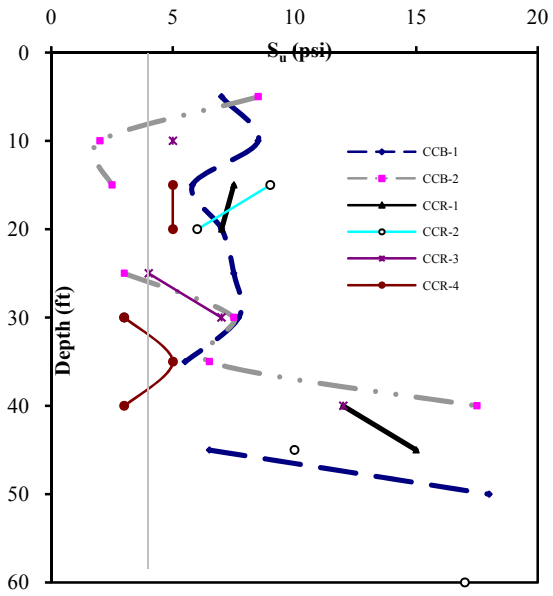

Fig. 3.19. Variation of Undrained Shear Strength with Depth (Project 3).

- **Consolidation properties (Project 3)**

The consolidation parameters, summarized in Table 3.15, were obtained from the standard incremental load consolidation test using samples from Boring CCR-3. Three consolidation tests were performed on samples collected from depth of 14 - 15 ft, 18 - 19 ft, and 23 - 24 ft.

Table 3.15. Consolidation Parameters Used for the Settlement Estimation (Project 3).

Settlement parameters								
Depth (ft)	Layers height (ft)	C_c	C_r	e_o	$C_{v\ Av}$ (in^2/day)	σ_p (psf)	σ_o (psf)	OCR
2.5	5.0	0.199	0.050	0.66	1.128	1500	300	5.0
7.5	5.0	0.199	0.050	0.66	1.128	1500	875	1.7
12.5	5.0	0.199	0.050	0.66	1.128	1500	1188	1.3
18.5	7.0	0.377	0.038	1.06	0.522	2600	1564	1.7
26.0	8.0	0.149	0.012	0.59	1.404	2200	2033	1.1
34.0	8.0	0.149	0.012	0.59	1.404	2200	2534	0.9
42.0	8.0	0.149	0.012	0.59	1.404	2200	3035	0.7

The soil sample from the 14 - 15 ft depth had a void ratio (e_0) of 0.66 and an average compression (C_c) and recompression indices (C_r) of 0.199 and 0.050, respectively, with a preconsolidation pressure of 1500 psf and an average coefficient of consolidation of 1.128 in^2/day. These parameters were used for the top 15 ft, divided into three layers of 5 ft each (Table 3.15).

The soil sample at the 18 – 19 ft depth had a void ratio (e_0) of 1.06 and average compression and recompression indices of 0.377 and 0.038, respectively. The preconsolidation pressure was 2,600 psf and an average coefficient of consolidation of 0.522 in^2/day. Its settlement parameters were used for the 7-ft layer underlying the top 15 ft (Table 3.15).

Finally, the soil sample at the 23 – 24 ft depth had a void ratio of 0.59 and average compression and recompression indices of 0.149 and 0.012, respectively, with an average coefficient of consolidation of 1.404 in^2/day. Its settlement parameters were used for the bottom 24 ft divided into three layers of 8 ft each (Table 3.15).

- **Stress Dependency Phenomena (C_c)**

The stress dependency of the compression index was investigated based on the available data. The samples were loaded from 0.25 tsf to 12 tsf. The slope -de / d$log\sigma$' was determined for each load increment (Fig. 3.20(b)). The three samples showed similar stress dependent patterns. The incremental compression index (C'_c) increased with the increasing stress from 0.25 tsf to 2.50 tsf, then decreased despite the increased stress to 5.50 tsf, and then increased with the increased stress up to 12 tsf. The conventional compression index C_c was determined and used in the settlement calculation (Table 3.16).

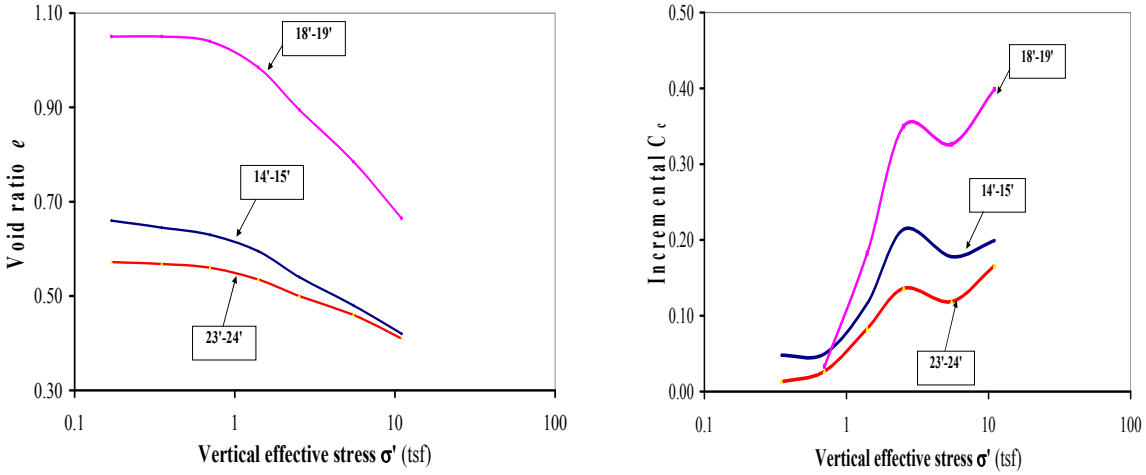

a) b)

Fig. 3.20. (a) e – log σ' Relationship for the Three Samples and (b) Variation of Compression Index with log σ' (Project 3).

- **Stress Increase due to the embankment loading (Project 3)**

The stress increase in the soil mass due to the embankment loading ($\Delta\sigma$) was calculated at the center and the toe of the embankment using the Osterberg method. A surcharge of 240 psf was added to the total stress induced by the embankment, complying with the TxDOT design method (Table 3.16). The average height of the embankment was taken to be 9 ft.

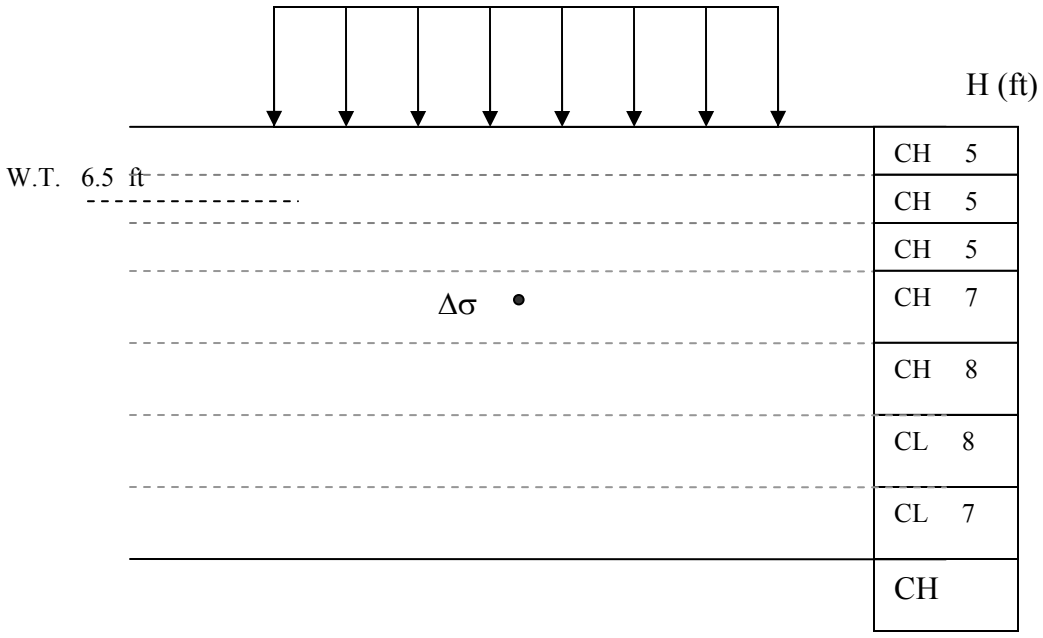

Fig. 3.21. Profile of the Soil Layers for Settlement Calculation (Project 3).

Table 3.16. Summary Stress Increase in the Soil Mass (Project 3).

				Stress increase			
Soil parameters				Center of the embankment		Edge of the embankment	
Depth (ft)	σ_p (psf)	σ_o (psf)	OCR	Center $\Delta\sigma$ (psf)	$\sigma_o+\Delta\sigma$ (psf)	Edge $\Delta\sigma$ (psf)	$\sigma_o+\Delta\sigma$ (psf)
2.5	1500	300	5.0	1320	1620	0	300
7.5	1500	875	1.7	1319	2194	166	1041
12.5	1500	1188	1.3	1313	2501	292	1480
18.5	2600	1564	1.7	1297	2861	417	1981
26.0	2200	2033	1.1	1265	3298	475	2508
34.0	2200	2534	0.9	1216	3750	511	3045
42.0	2200	3035	0.7	1159	4194	531	3566

The variation of the stress increase with depth is shown in Fig. 3.22. The ratio of the stress increase at the center to stress increase at the toe varied from infinite at the top to 2.66 at the 26 ft depth.

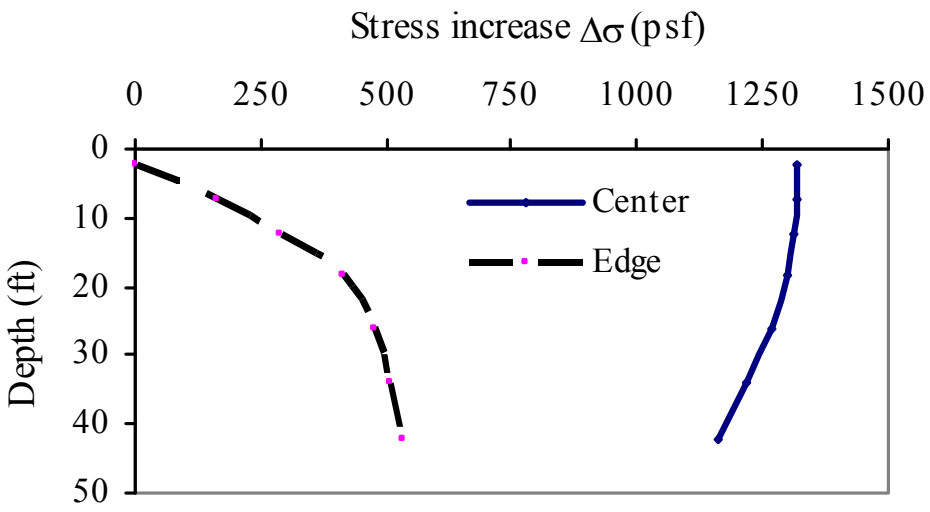

Fig. 3.22. Variation of Stress Increase with Depth at the Center and at the Toe of the Embankment Using the Osterberg Method (Project 3).

- **Total settlement at the center (Project 3)**

Based on the information provided by TxDOT, the total primary settlement was 8.50 in.

UH Check: In all the layers, the total stress ($\Delta\sigma' + \sigma'_o$) was higher than the preconsolidation pressure (σ_p). Therefore, both the compression and recompression indices were the governing parameters for the total primary settlement S_p,

$$S_p = \frac{C_r H}{1+e_0} log\left(\frac{\sigma_p}{\sigma_0'}\right) + \frac{C_c H}{1+e_0} log\left(\frac{\sigma_0' + \Delta\sigma'}{\sigma_p}\right). \qquad 2\text{-}12$$

Using the Osterberg method, the stress increase results at the center of the embankment (Table 3.16), and the following results were obtained for 45 ft of soil:

Layer 1: $S_p = \frac{0.05x5}{1+0.66} log\left(\frac{1500}{300}\right) + \frac{0.199x5}{1+0.66} log\left(\frac{1620}{1500}\right) = 0.1253\ ft$

Layer 2: $S_p = \frac{0.05x5}{1+0.66} \log\left(\frac{1500}{875}\right) + \frac{0.199x5}{1+0.66} \log\left(\frac{2194}{1500}\right) = 0.1342\ ft$

Layer 3: $S_p = \frac{0.05x5}{1+0.66} log\left(\frac{1500}{1188}\right) + \frac{0.199x5}{1+0.66} log\left(\frac{2501}{1500}\right) = 0.1483\ ft$

Layer 4: $S_p = \frac{0.038x7}{1+1.06} log\left(\frac{2600}{1564}\right) + \frac{0.377x7}{1+1.06} log\left(\frac{2861}{2600}\right) = 0.0817\ ft$

Layer 5: $S_p = \frac{0.012x8}{1+0.59} log\left(\frac{2200}{2033}\right) + \frac{0.149x8}{1+0.59} log\left(\frac{3298}{2200}\right) = 0.1339\ ft$

Layer 6: $S_p = \frac{0.149x8}{1+0.59} log\left(\frac{3750}{2534}\right) = 0.1276\ ft$

Layer 7: $S_p = \frac{0.149x7}{1+0.59} log\left(\frac{4194}{3035}\right) = 0.0921\ ft$.

Hence the total primary settlement at the center of the embankment was

Sp = 0.1253 + 0.1342 + 0.1483 + .0817 + 0.1339 + 0.1276 + 0.1053 = 0.8431 ft

= 10.11 in.

The difference between the UH check result (10.11 in.) and the TxDOT estimation (8.50 in.) was due to the thickness of soft soil considered for the settlement estimation (Fig. 3.23). It was noted that if only the top 30 ft of soft soil was considered, the total settlement would be 7.48 in.

- **Rate of settlement at the center (Project 3)**

  TxDOT

The TxDOT rate of settlement estimation, using C_v values in Table 3.15, predicted a settlement of 5.10 in. after 1 year which represents 60% of the total primary settlement (8.50 in.).

UH Check: Using the TxDOT method, as described in Project 1A and 2, it was considered that each clay layer had two drainage surfaces (top and bottom); the total settlement reached in 2007, 14 years after construction, was determined as follows.

(a) Calculation

14 years = 168 months =14 x 365 = 5110 days

$$T_v = \frac{c_v t}{H_{dr}^2} \qquad 2\text{-}13$$

$$\frac{U\%}{100} = \frac{(4T_v/\pi)^{0.5}}{\left[1+(4T_v/\pi)^{2.8}\right]^{0.179}} \quad \text{(Das 2006).} \qquad 3\text{-}1$$

Layer 1 to 3 $T_v = \frac{1.128(5110)}{(2.5x12)^2} = 6.405 \longrightarrow$ U% = 99.7

Layer 4 $T_v = \frac{0.522(5110)}{(3.5x12)^2} = 1.512 \longrightarrow$ U% = 97.31

Layer 5 to 7 $T_v = \frac{1.404(5110)}{(4x12)^2} = 3.114 \longrightarrow$ U% = 99.46.

Consequently, the total settlement S_{p168} after 14 years was

S_{p168} = (0.997 x 0.1253) + (0.997 x 0.1342) + (0.997 x 0.1483) + (0.973 x 0.0817) + (0.994 x 0.1339) + (0.994 x 0.1276) + (0.994 x 0.0921)

= 0.8376 ft

= 10.05 in.

When considering the top 30 ft of soft clay layers,

S_{p168} = 7.43 in.

Using the same calculation procedure, Fig. 3.23 was obtained.

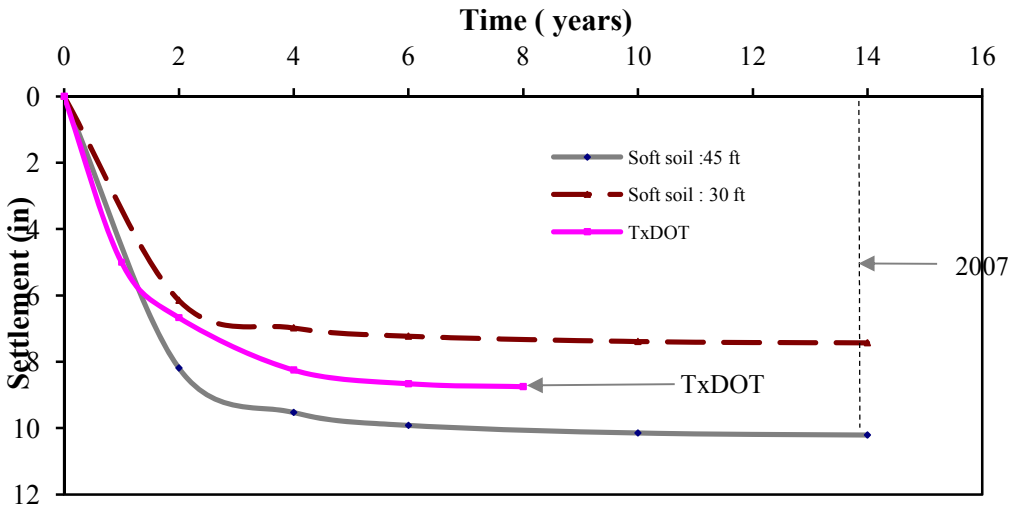

Fig. 3.23. Comparison of TxDOT Rate of Settlement Estimation at the Center of the Embankment with New Estimation Using the Same Data.

Based on this procedure, more than 90% of the total settlement was completed in 1999, six years after construction in all three cases at the center of the embankment. Consequently, the settlement of the embankment can be complete in 2007, 14 years later.

One-layer consideration

Method 1

Considering two drainage surfaces (top and bottom), the primary settlement reached after 14 years (168 months), in 2007, was calculated using the following procedure:

Weighted average of the coefficient of consolidation

$$C_v = \frac{\sum C_{vi} H_i}{\sum H_i} = \frac{(15x1.128) + (7x0.522) + (23x1.404)}{45} = 1.175\, in^2 / day$$

$$T_v = \frac{c_v t}{H_{dr}^2} = \frac{1.175(5110)}{(22.5x12)^2} = \longrightarrow U\% = 32.37$$

S_{p168} = 10.11 x 0.3237 = 3.27 in.

Based on this approach, the settlement reached in 2007 would be 3.27 in., representing about 32% of the total primary settlement at the center of the embankment.

When 30 ft of soft soil layers was considered, the total settlement 14 years later was 48% (U= 0.484190) of the primary settlement and S_{p168} = 3.58 in. After 15 years, the 50% total settlement (U=0.50093) will be S_{p180} = 3.72 in. After 16 years the 51.7% total settlement (U=0.51698) will be S_{p180} = 3.84 in. Hence the expected consolidation settlement under the center of the embankment in one year and two years after 14 years will be 0.14 in. and 0.26 in., respectively.

Method 2

Considering two drainage surfaces (top and bottom), the necessary time to reach 90% of primary settlement can be calculated using the following procedure:

Weighted average of the coefficient of consolidation

$C_v = 1.175\ in^2\ /\ day$.

With U% = 90%, T_v = 0.848 and the time necessary time *t* is given by

$$t = \frac{T_v H_{dr}^2}{C_v} = \frac{0.848(22.5x12)^2}{1.175} = 52612\ day = 144 \text{ years.}$$

This result of 144 years was about 24 times what was predicted by the TxDOT project approach (6 years) to reach 90% of the primary settlement at the center of the embankment (Fig. 3.24).

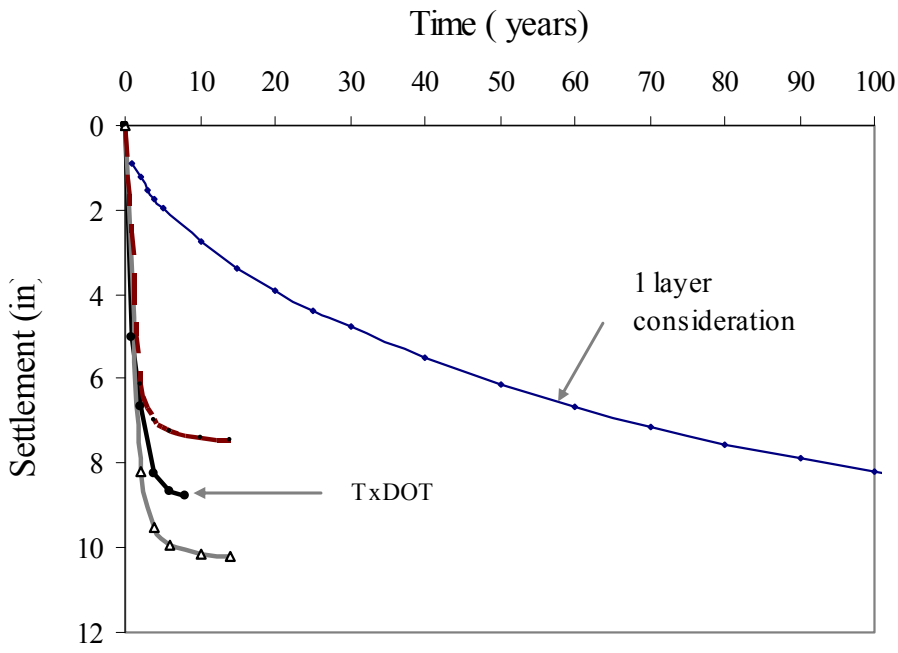

Fig. 3.24. Comparative Graph Showing the Effect of Layering on the Rate of Settlement at the Center of the Embankment (Project 3).

- **Total settlement at the toe (Project 3)**

Using the Osterberg method, stress increase results at the toe of the embankment (Table 3.16) and considering 45 ft of soft soil layers, the following results were obtained:

Layer 1: $S_p = \frac{0.05x5}{1+0.66} log\left(\frac{300}{300}\right) = 0\ ft$

Layer 2: $S_p = \frac{0.05x5}{1+0.66} log\left(\frac{1041}{875}\right) = 0.0114\ ft$

Layer 3: $S_p = \frac{0.05x5}{1+0.66} log\left(\frac{1480}{1188}\right) = 0.0.0144\ ft$

Layer 4: $S_p = \frac{0.038x7}{1+1.06} log\left(\frac{1981}{1564}\right) = 0.0133\ ft$

Layer 5: $S_p = \frac{0.012x8}{1+0.59} log\left(\frac{2200}{2033}\right) + \frac{0.149x8}{1+0.59} log\left(\frac{2508}{2200}\right) = 0.0447\ ft$

Layer 6: $S_p = \frac{0.149x8}{1+0.59} log\left(\frac{3045}{2534}\right) = 0.0598\ ft$

Layer 6: $S_p = \frac{0.149x7}{1+0.59} log\left(\frac{3566}{3035}\right) = 0.0459\ ft$.

Hence the total primary settlement at the toe of the embankment was

Sp = 0 + 0.0114 + 0.0144 + 0.0133 + 0.0477 + 0.0598 + 0.0459 = 0.1895 ft

= 2.27 in.

Hence the total settlement 14 years later was 32% (U= 0.3237) of the primary settlement and S_{p168} = 0.73 in. After 15 years, the 33.5% total settlement (U=0.3351) will be S_{p180} = 0.76 in. After 16 years, the 34.6% total settlement (U=0.3460) will be S_{p180} = 0.79 in. Hence the expected consolidation settlement in the edge of the embankment in one year and two years after 14 years will be 0.03 in. and 0.06 in., respectively.

Considering 30 ft of soft clay layer, $S_{p\ (toe)}$ = 1.01 in. The total settlement 14 years later was 48% (U= 0.484190) of the primary settlement occurs and S_{p168} = 0.48 in. After 15 years, the 50% total settlement (U=0.50093) will be S_{p180} = 0.50 in. After 16 years, the 51.7% total settlement (U=0.51698) will be S_{p180} = 0.52 in. Hence the expected consolidation settlement in the edge of the embankment in one year and two years after 14 years will be 0.02 in. and 0.04 in., respectively.

- **Rate of settlement at the toe (Project 3)**

Using the same procedure used to calculate the rate of settlement at the center of the embankment, Fig. 3. 25 and Fig. 3.26 were obtained. Ninety percent of the total settlement (2.04 in.) was reached at the toe of the embankment four years after construction using the TxDOT method. After 14 years in 2007, 99.6% (2.26 in.) of the

total settlement was reached. Therefore, based on this method, the primary settlement is considered over (Fig. 3.26).

When one layer was assumed for the soft soil, the resulting rate of settlement predicted 32.3% of the total settlement at the toe (0.73 in.), which was reached in 2007. It was three times less than the one obtained by using the TxDOT method (Fig. 3.26).

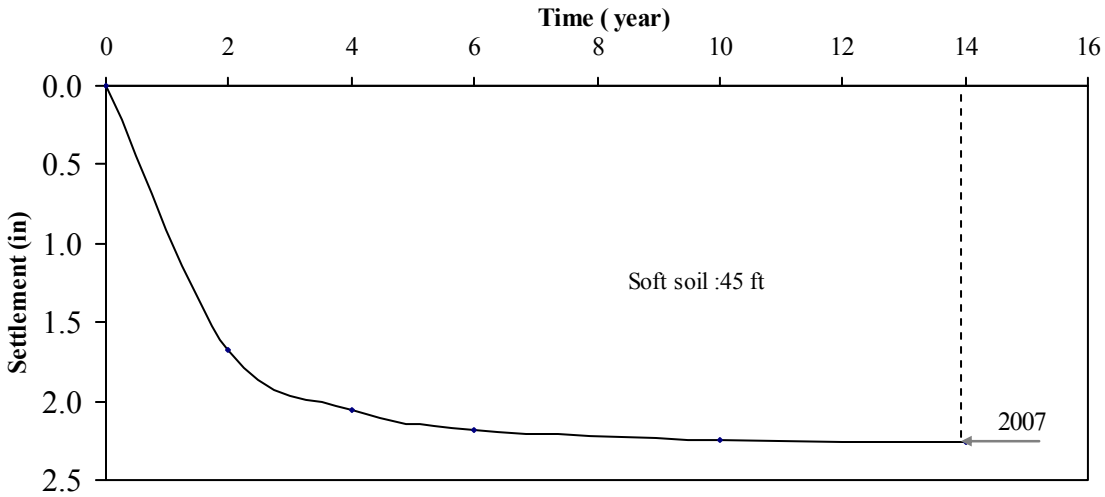

Fig. 3.25. Rate of Settlement at the Toe of the Embankment Using TxDOT Method.

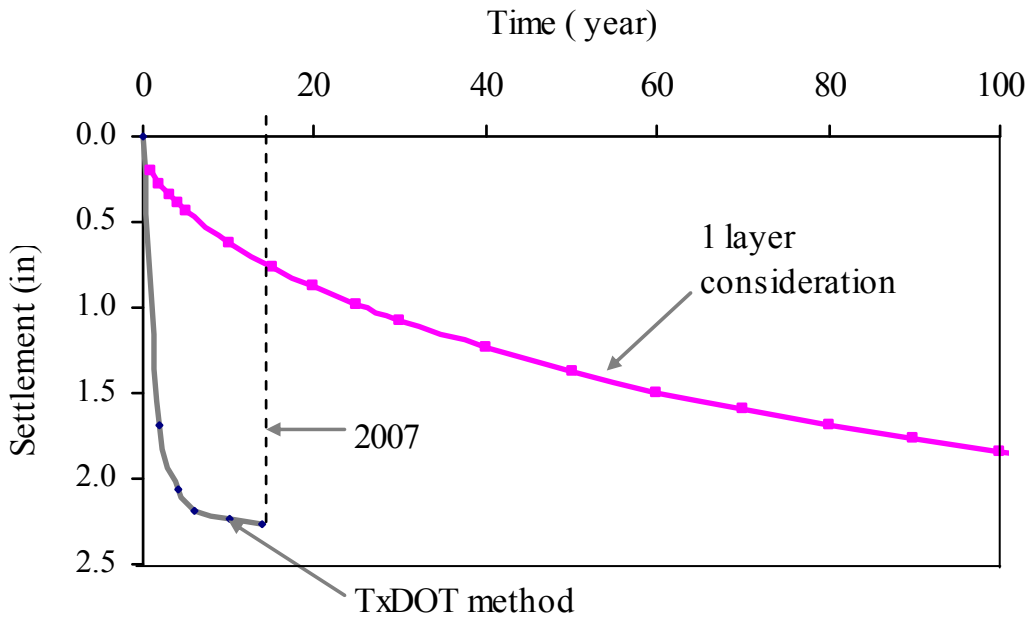

Fig. 3.26. Comparative Graph Showing the Effect of Layering on the Rate of Settlement at the Toe of the Embankment.

- **Excess Pore Water Pressure**

Considering the 14 years of the embankment in place, we have the following consideration:

u_o = initial excess pore water pressure at the construction of the embankment in 1993

u_i = excess pore water pressure at a specific time t.

In Section 3.2.6, by considering one layer of soft soil and two drainage surfaces and the consolidation parameters of 1991, it was ascertained that 32.37% of the consolidation (total thickness of 45 ft) was completed in 2007.

$$U = 1 - \frac{u_i}{u_o} = 0.324 \longrightarrow u_i = 0.676 u_o .$$

Assuming that $u_o = \Delta\sigma'$, the remaining excess pore water pressure u_i is given by

$$u_i = 0.676 u_o = 0.676 \Delta\sigma'$$

Using the increase in stress due to the embankment at the 26 ft depth below the toe of the embankment the pore water pressure is 475 psf (Table 3.16). Hence the excess pore water pressure will be 2.23 psi.

If the total thickness was 30 ft, then the pore water pressure will be $0.516\Delta\sigma'$. Hence the excess pore water pressure will be 1.70 psi.

Comment on the settlement prediction (Project 3)

- All the predictions were based on three consolidation tests. These three tests were representing 45 ft of soil. The number of tests is not representative of the variability in deltaic soil deposits. At least one consolidation test should be done every 6 ft of depth to better estimate the consolidation properties.
- The method used to estimate the stress increase was closer to the Osterberg method. The soft clay soil was overconsolidated, and in all six layers the total effective stress was higher than the preconsolidation pressure. Therefore, both compression and recompression indices are governing parameters of the total primary settlement. The type of the recompression index used for the calculation was not clear.
- The TxDOT project approach used layers of soft soils to estimate the time of settlement. This approach underestimated the time of settlement and is not correct based on theory because of the assumed drainage condition for each layer.

3.1.6. Project No 4 (NASA Road 1 @ Taylor Lake)

At the time of review of the data in 2007, the highway embankment had been in service for seven years. The designed embankment height varied from 10 to 15 ft, and the base width (W) was 60 ft (Fig. 3.27). The ratio $\frac{H}{W}$ varied then from 0.17 to 0.25. About 11 borings were taken on site to collect the geotechnical information from 1994 through 2007 for construction, and monitoring of the road as follow:

- Three borings (TB-1, TB-2, and TB-3) were drilled in March 1994. TCP (Texas Cone Penetrometer) tests were conducted during the drilling and soil samples were taken for laboratory testing. The embankment and the bridge were both constructed in September 2000.
- In April 2005, due to the observed embankment settlements four more borings were drilled for further investigation (AT-1, AT-2, AT-3, and AT-4). Prior to asphalt patching in 2006, 1 to 2.5 inches of elevation difference was measured between bridge and embankment sides.
- In April 2007, four boreholes (UH-1, UH-2, UH-3, and UH-4) located along the embankment, were drilled on the roadway (Fig 3.28). During drilling, the TCP blow counts were recorded to determine the consistency of the soil along the depth.

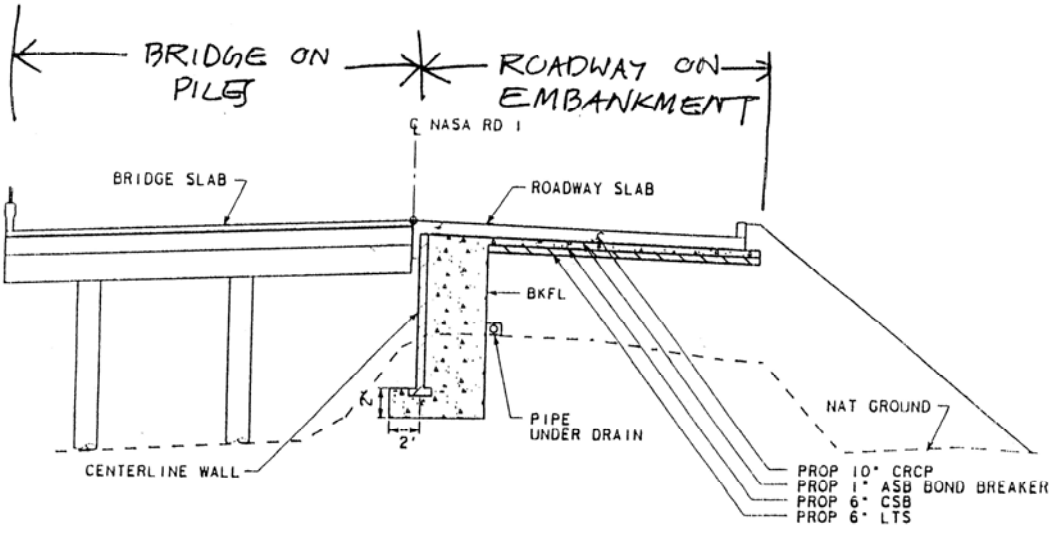

Fig. 3.27. Cross Section of the Bridge and the Embankment at Nasa Road 1 Site.

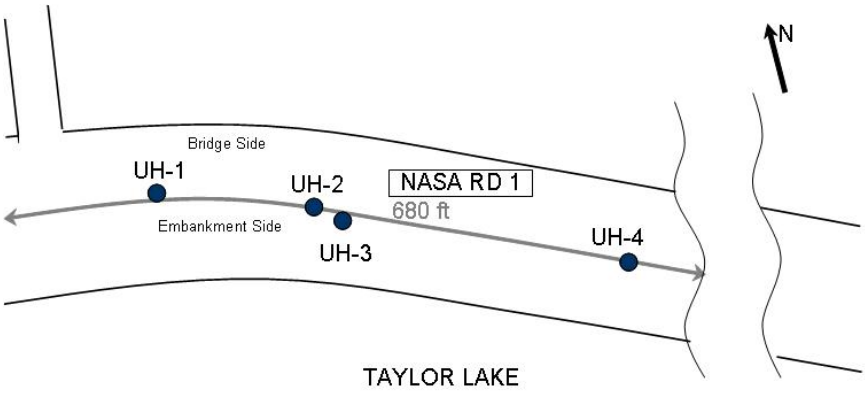

Fig. 3.28. Approximate Borehole Locations Drilled in April 2007 (Not to Scale).

- **Stress Increase due to the embankment loading (Project 4)**

The stress increase in the soil mass due to the embankment loading ($\Delta\sigma$) was calculated at the center and the toe of the embankment using the Osterberg method. A surcharge of 240 psf was added to the total stress induced by the embankment, complying with the TxDOT design method (Table 3.17). The average height of the embankment was taken to be 20 ft.

Table 3.17. Summary of Stress Increase in the Soil Mass.

Soil Parameters						Center	Edge	Center	Edge
Depth	e_o	Cc	Cr	σ_p (psf)	σ_o (psf)	$\Delta\sigma$ (psf)	$\Delta\sigma$ (psf)	$\sigma_o+\Delta\sigma$ (psf)	$\sigma_o+\Delta\sigma$ (psf)
1.5	0.618	0.2	0.04	4800	93.6	2741	108	2834	202.
6.5	0.618	0.2	0.04	4800	405.6	2725	433	3131	838
12.5	0.618	0.2	0.04	4800	780	2648	702	3428	1482
17.5	1.329	0.26	0.01	3400	1092	2531	844	3623	1936
30	0.656	0.126	0.062	4000	1872	2143	1067	4015.	2939
52.5	0.85	0.241	0.061	3800	3276	1536	1129	4812	4405

The variation of the stress increase with depth is shown in Fig. 3.29. The ratio of the stress increase at the center to stress increase at the toe varied from 25.3 near the top to 1.36 at the 52.5 ft depth.

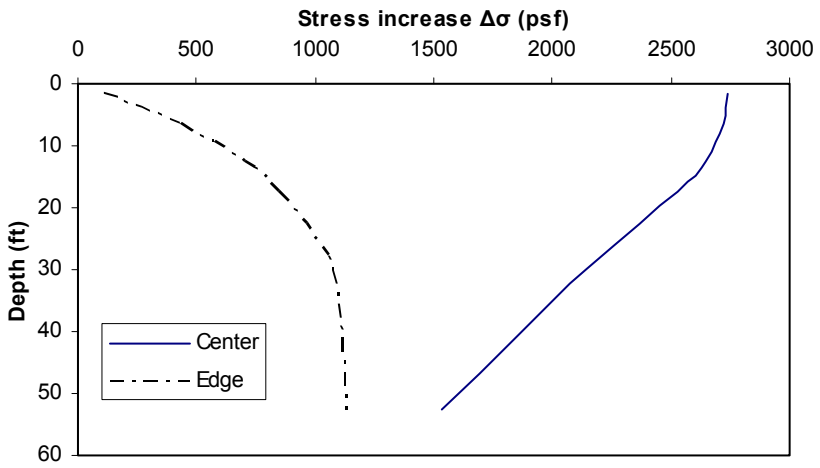

Fig. 3.29. Variation of Stress Increase with Depth at the Center and at the Toe of the Embankment Using the Osterberg Method (Project 4).

- **Total settlement at the center (Project 4)**

Based on the information provided by TxDOT, the total primary settlement was 37.87 in.

<u>UH Check (total thickness of 65 ft)</u>: In three layers, the total stress ($\Delta\sigma' + \sigma'_o$) was higher than the preconsolidation pressure (σ_p). Therefore, both the compression and recompression indices were the governing parameters for the total primary settlement S_p,

$$S_p = \frac{C_r H}{1+e_0} log\left(\frac{\sigma_p}{\sigma_0'}\right) + \frac{C_c H}{1+e_0} log\left(\frac{\sigma_0' + \Delta\sigma'}{\sigma_p}\right)$$

Using the Osterberg method, the stress increase results at the center of the embankment (Table 3.17), and the total primary settlement at the center of the embankment was calculated as follows

$$\text{Layer 1: } S_p = \frac{0.04x3}{1+0.618}\log\left(\frac{2834.8}{93.6}\right) = 1.32\ in.$$

Layer 2: $S_p = \frac{0.04x7}{1+0.618}\log\left(\frac{3131.5}{405.6}\right) = 1.84\ in.$

Layer 3: $S_p = \frac{0.04x5}{1+0.618}\log\left(\frac{3428.4}{780}\right) = 0.95\ in.$

Layer 4: $S_p = \frac{0.01x5}{1+1.329}\log\left(\frac{3400}{1092}\right) + \frac{0.26x5}{1+1.329}\log\left(\frac{3623.5}{3400}\right) = 0.31\ in.$

Layer 5: $S_p = \frac{0.062x20}{1+0.656}\log\left(\frac{4000}{1872}\right) + \frac{0.126x20}{1+0.656}\log\left(\frac{4015.2}{4000}\right) = 2.99\ in.$

Layer 6: $S_p = \frac{0.061x25}{1+0.85}\log\left(\frac{3800}{3276}\right) + \frac{0.241x25}{1+0.85}\log\left(\frac{4812.9}{3800}\right) = 4.65\ in.$

S_p =1.32 in. + 1.84 in. + 0.95 in. + 0.31 in. + 2.99 in. + 4.65 in. = 12.06 in.

The difference between the UH check result (12.06 in.) and the TxDOT estimation (37.86 in.) was due to the fact that overconsolidation of the layers were taken into account in the UH approach in addition to the recompression index, C_r, for the settlement estimation. If only the top 10 ft thickness of the soft soil was considered, the total primary settlement at the center of the embankment would be 4.1 in. The consolidation settlement for the top 20 ft thickness of soft soil would be 4.43 in. It must be noted that these depths were analyzed because the embankment was instrumented to these two depths.

Rate of Settlement (Project 4)

One-layer consideration

Considering two drainages surfaces (top and bottom), the primary settlement reached after 7 years (84 months), in 2007, was calculated using the following procedure:
Weighted average of the coefficient of consolidation

$$C_v = 1.97x10^{-4}\ in^2/\sec$$

$$T_v = \frac{c_v t}{H_{dr}^2} = \frac{1.97x10^{-4}\left(2.21x10^8\right)}{\left(32.5x12\right)^2} = \longrightarrow U\% = 59.72$$

S_{p84} = 4.43 x 0.5972 = 2.64 in.

Based on this approach, the settlement reached in 2007 (after 7 years) for 20 ft thickness of the soil would be 2.64 in., representing about 59.7% of the total primary settlement at the center of the embankment. After 8 years, U =0.6356 and total settlement was 63.5% with the settlement being S_{p96} = 2.81 in. Hence, the expected consolidation settlement in the center of the embankment in one year (between 7 and 8 years) would be 0.17 in. in the 20-ft thick layer.

The settlement reached in 2007 (U=0.5972) in the top 10-ft thickness of the soft soil would be 2.49 in. After 8 years the settlement will be 63.5% of the total settlement (U=0.6356) and would be S_{p96} = 2.01 in. Hence the expected consolidation settlement in the 10-ft thick top layer center of the embankment in one year will be 0.12 in.

In Fig. 3.30 the rate of settlement predicted by TxDOT and UH approaches are compared. The time required for 99% of the consolidation as predicted by UH was 43.6 years. Based on the TxDOT calculations the time required for 99% of the consolidation was 38.4 years.

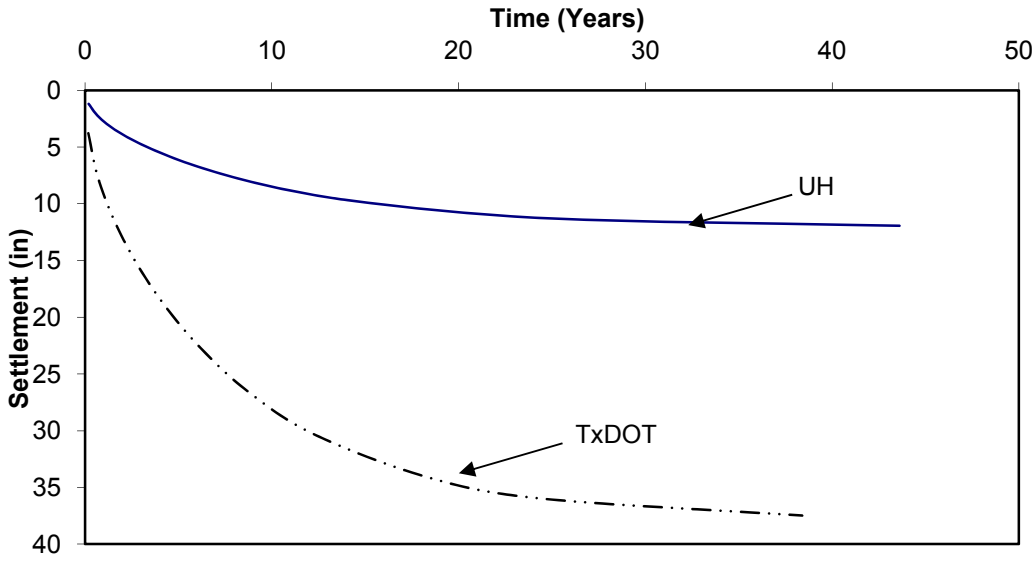

Fig. 3.30. Comparison of Rate of Settlement (Project 4).

3.2. Summary and Discussion

A total of four TxDOT projects were reviewed to ascertain the procedures used by TxDOT to predict the settlement of embankments on soft soils. Based on the review of the design and analyses the following observations can be advanced:

(1) The method currently used in TxDOT projects to determine the increase in in-situ stress is comparable to the Osterberg method and is acceptable. The approach used in TxDOT projects to determine the preconsolidation pressure is acceptable (Casagrande Method).

(2) The total settlement has been estimated in TxDOT projects based on very limited consolidation tests. Since the increase in in-situ stresses due to the embankment are relatively small (generally less than the preconsolidation pressure), using the proper recompression index is import. Reviewing of the TxDOT project

approaches indicates that there is no standard procedure to select the recompression index.

(3) The procedure used in TxDOT projects to determine the rate of settlement is not acceptable. In determining the rate of settlement, the thickness of the entire soil mass must be used with the average soil properties and not the layering method. The layered approach will not satisfy the drainage conditions needed to use in the time factor formula and determine the appropriate coefficient of consolidation.

(4) The consolidation index (C_c) was stress dependent. Hence, when selecting representative parameters for determining the total settlement, expected stress increases in the ground should be considered.

(5) The number of consolidation tests used to determine the consolidation properties of the soils in each project must be increased. Due to the variability in properties of deltaic deposited clay soils, it is recommended to use one consolidation test for each 6 ft depth of soil used for settlement analyses.

4. LABORATORY TESTS AND ANALYSIS

4.1. Introduction

Soil samples were collected from SH3 at Clear Creek (CSJ 0051-03-069) and NASA Road 1 at Taylor Lake (CSJ 0981-01-104) (Fig. 4.1) for laboratory study. Shelby tubes, 3 inches in diameter and 30 in. in length, with an average area ratio of 9.5% were used to collect the soil samples. While some samples were extruded, wrapped in aluminum foil, put in transparent plastic bags and stored in 3'' by 6'' or 3'' by 12'' containers for index tests, others remained in the Shelby tubes for use in consolidation and strength tests. Samples were stored vertically in plastic buckets and transported to the University of Houston's Geotechnical Laboratory for testing. Information on the collected samples is summarized in Table 4.1. In addition to performing standard geotechnical tests, soil samples were used to perform a limited amount of constant rate of strain (CRS) tests to determine the consolidation parameters.

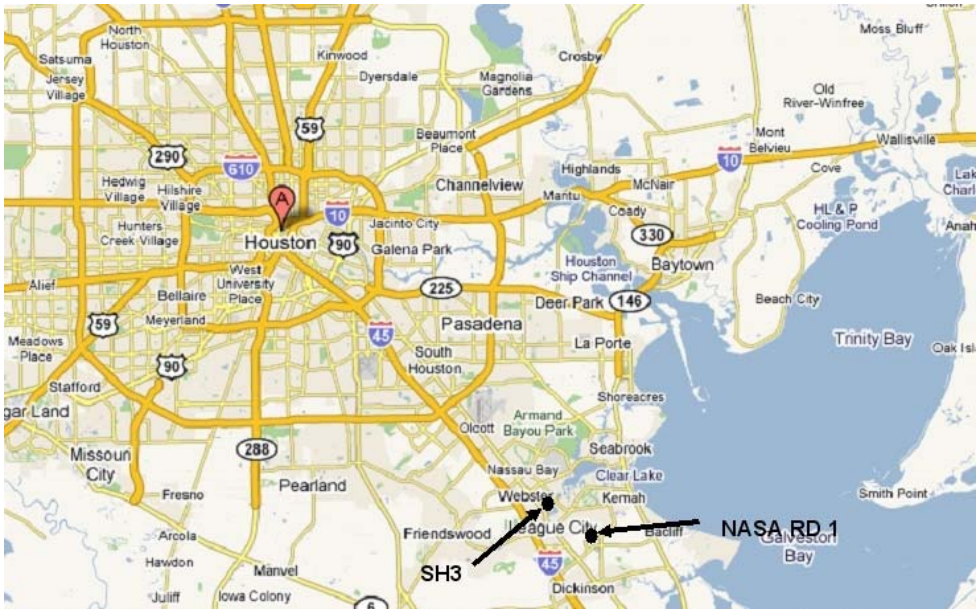

Fig. 4.1. Location of the Two Field Sites in Houston, Texas.

Table 4.1. Summary of the Samples Collected.

Details	SH3	NASA Rd. 1
Depth of Samples (ft)	20 to 30	30 to 50
Number of Samples Collected	56	20
Total Number of Boreholes	5	4
Total Length of Samples (in)	876	282

4.2. Tests Results

A series of soil tests included index properties, consolidation, and unconfined compressive strength.

4.2.1. SH3 at Clear Creek site

- **Natural moisture content:** A total of 50 moisture content (MC) tests were performed to determine the variation of MC with depth in all five borings (Fig. 4.2). The highest MC was 60.8% in the CH soil at a depth of 17 ft in Borehole B4. The lowest MC was 18.7% in the CH soil at a depth of 3 ft in Borehole B2. The highest change was observed between 10 and 20 ft (representing a change in moisture content of 25%) and it was also represented by the transition from the CH to the CL clay soil. The minimum and maximum MCs reported by TxDOT based on the tests done in early 1990s and before were 18% and 44%, respectively. The maximum MC of 44% was in the CH soil at a depth of 20 to 25 ft. This is also an indication of the variability that can be expected in a deltaic deposit (Vipulanandan et al. 2007).

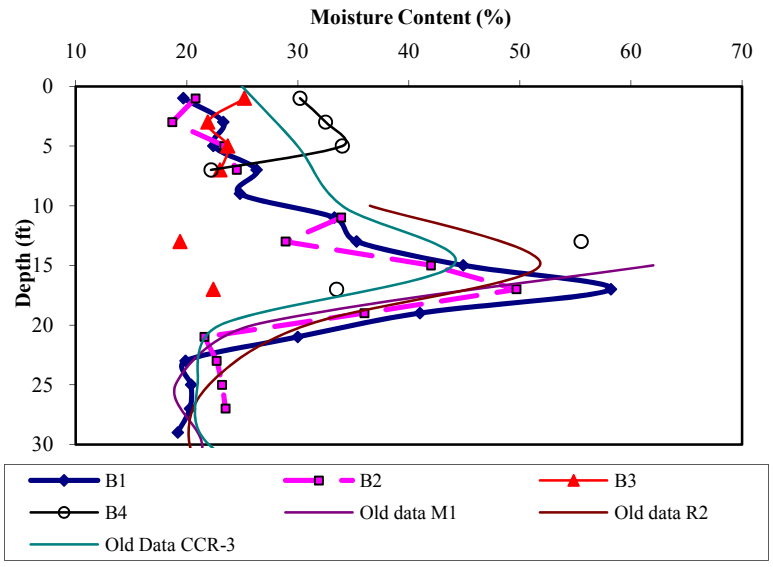

Fig. 4.2. Variation of Moisture Content with Depth in All the Boreholes (SH3).

- **Liquid limit: A** total of 27 liquid limit (LL) tests were performed to determine the type of clay soil and its variation with depth (Fig. 4.3). The highest LL was 91% in the CH soil at a depth of 15 ft. The lowest LL was 27.4% in the CL soil at a depth of 11 ft. Previous study based on 97 data sets on soft deltaic clay soils in this region showed that the LL varied from 24% to 93% with a mean of 53.6%, standard deviation of 22.7%, and coefficient of variation of 2.36% (Vipulanandan et al. 2007). Hence the data from the four boreholes were within the range reported in the literature.

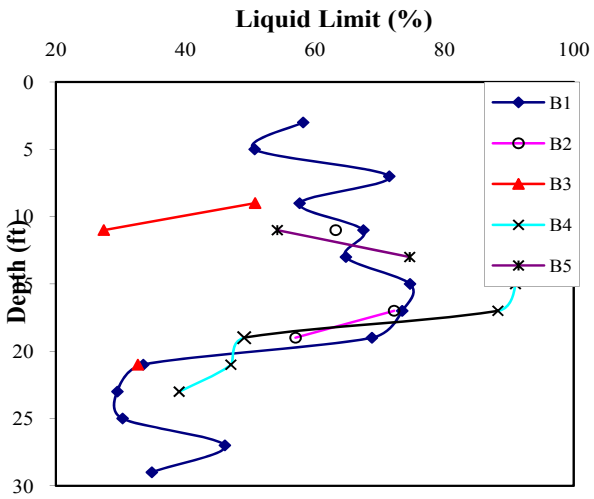

Fig. 4.3. Variation of Liquid Limit with Depth (SH3).

- **Plastic limit:** A total of 27 plastic limit (PL) tests were performed to determine the type of clay soil and its variation with depth in boreholes (Fig 4.4). The highest PL was 24.6% in the CH soil at a depth of 13 ft. The lowest PL was 15.3% in the CL soil at a depth of 27 ft. Previous study based on 97 data sets on soft deltaic clay soils in this region showed that the LL varied from 8 to 35% with a mean of 21.8%, a standard deviation of 6.9%, and coefficient of variation of 31.6% (Vipulanandan et al. 2007). Hence the data from the four boreholes were within the range reported in the literature.

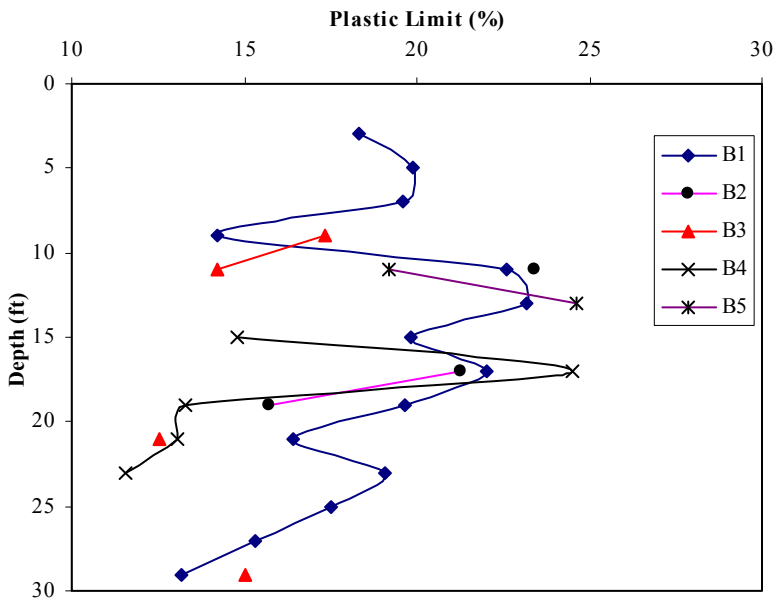

Fig. 4.4. Variation of Plastic Limit with Depth in Boring B1 (SH3).

- **Undrained shear strength** (S_u): A total of 26 undrained shear strength tests were performed to determine the strength of the soil and its variation with depth in four the four boreholes (Table 4.3 and Fig. 4.5). The highest S_u was 17.7 psi in the CH soil at a depth of 7 ft in Boring B3. The lowest S_u was 2.14 psi in the CH soil at a depth of 17 ft in Boring B4. The undrained shear strength from previous testing at this location varied from 2 psi to 18 psi (Table 3.14). The variation in the strength results is comparable.

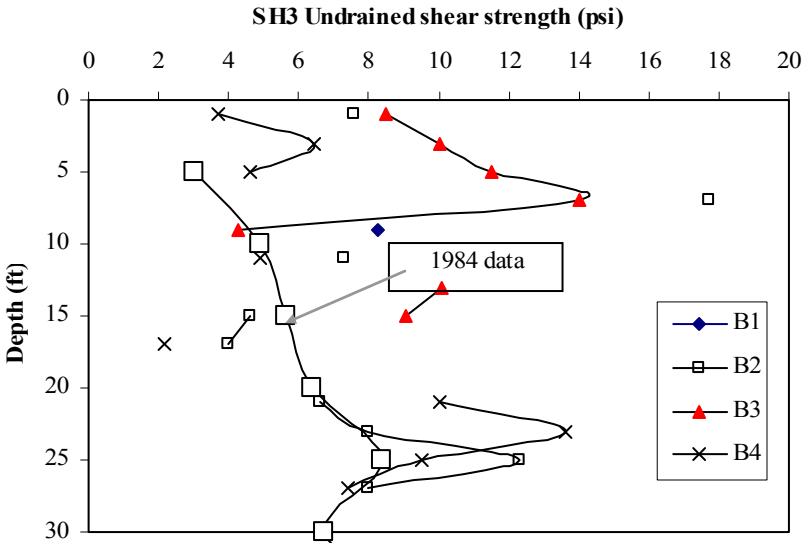

Fig. 4.5. Variation of S_u with Depth in Borings B1, B2, B3, and B4 (SH3).

- **Overconsolidation ratio** (OCR): A total of 27 incremental load (IL) consolidation tests were performed, and the overconsolidation ratio variation with depth in Borehole B1 is summarized in Table 4.4 and plotted in Fig. 4.6. The highest OCR was 9.6 in the CH soil at a depth of 3 ft in boring. The lowest OCR was 1 in the CL soil at a depth of 25 and 29 ft. The clay soil was overconsolidated (OCR > 1) up to 23 ft in CH clay soil. The OCR from previous testing at this location varied from 1 to 5 (Table 3.15). Although the magnitudes were somewhat different, the variation in the OCR with depth was comparable.

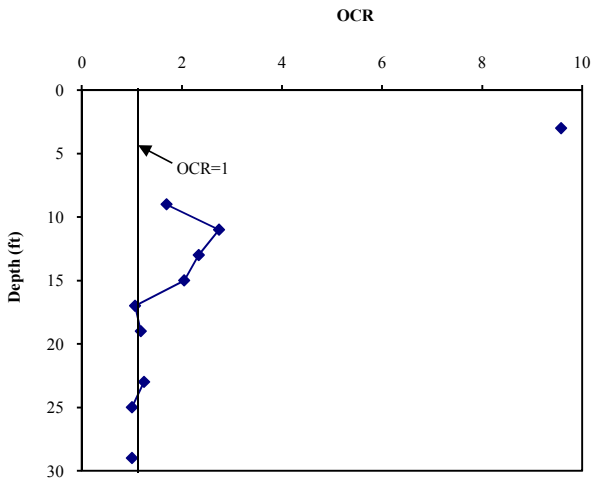

Fig. 4.6. Variation of Overconsolidation Ratio with Depth in Borehole B1 (SH3).

- **Compression index** (C_c): A total of 10 compression indices were determined from 10 IL consolidation tests on samples from Boring B1 (Table 4.4), and their variation with depth is shown in Fig. 4.7. The highest C_c was 0.446 in the CH soil at a depth of 17 ft. The lowest C_c was 0.086 in the CL soil at a depth of 23. The minimum and maximum C_c reported by TxDOT based on the tests done in the early 1990s and before were 0.149 and 0.377, respectively (based on three consolidation tests). There was an 18% difference in the maximum C_c.

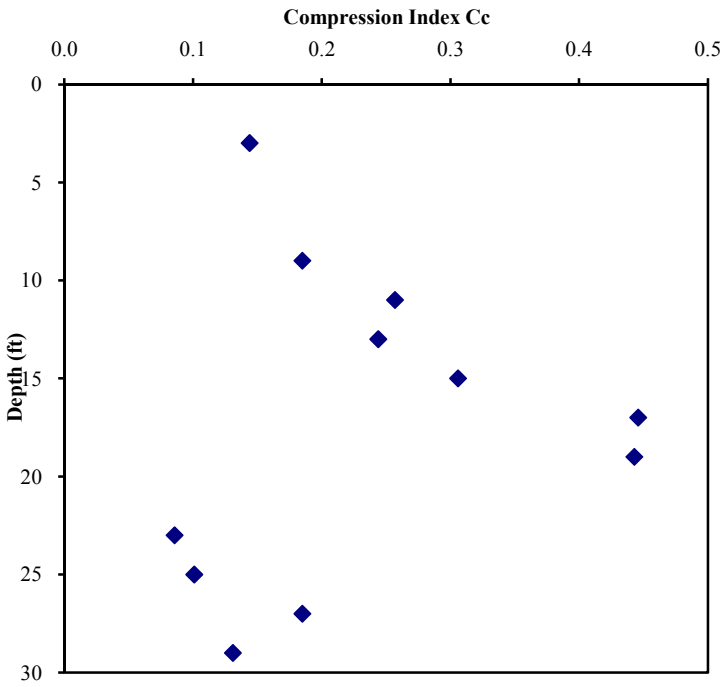

Fig. 4.7. Variation of Compression Index with Depth in Boring B1 (SH3).

- **Recompression index** (C_r): A total of 28 recompression indices of three types (C_{r1}, C_{r2}, and C_{r3}) were determined from 10 IL consolidation tests on samples from Borehole B1 (Table 4.4). The different types of recompression indices were introduced and discussed in Section 4.6.1. The minimum and maximum C_r reported by TxDOT based on the tests done in the early 1990s and before were 0.012 and 0.050, respectively, and were comparable to the C_{r1} of the current study.
- **Coefficient of consolidation** (C_v): A total of seven coefficients of consolidation were determined from seven IL consolidation tests on samples from Borehole B1 (Table 4.4), and their variation with depth is shown in Fig. 4.8. The highest C_v was 24.90 in^2/day in the CL soil at a depth of 29 ft. The lowest C_v was

1.37 in^2/day in the CH soil at a depth of 19 ft. The minimum and maximum C_v reported by TxDOT based on the tests done in the early 1990s and before were 0.522 in^2/day and 1.404 in^2/day, respectively (Table 3.15). The difference in C_v will affect the rate and total time for consolidation.

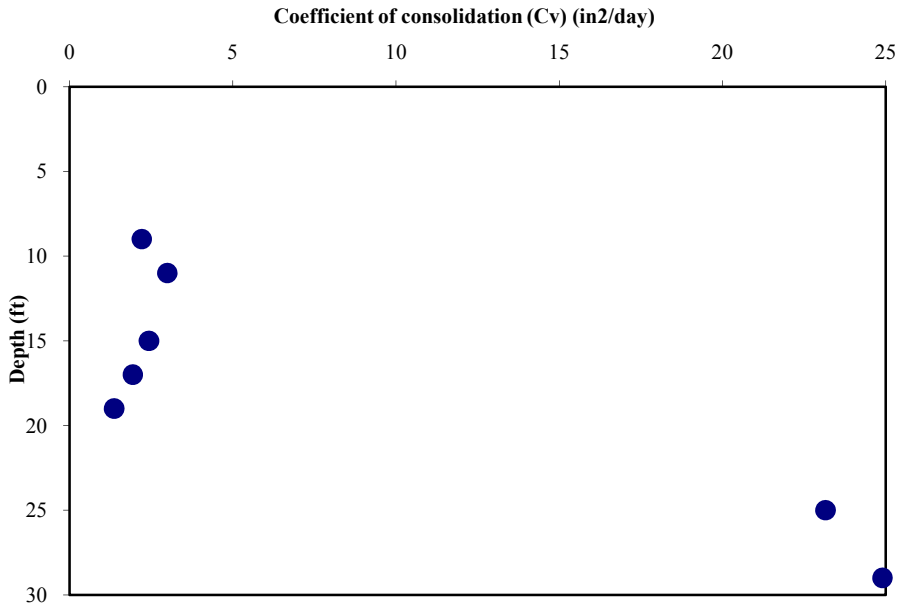

Fig. 4.8. Variation of Coefficient of Consolidation with Depth in Borehole B1 (SH3).

Table 4.2. Summary of Soil Type Parameters (SH3).

Depth (ft)	MC (%)					LL (%) B1	PL (%) B1	TYPE
	B1	B2	B3	B4	B5			
1	19.7	20.8	25.2	34.6	30.2			
3	23.3	18.7	21.9	29.7	32.5	58.2	18.3	CH
5	22.4	23.4	23.7	31.8	34.0	50.7	19.9	CH
7	26.3	24.5	23.0	27.0	22.2	71.5	19.6	CH
9	24.8							
11	33.3	33.9		35.7		67.5	22.6	CH
13	35.3	28.9	19.4	52.9	55.5	64.8	23.2	CH
15	44.9	42.0				75	19.8	CH
17	58.2	49.7	22.4	60.8	33.5	73.5	22	CH
19		36.0						
21	30.0	21.6		22.3		33.5	16.4	CL
23	19.9	22.7				29.5	19.1	CL
25	20.4	23.2		21.5		30.3	17.5	CL
27	20.3	23.5		23.3		46.1	15.3	CL
29	19.2							

Table 4.3. Summary of Strength Parameters (SH3).

Depth (ft)	Unit weight (pcf)				Undrained Shear strength (psi)			
	B1	B2	B3	B4	B1	B2	B3	B4
1	131.0	127.2	125.0	114.8		7.60	8.50	3.70
3	128.7	125.1	126.1	121.1			10.00	6.45
5	132.6	133.7	133.4	115.4			11.50	4.63
7	126.4	134.7	131.6			17.70	14.00	
9	123.0	128.7	116.0		8.25		4.30	
11	120.5	122.7		121.9		7.32		4.89
13	116.8	124.4	138.8				10.08	
15	116.0	115.0	151.8			4.60	9.04	
17	106.3	110.1		100.7		4.00		2.14
19	119.0	112.7						
21	131.7	127.7		130.6		6.60		10.03
23	129.8	125.8		132.6		8.00		13.61
25	134.8	129.3		131.6		12.30		9.52
27	128.4	132.2		128.6		8.00		7.42
29		132.2						

Table 4.4. Summary of Consolidation Parameters (SH3).

								IL TEST						
Depth (ft)	G_s (B1)	Void ratio					σ'_v (psf) (B1)	σ_p (psf) (B1)	OCR	Compressibility parameters of B1				C_v in^2/day
		B1	B2	B3	B4	B5				Cc	C_{r1}	C_{r2}	C_{r3}	
1		0.52	0.55	0.67	0.92	0.80	131							
3		0.62	0.50	0.58	0.79	0.86	388	3720	9.6	0.144	0.018	0.049	0.062	
5		0.59	0.62	0.63	0.84	0.90	654							
7		0.70	0.65	0.61	0.72	0.59	906							
9		0.66					1028	1950	1.9	0.185	0.018	0.057	0.068	2.21
11		0.88	0.90		0.95		1144	3820	3.3	0.257	0.032	0.081	0.099	2.99
13	2.672	0.94	0.77	0.51	1.40	1.47	1253	3800	3.0	0.244	0.022	0.065	0.080	
15		1.19	1.11				1360	3800	2.8	0.306	0.041	0.099	0.111	2.43
17		1.54	1.32	0.59	1.61	0.89	1448	2720	1.9	0.446	0.025	0.162	0.190	1.94
19		1.10	0.95				1561	2720	1.7	0.443	0.026	0.117	0.136	1.37
21		0.80	0.57		0.59		1699							
23	2.693	0.53	0.60				1834	1934	1.1	0.086	0.014	0.018	0.016	
25	2.679	0.54	0.61		0.57		1979	1979	1.0	0.101	-	0.015	0.017	23.15
27		0.54	0.62		0.62		2111			0.185				
29		0.51					2243	2243	1.0	0.131	-	0.024	0.017	24.90

4.2.2 NASA Road 1

Moisture Content

Test results showed that the soil moisture content was gradually increasing with depth (Fig. 4.9). The moisture content was approximately 15% at shallow depths less than 5 ft and reached to 38.5% at the 38 ft depth. The maximum moisture content at this location was much lower than what was observed at the SH3 site.

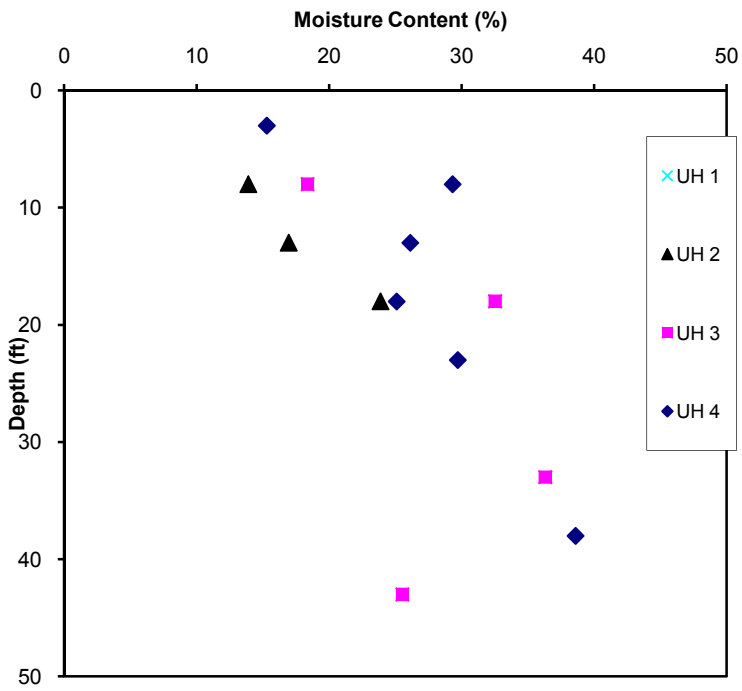

Fig. 4.9. Variation of Moisture Content with Depth at NASA Rd. 1.

Liquid Limit and Plastic Limit Tests

Liquid limit and plastic limit tests were conducted on eight soil samples. Since the top 20 ft of the soil was embankment, tests were conducted on samples below the embankment. Both liquid limit and plastic limit were relatively high around the 23 ft depth. The liquid limit was in the range of 60% and 70% while the plastic limit was in the range of 15% and 25% as shown in Fig. 4.10.

As the depth increased, the liquid limit decreased to 34% (except for one datum point (Fig. 4.10)) and the plastic limit to 7%. Data in the TxDOT report on NASA Rd. 1 indicted that the liquid limit varied from 56 to 80% and it increased with depth. Still, the LL at NASA Rd.1 was within the range of LL measured at the SH3 site.

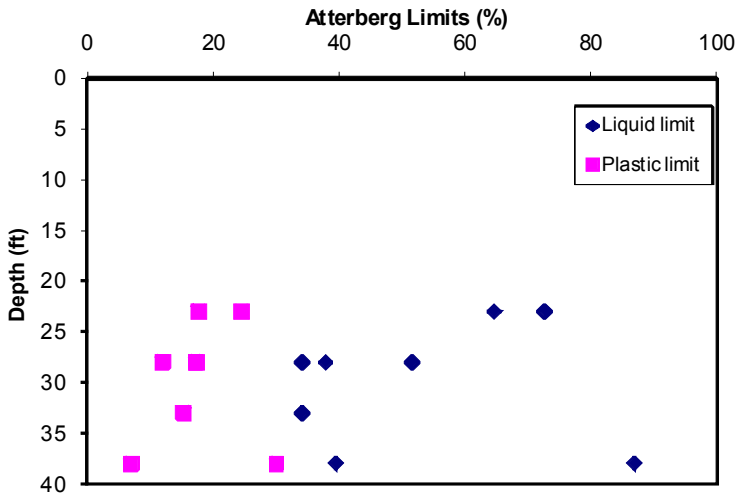

Fig. 4.10. Liquid Limit and Plastic Limit of the Soils along the Depth.

Unconfined Compressive Strength Tests

Nine strength tests were conducted on the soil samples collected. The depth of the samples ranged from 18 ft to 40 ft. The shear strength of the soil ranged between 3 psi and 6 psi up to the 38 ft depth (Fig 4.11). Much higher soil strength was observed near the 39 ft depth and it was 14.5 psi. The shear strength at the SH3 site varied from 2 psi to 18 psi. So the soil at the SH3 site had comparable strength to the NASA Rd.1 site.

Incremental Load (IL) Consolidation Tests

Seven traditional consolidation tests were conducted on the samples collected from the depths between 20 and 40 ft below the ground surface. For all the consolidation tests, pre-consolidation pressure, compression index, and three recompression indices were obtained. The parameters obtained from consolidation tests are summarized in Table 4-5**.**

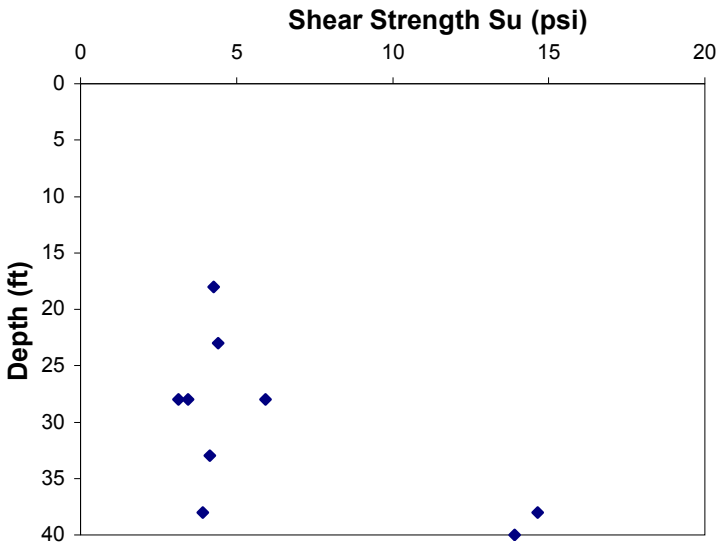

Fig. 4.11. Shear Strength Variation with Depth at NASA Rd. 1.

Table 4-5. Consolidation Parameters from IL Consolidation Tests for NASA Rd. 1.

Sample	Depth (ft)	e_0	σ_p (psf)	C_c	C_{r1}	C_{r2}	C_{r3}	Comment
UH-1 27-29	28	1.065	2144	0.546	0.069	0.119	0.127	Soft*
UH-1 37-39	38	0.830	2406	0.173	0.030	0.076	0.081	Soft**
UH-2 22-24	23	0.972	2094	0.375	0.019	0.079	0.077	Very Soft**
UH-3 22-24	23	0.736	3820	0.333	0.037	0.067	0.070	Very Soft**
UH-3 27-29	28	0.900	2352	0.296	0.028	0.041	0.047	Soft*
UH-3 32-34	33	0.735	3820	0.284	---	0.040	0.044	Very Soft**
UH-3 37-39	38	1.041	3032	0.298	0.028	0.047	0.052	Very Soft**

* Based on the unconfined compressive strength test results for $S_u \leq 3.63$ psi (Terzaghi and Peck 1967)

** Based on the TCP values (TxDOT Geotechnical Manual 2006)

In Fig. 4.12, the C_c and C_r values obtained during this study are compared with data from earlier investigations performed in 1994 and 2005. As seen in Fig. 4.12, the compression index values compare well with the new data. The recompression index values (C_{r2}) were also in good agreement except for the two data points from the 2005 consolidation tests. These two recompression indices were comparable to the C_{r1} from the current study.

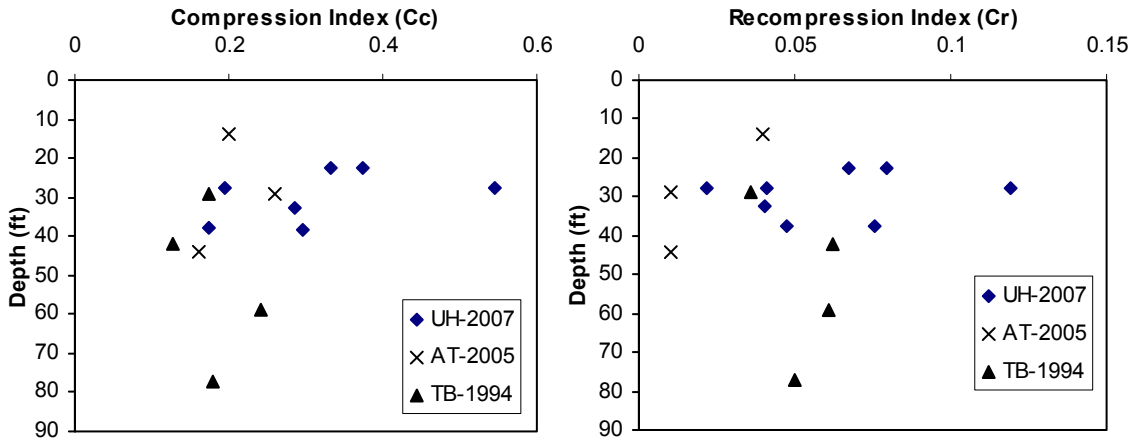

(a) C_c (b) C_{r2}

Fig. 4.12. Variation of New and Old (a) C_c and (b) C_{r2} with Depth.

Incremental Load Consolidation Test with Multiple Unloading–Reloading

To investigate the effect of the unloading stress level on the recompression index, three consolidation tests were conducted with multiple unloading–reloading cycles. General properties of the soil samples are given in Table 4.6**.** Two of the soil samples were high plasticity clay, CH, while one of them was low plasticity clay, CL.

Table 4-6. Soil Parameters of the Samples Used for Consolidation Tests with Multiple Loops.

Sample	Depth (ft)	e_0	LL (%)	PI	Soil Type	Comment
UH-2 22-24	23	1.057	72.67	55.02	CH	Very Soft*
UH-2 27-29	28	0.682	34.10	16.85	CL	Very Soft*
UH-3 22-24	23	0.736	64.65	40.16	CH	Very Soft*

* Based on the TCP values (TxDOT Geotechnical Manual 2006)

Typical vertical effective stress versus void ratio relationships for a soil sample (UH-2-22-24) is shown in Fig. 4.13. Similarly the consolidation tests for UH-3 22-24 had four loops, while soil sample UH-2 27-29 had six loops. It can be observed that the slope of the unloading–reloading curves increased while vertical effective stress was increased.

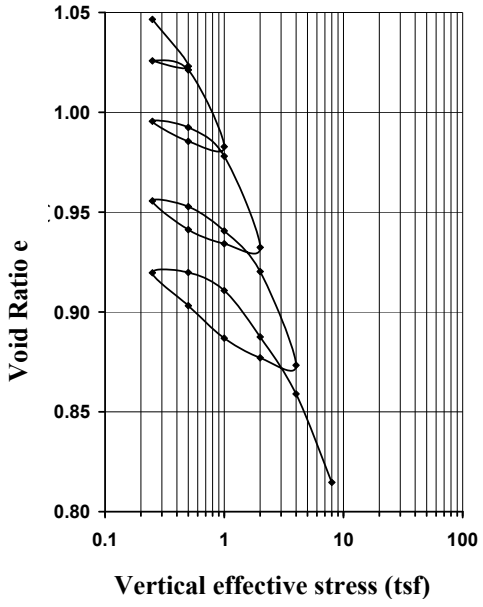

Fig. 4.13.Void Ratio versus Vertical Effective Stress Relationship for CH Soil (Sample UH-2 22-24) with Multiple Loops.

4.3. Soil Characterization

- The data from SH3 and NASA Rd. 1 are compared to the other published data in the literature (Vipulanandan et al. 2007) on deltaic clays using the Casagrande plasticity chart (Fig. 4.14). The results are comparable and within the A and U-lines on the plasticity chart.

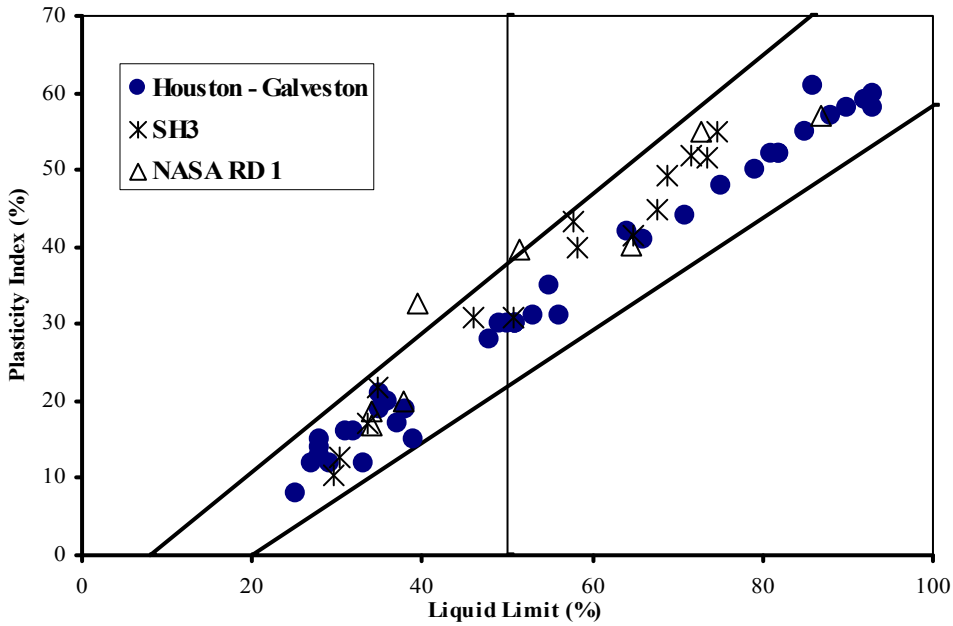

Fig. 4.14. Comparing the SH3 and NASA Rd.1 Data on Casagrande Plasticity Chart.

4.4. Preconsolidation Pressure (σ_p)

The preconsolidation pressure of a clay soil is defined as the highest stress the clay soil ever felt in its history. It is also defined as the yield stress of the soil. Several methods were developed to determine the preconsolidation pressure, σ_p, and they are as follows (Şenol and Sağlamer 2000):

1. Casagrande method (e - log σ')
2. Schmertmann method (e - log σ')
3. Janbu methods ($\Delta H/H$ - σ' and M_c - σ')
4. Butterfield method (ln(1 + e) – log P')
5. Tavenas method ($\Delta H/H$ - σ')
6. Old method ($\Delta H/H$ – log σ')
7. Van Zelst method ($\Delta H/H$ – log σ').

They are classified into two main groups:

- the direct determination methods: Janbu and Tavenas methods (Fig. 4.16)
- the graphical methods: the five remaining methods (Figs. 4.15 and 4.17.).

The Casagrande graphical method (e - log σ') is the most widely used and the one used by TxDOT (Fig. 4.15).

Data obtained from the standard incremental load consolidation performed on a clay sample obtained from SH3 Borehole B1 at a depth of 18-20 ft were used to determine the preconsolidation pressure using the different existing methods. It was a high plasticity clay with LL = 73.5% and PI = 51.5% and classified as CH clay according to the USCS system.

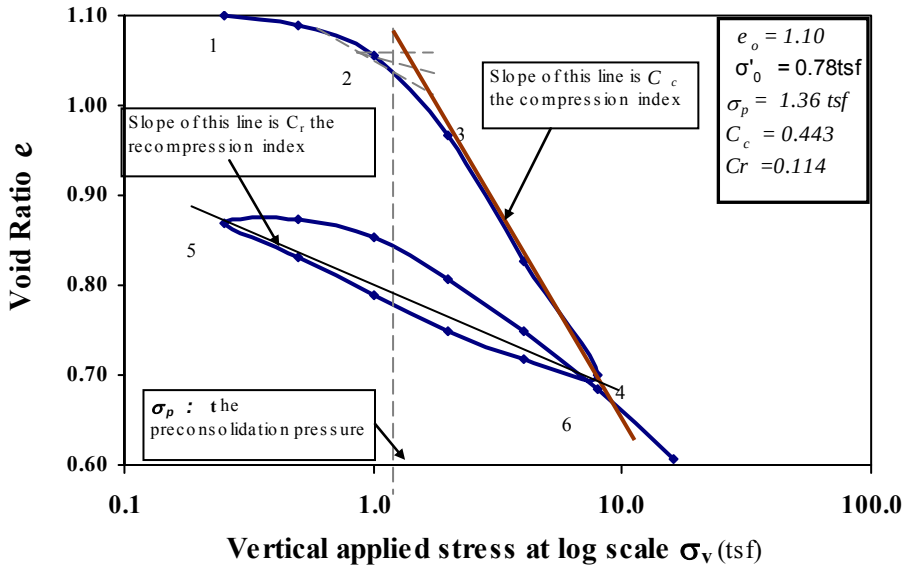

Fig. 4.15. e – log σ' Curve Showing Casagrande Graphical Method (Method 1) for σ_p Determination (Clay Sample from SH3 Borehole 1, Depth 18-20 ft, CH Clay).

Table 4.7. Estimated Preconsolidation Pressure.

No	Methods	σ_p (tsf)	OCR
1	Casagrande	1.36	1.74
2	Janbu	2.00	2.56
3	Tavenas	2.00	2.56
4	Schmertmann	1.15	1.47
5	Butterfield	1.40	1.79
6	Old	1.00	1.28
7	Van Zelst	1.76	2.26

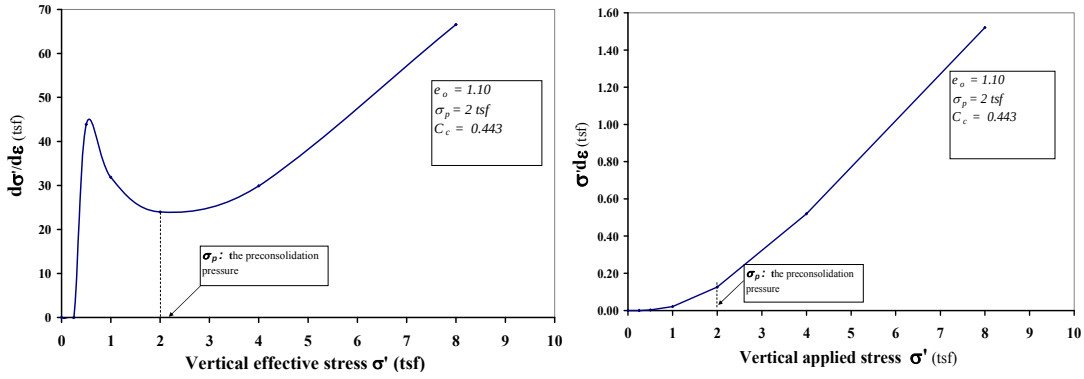

Janbu method Tavenas method

Fig. 4.16. Direct Determination Methods for Preconsolidation Pressure.

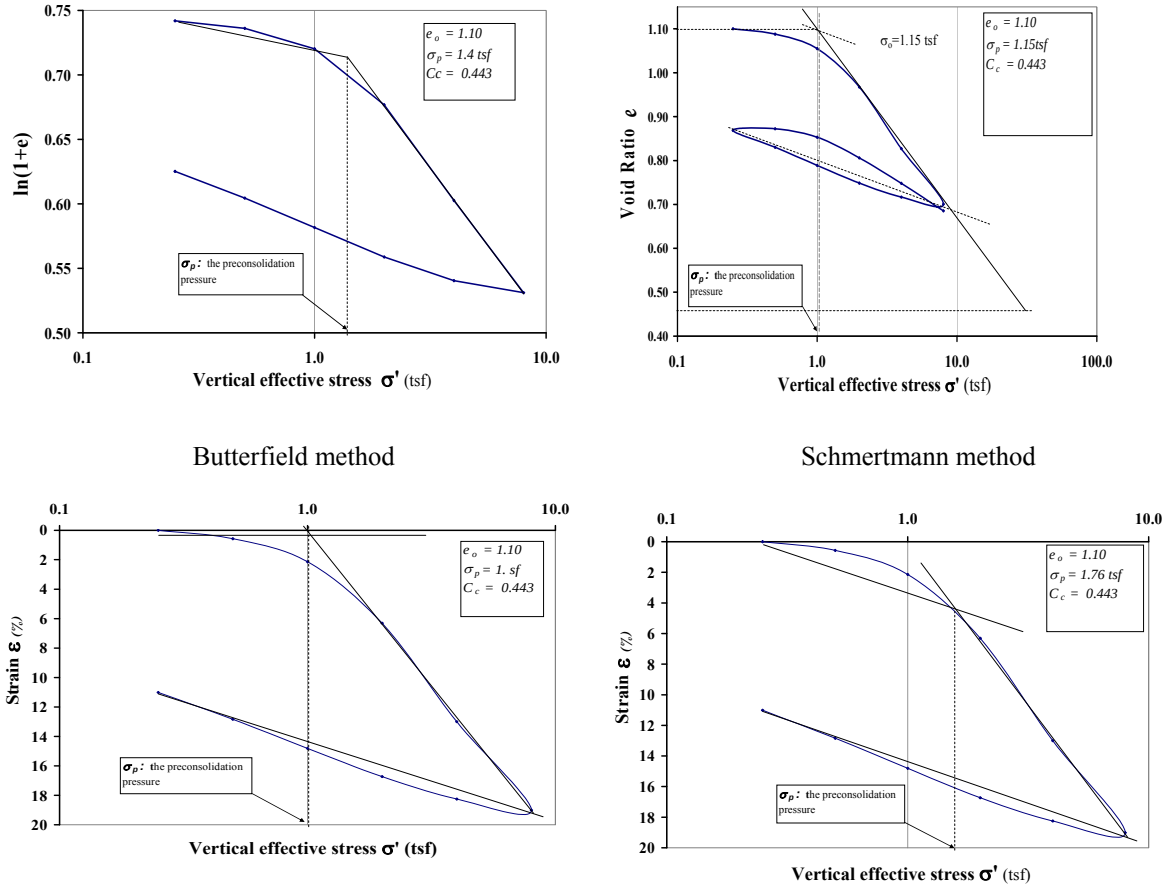

Fig. 4.17. Graphical Methods of Determining the Preconsolidation Pressure.

The direct determination methods give the highest preconsolidation pressure of 2 tsf; it was noted that their accuracies depended on the load increment, and hence, the error is higher with higher value of preconsolidation pressure. For the record, the Tavenas method is the strain energy method.

Using the graphical methods, preconsolidation pressure varied from 1 tsf using the Old method to 1.76 tsf using the Van Zelst method. The preconsolidation pressure being the yield stress of the clay soil, and assuming the reliability of the consolidation

test, the Casagrande method, which consists of determining the yield point on the consolidation curve, was a relatively easy method and the results were reproducable. The remainder of the graphical methods, Schmertmann, Butterfield, Old, and Van Zelst methods, are all based on approximate linearization of the real consolidation curve. In particular, the Butterfield method is based on critical state theory. It is useful in cases of considerable disturbance of the clay soil sample. Consequently, the Casagrande method is the most widely used and is the one used in this study.

4.5. Compression Index (C_c)

The compression index (C_c) is the slope of the virgin compression part of the $e - log\ \sigma$' curve and is defined as follows:

$$C_c = \frac{\Delta e}{log \frac{\sigma_2}{\sigma_1}} \qquad 4\text{-}1$$

This represents the slope of section 3-4 in Fig. 4.15 and is represented as

$$C_c = \frac{-(e_4 - e_3)}{log \frac{\sigma_4}{\sigma_3}} \qquad 4\text{-}2$$

The compression index (C_c) for various soils are summarized in Table 4.8. At the SH3 site, C_c for the CH clay varies from 0.14 to 0.45, which was in the range of medium sensitive clay, Chicago clay and Boston Blue clay (Table 4.8). At the NASA Rd.1 site, the C_c varied from 0.28 to 0.55, closer to the Boston Blue clay.

Table 4.8. Summary Table of Compression Indices for Various Clay Soils (Holtz and Kovacs 1981).

Soil	Deposition type	C_c
Normally consolidated medium sensitive clays	-	0.2 to 0.5
Chicago silty clay (CL)	glacial	0.15 to 0.3
Boston blue clay (CH)	marine	0.3 to 0.5
Vicksburg Buckshot clay (CH)	-	0.5 to 0.6
Swedish medium sensitive clays (CL-CH)	marine	1 to 3
Canadian Leda clays (MH)	marine	1 to 4
Mexico City clay (MH)	volcanic	7 to 10
Organic clays (OH)	-	4 and up
Peats (Pt)	-	10 to 15
Organic silt and clayey silts (ML-MH)	-	1.5 to 4.0
San Francisco Bay Mud (CL)	-	0.4 to 1.2
San Francisco Old Bay clays (CH)	-	0.7 to 0.9
Bangkok clay (CH)	marine	0.4

4.5.1. Compression index correlation

Several correlations have been developed to determine the compression index from the natural moisture content (W_n) or liquid limit (LL) for some specific clay soils (Table 4.9).

Ganstine (1971) proposed several linear correlations for the Beaumont clay in the Houston area. Based on the data collected by Ganstine (1971) and using the data from the current study, it is being proposed to relate the C_c to the moisture content and unit weight of the soil (Fig. 4.18 and Fig. 4.19).

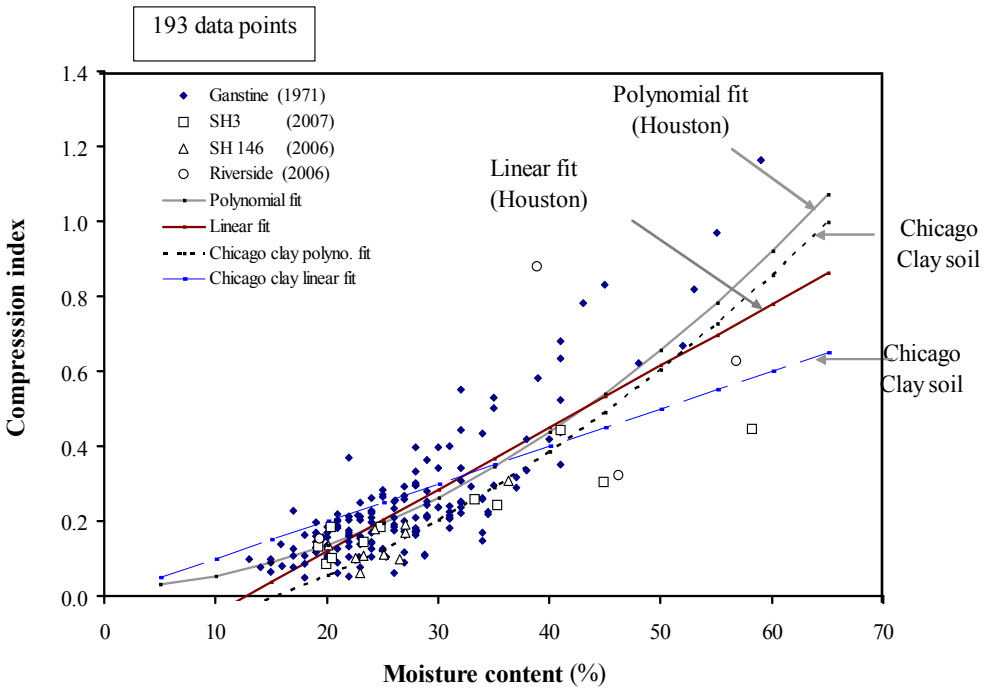

Fig. 4.18. Correlation of Compression Index of Houston/Beaumont Clay Soil with In-situ Moisture Content.

One hundred ninety-three compression indices of the Houston clay, obtained from the standard incremental load consolidation test, were used to develop the correlations.

- C_c versus moisture content

The *second order polynomial* relationship is as follows:

$$C_c = 2.298.10^{-4}W_n^2 + 1.297.10^{-3}W_n + 1.756.10^{-2} \qquad 4\text{-}3$$

with a coefficient of correlation (R) = 0.83.

The *linear* relationship is as follows:

$$C_c = 1.65.10^{-2}W_n - 0.2108 \qquad 4\text{-}4$$

with R = 0.81.

Based on Fig. 4.18, it is recommended using the *linear fitting* correlation equation for natural moisture content within the range of 20% and 40% for a good estimation of the recompression index. The *second order polynomial* relationship is the better one and can be used for any value of in-situ moisture content. These correlations were established independently of the type of clay (CL or CH) and are quite useful for estimating the compression index, knowing only the in-situ moisture content and without performing any consolidation or even an Atterberg's limit tests.

Houston clay soil has higher compressibility compared to Chicago clay soils (Fig. 4.18). Chicago clay soil correlations are summarized in Table 4.9.

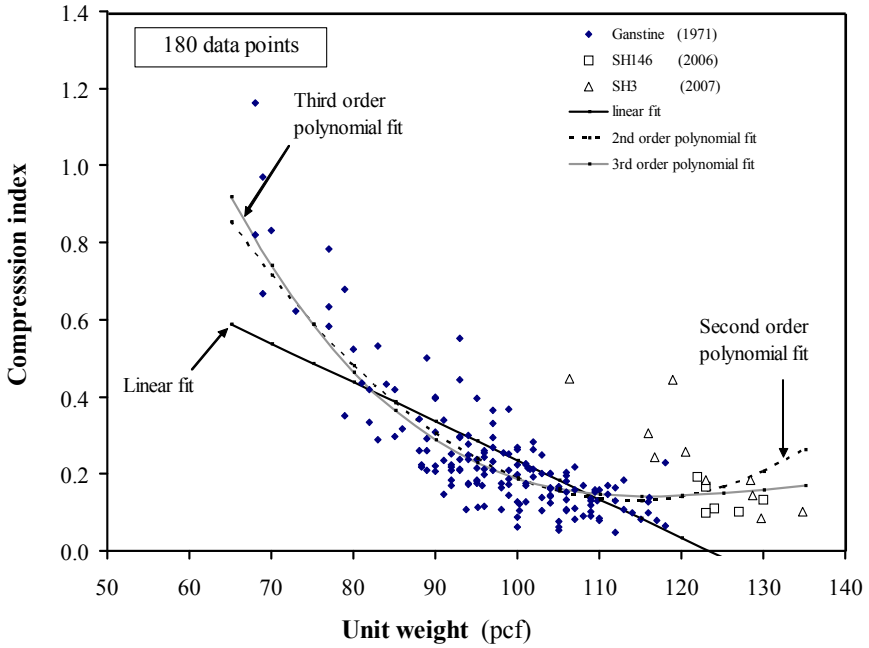

Fig. 4.19. Correlation of Compression Index of Houston/Beaumont Clay Soil with In-situ Unit Weight.

- C_c Versus Unit weight of Soils

The *linear* relationship is as follows:

$$C_c = -1.01.10^{-2} W_n + 1.245 \qquad 4\text{-}5$$

with R = 0.7

The *second order polynomial* relationship is as follows:

$$C_c = 3.10^{-4} \gamma^2 - 6.87.10^{-2} \gamma + 4.0458 \qquad 4\text{-}6$$

with R = 0.8.

The *third order polynomial* relationship is as follows:

$$C_c = -3.10^{-6} \gamma^3 + 1.3.10^{-3} \gamma^2 - 0.1626\gamma + 7.0264 \qquad 4\text{-}7$$

with R = 0.81.

Based on prediction error, it is recommended to use the linear relationship to estimate the C_c when the unit weight is in the range of 80 and 110 pcf. The *second order polynomial relationship* is as good as the *third order* up to a unit weight of 120 pcf. Over 120 pcf, it is better to use the third order polynomial relationship for estimating the recompression index.

Table 4.9. Correlations for C_c (Azzouz et al. (1976); Holtz and Kovacs (1981)).

Equations	Regions of Applicability
$C_c = 0.007(LL - 7)$	Remolded clays
$C_c = 0.208e_o + 0.0083$	Chicago clays
$C_c = 17.66x10^{-5}w_n^2 + 5.93x10^{-3}w_n - 0.135$	Chicago clays
$C_c = 1.15(e_o - 0.35)$	All clays
$C_c = 0.3(e_o - 0.27)$	Inorganic, cohesive soil; silt, some clay; silty clay;clay
$C_c = 1.15x10^{-2}w_n$	Organic soils-meadow mats, peats, and organic silt and clay
$C_c = 0.75(e_o - 0.50)$	Soils of very low plasticity
$C_c = 0.156e_o + 0.0107$	All clays
$C_c = 0.01w_n$	Chicago clays

4.5.2. Stress dependency of incremental compression index (C'_c)

The stress dependency of the compression index was mentioned by Leroueil et al. (1990), in which a representative value of the field condition is to be chosen for settlement calculation and that the current practice usually takes the slope of the secant drawn across the experimental curve from σ'_p *to* $\sigma'_{v0} + \Delta\sigma_{vi}$ (Fig. 4.15). In this study, incremental load consolidation test results from SH3 samples were used for more detail analyses. The incremental compression index (de/d(logσ) was determined from the primary consolidation relationships. From laboratory consolidation tests on the Houston clay soil, it was noticed that the recompression index, in fact, is stress dependent as can be seen in Fig. 4.20(a, b, c, d, e, f, g, and h). The C_c was stress dependent and this observation was true for both CL and CH clays.

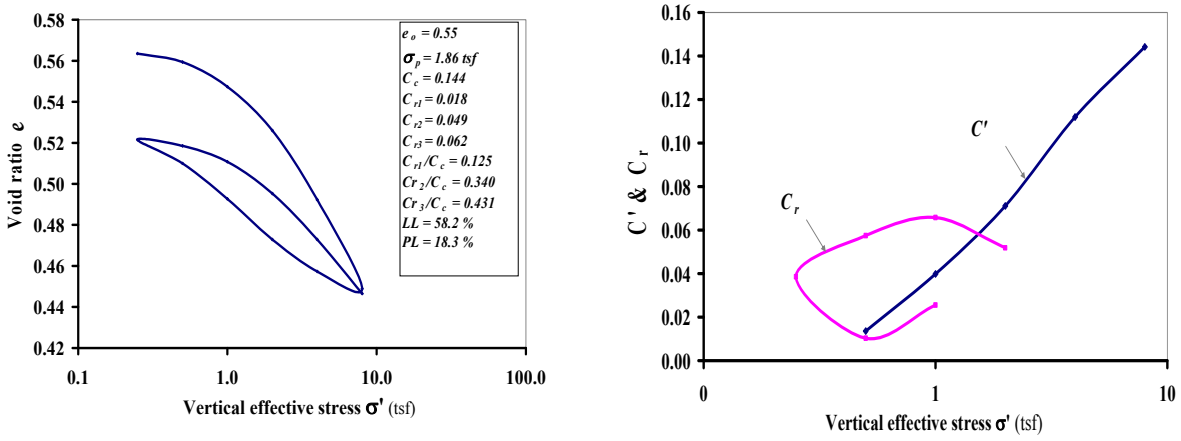

a) SH3 B1_2 – 4 ft (CH)

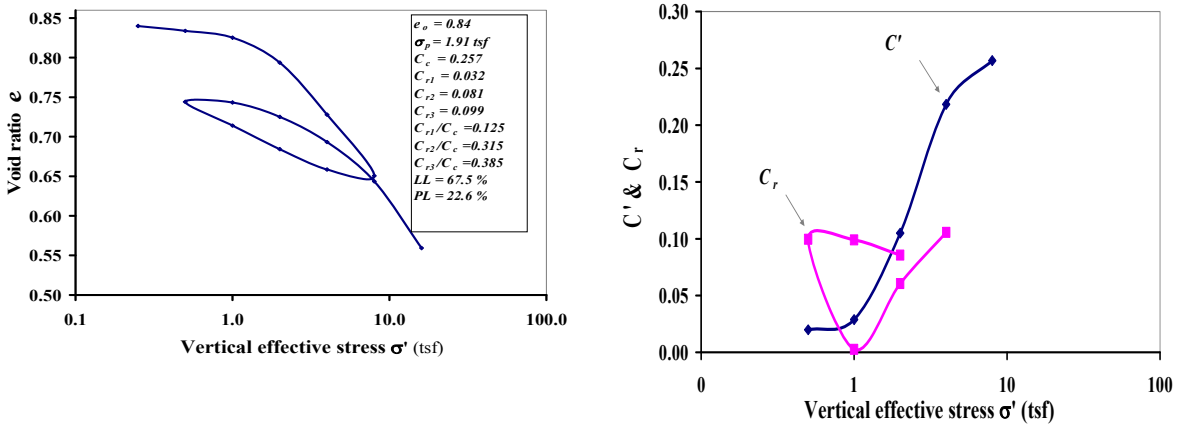

b) SH3 B1_10 – 12 ft (CH)

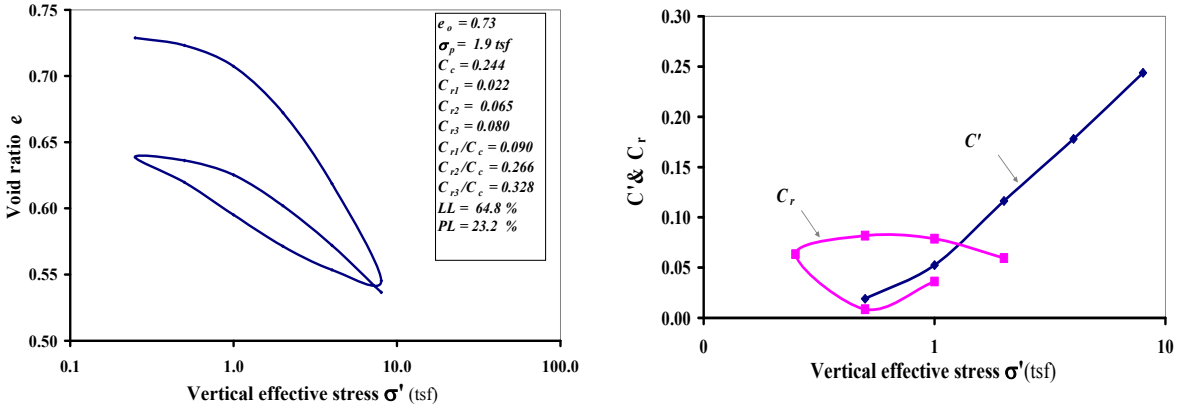

c) SH3 B1_12 – 14 ft (CH)

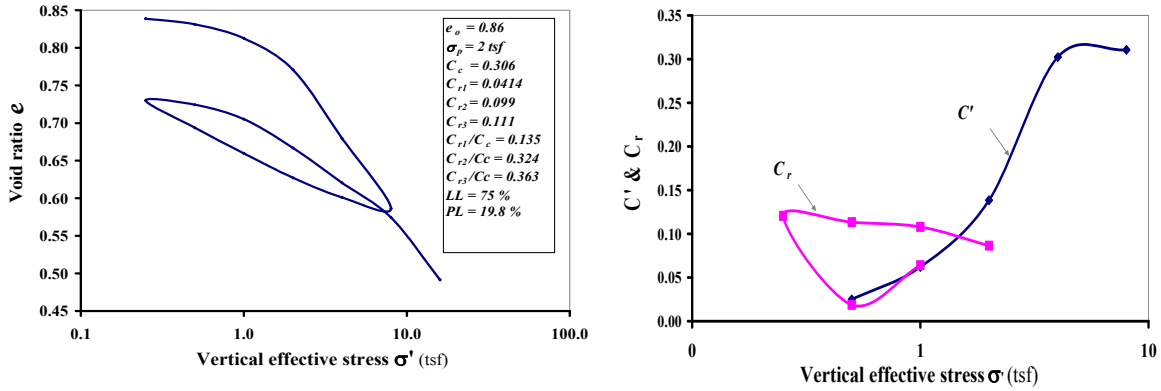

d) SH3 B1_14 – 16 ft (CH)

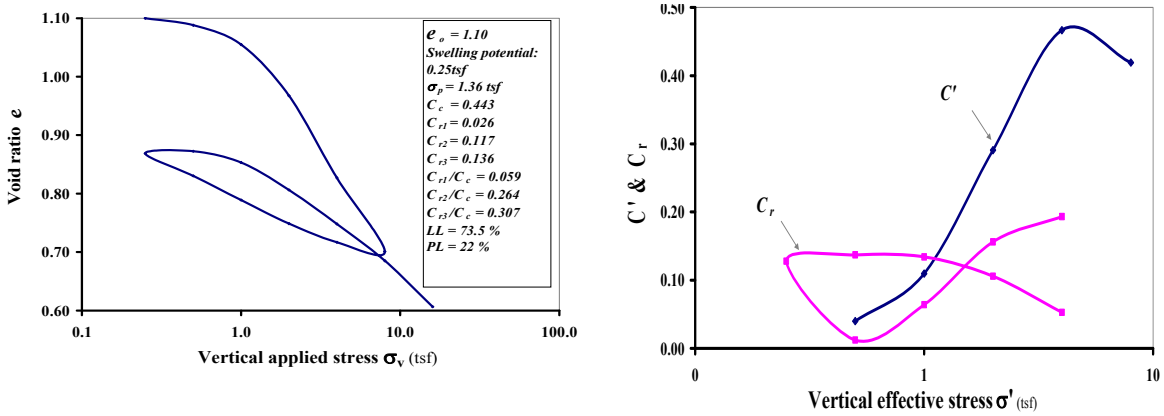

e) SH3 B1_18 – 20 ft (CH)

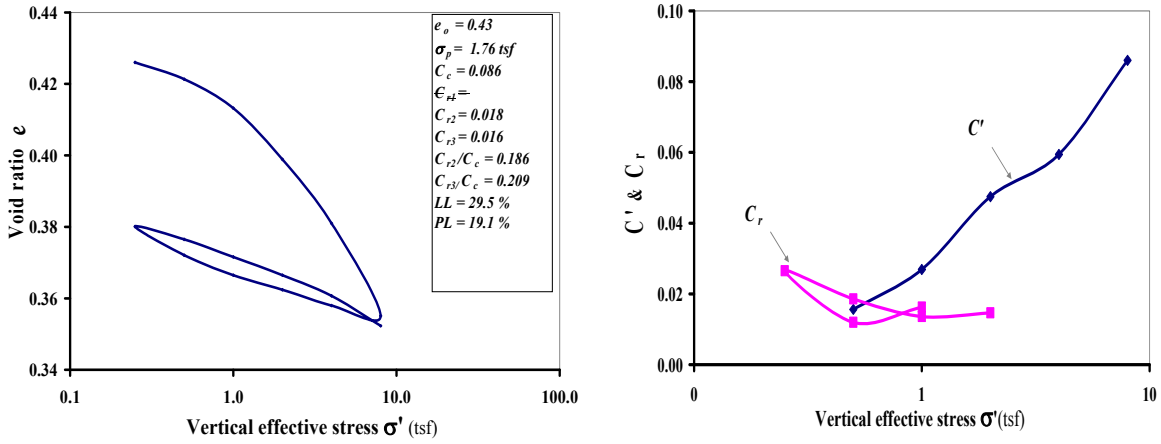

f) SH3 B1_22 – 24 ft (CL)

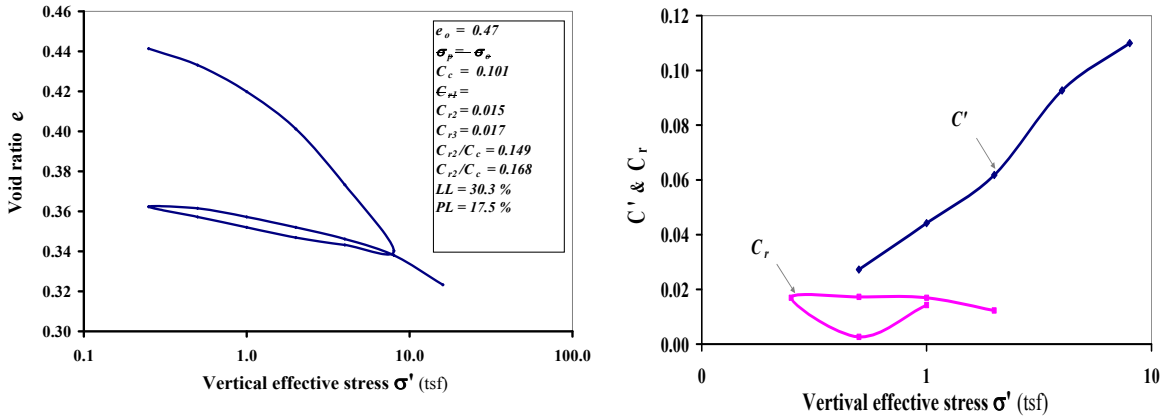

g) SH3 B1_24 – 26 ft (CL)

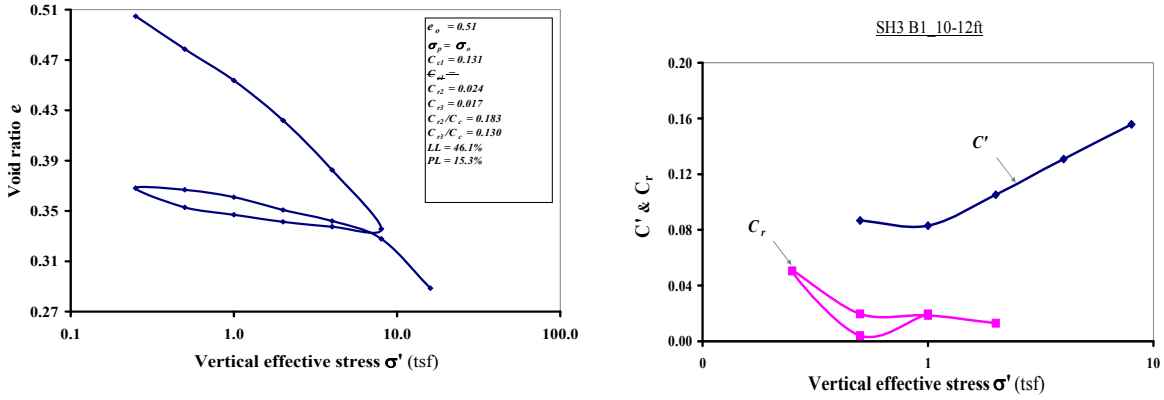

h) SH3 B1_28 – 30 ft (CL)

Fig. 4.20. e – log σ' of Different Clay Samples from SH3 at Clear Creek Bridge and Their Respective Compression and Recompression Index versus log σ' Curves.

4.6. Recompression Index (C_r)

The recompression index (C_r) is the compressibility of the clay soil up to the preconsolidation pressure (σ_p), meaning the slope of Section 1-2 in Fig. 4.21 for an undisturbed sample, but since there is no real undisturbed sample, the unloading and reloading section of the consolidation curve is used to determine the recompression index.

The interest in the recompression index determination is due to the fact that the Houston clay is mostly overconsolidated, and the stress increase due to the embankment and the retaining walls, constructed by TxDOT, is mainly around the preconsolidation pressures. Consequently, the determination of the recompression is highly critical for settlement estimation.

The objective of this study is to investigate the different methods used to determine the recompression index and to quantify its variation for the Houston overconsolidated clay.

4.6.1. Recompression indices

There is no clear definition for determining the recompression index. A recent observation was that the recompression index C_r can be determined by three different methods (Fig. 4.21) giving three different values that are named in this study by $C_{r1,}$ C_{r2}, and C_{r3} (Vipulanandan et al. 2008). This fact needs to be investigated and is due to the stress dependency of the recompression index during the unloading and reloading process in a consolidation test (Fig. 4.21).

(1) C_{r1} is the slope of the line joining the end of the unloading part (Point 5) and the intersection of the preconsolidation line and the reloading part of the recompression curve (Point 6) (Vipulanandan et al. 2008).

(2) C_{r2} is the average slope of the hysteretic loop (all the unloading and reloading) as shown in Fig. 4.21 (Holtz and Kovacs 1981).

(3) C_{r3} is the slope of the unloading section of the recompression curve (Das 2006).

Even if the value of the recompression index is very small, the difference in the

values can result in predicting substantially different settlement predictions in case of overconsolidated soft clay soils (Vipulanandan et al. 2008).

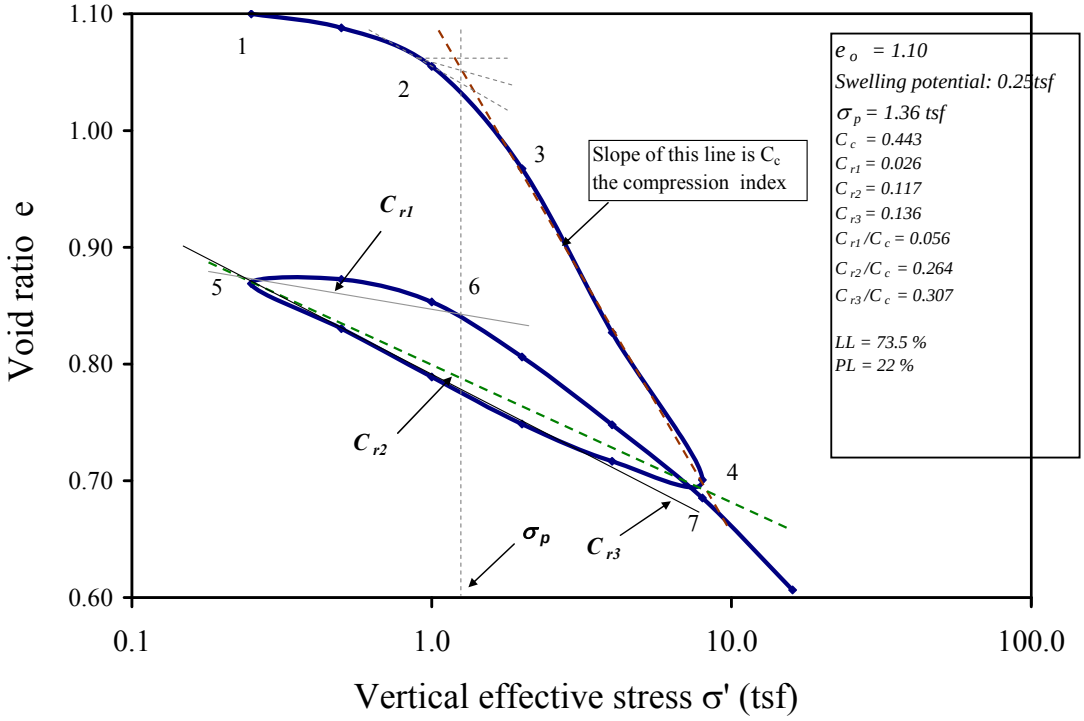

Fig. 4.21. e – log σ' Curve Showing the Three Recompression Indices (C_{r1}, C_{r2}, C_{r3}). Clay Sample from SH3 Borehole 1, Depth 18-20 ft, CH Clay.

Table 4.10. Summary of Compressibility Parameters for the Clay Soils (SH3 Bridge at Clear Creek).

		IL TEST									
Depth (ft)	Type	OCR	Compressibility parameters of B1				C_{r3}/C_{r1}	C_{r3}/C_{r2}	C_{r1}/C_c	C_{r2}/C_c	C_{r3}/C_c
			C_c	C_{r1}	C_{r2}	C_{r3}					
1	CH										
3	CH	9.6	0.144	0.018	0.049	0.062	3.44	1.27	0.125	0.340	0.431
5	CH										
7	CH										
9	CH	1.9	0.185	0.018	0.057	0.068	3.78	1.19	0.097	0.308	0.368
11	CH	3.3	0.257	0.032	0.081	0.099	3.09	1.22	0.125	0.315	0.385
13	CH	3.0	0.244	0.022	0.065	0.080	3.64	1.23	0.090	0.266	0.328
15	CH	2.8	0.306	0.041	0.099	0.111	2.71	1.12	0.134	0.324	0.363
17	CH	1.9	0.446	0.025	0.162	0.190	7.60	1.17	0.056	0.363	0.426
19	CH	1.7	0.443	0.026	0.117	0.136	5.23	1.16	0.059	0.264	0.307
21											
23	CL	1.1	0.086	0.014	0.018	0.016	1.14	0.89	0.163	0.210	0.187
25	CL	1.0	0.101	-	0.015	0.017		1.13	-	0.149	0.168
27	CL										
29	CL	1.0	0.131	-	0.024	0.017		0.71	-	0.183	0.130

From Table 4.10, it was observed that for the CH clay soils, C_{r3} was equal to 2.71 to 7.60 times the values of C_{r1}. This variation will be the same for the magnitude of settlement estimated using C_{r1} and C_{r3}, in the case of the overconsolidated clay, when the total primary settlement S_p is

$$S_p = \frac{C_r}{1+e_0} H \log\left(\frac{\sigma_o + \Delta\sigma}{\sigma_o}\right) \qquad 4\text{-}8$$

Based on the analysis of the data there was no direct correlation between C_{r1} and C'_c. But there was a linear correlation between C_c and other recompression indices: $C_{r2} = 0.305$, C'_c and $C_{r3} = 0.356\ C'_c$.

As shown on Fig. 4.23, the ratio of recompression indices (C_{r2} and C_{r3}) and the compression of the SH3 at Clear Creek clay soil were higher than the New Orleans clay ratios, except for C_{r1}.

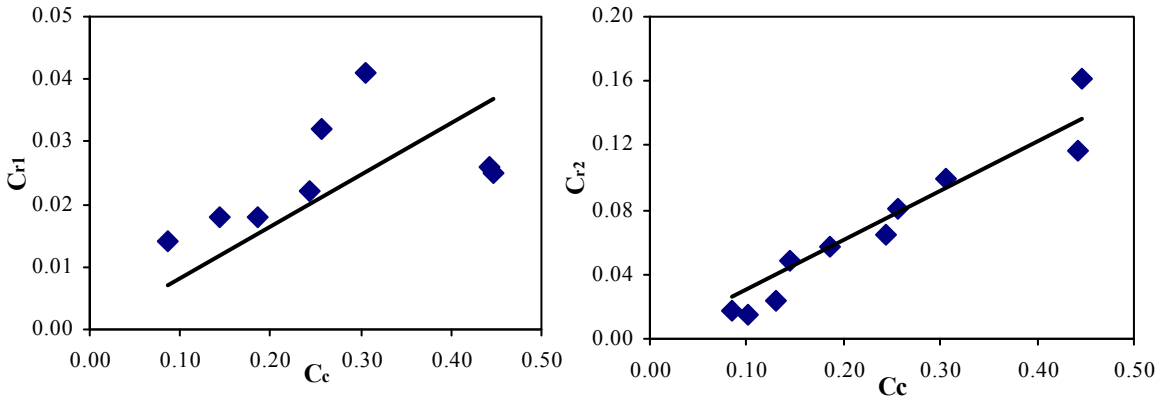

a) C_{r1} vs C_c b) C_{r2} vs C_c

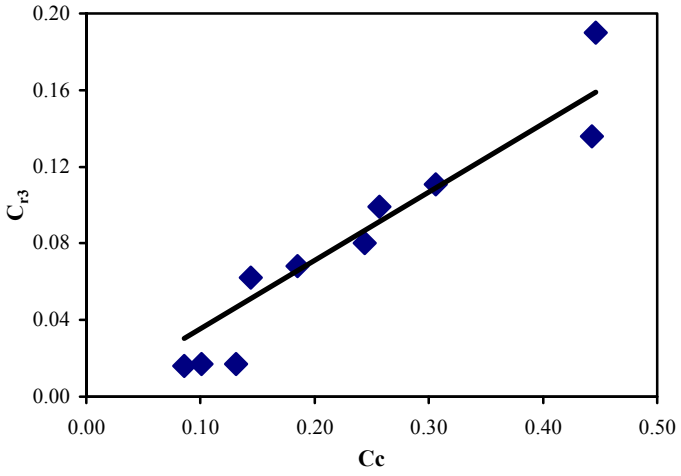

c) C_{r3} vs C_c

Fig. 4.22. Correlation of the Different Types of Recompression Indexes with the Compression Index a) C_{r1} vs. C_c, b) C_{r2} vs. C_c, and c) C_{r3} vs. C_c.

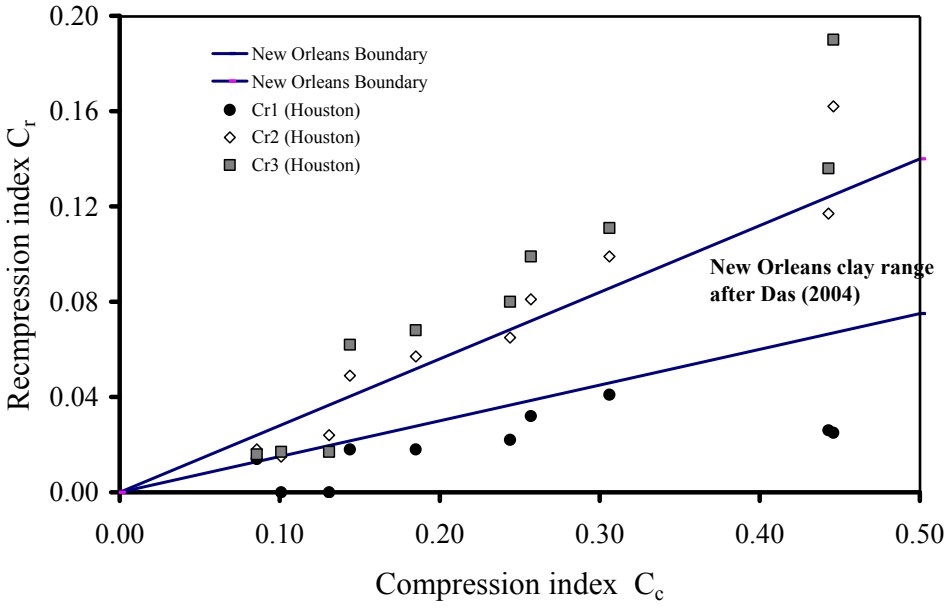

Fig. 4.23. Comparison of the Different Recompression Indices of Houston SH3 Samples with New Orleans Clay C_r/C_c Range.

4.7. Coefficient of Consolidation (C_v)

The coefficient of consolidation derived from Terzaghi's (1925) 1-D consolidation theory is the parameter used to determine the percent of the total primary settlement completed at any time, and is given by the following relationship:

$$c_v = \frac{T_v H_{dr}^2}{t} \qquad 4\text{-}9$$

where H_{dr} is the maximum drainage path.

There are two commonly used methods to calculate the coefficient of consolidation C_v:

- Casagrande's log time method giving

$$c_v = \frac{0.197 H^2_{dr}}{t_{50}} \qquad 4\text{-}10$$

- Taylor's square root of time method giving

$$c_v = \frac{0.848 H^2_{dr}}{t_{90}} \qquad 4\text{-}11$$

As reported in the literature, Taylor's square root of time method C_v values are generally higher than Casagrande's logarithm-of-time method values, as was observed in the current study. For CH clay soils, the coefficient of consolidation was very high before the preconsolidation pressure and then decreased rapidly thereafter (Fig. 4.24).

In the case of the CL clay soils (silty clay), the coefficient of consolidation reduced with the stress increase. The Casagrande log-of-time method was not convenient for the CL soils to the determination of C_v since the standard shape of the deformation versus log time was not obtained (Fig. 4.25).

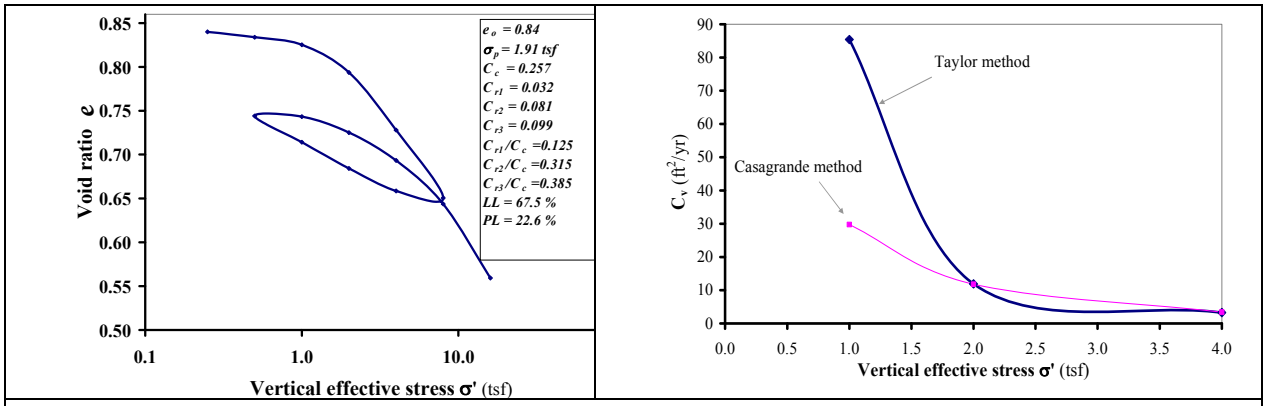

a) SH3 B1 10 – 12 ft (CH)

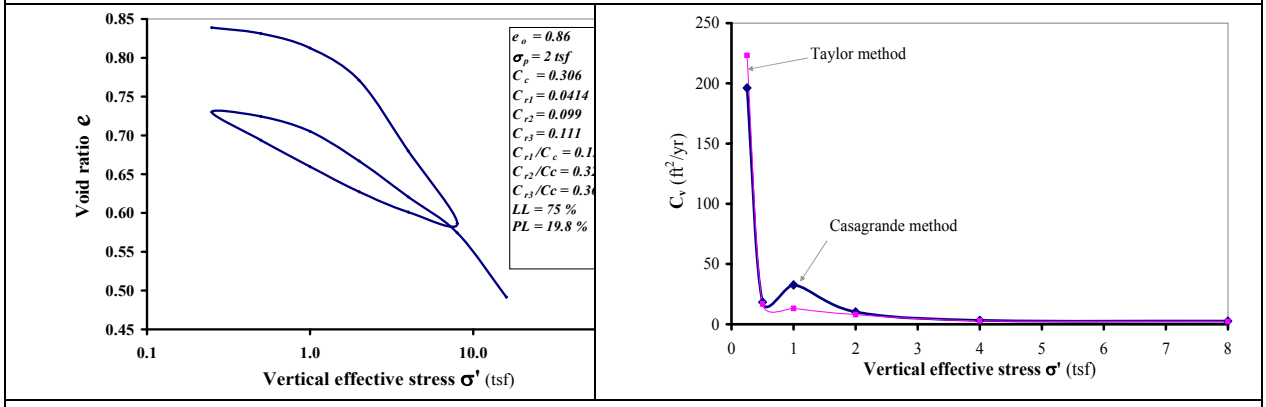

b) SH3 B1 14 – 16 ft (CH)

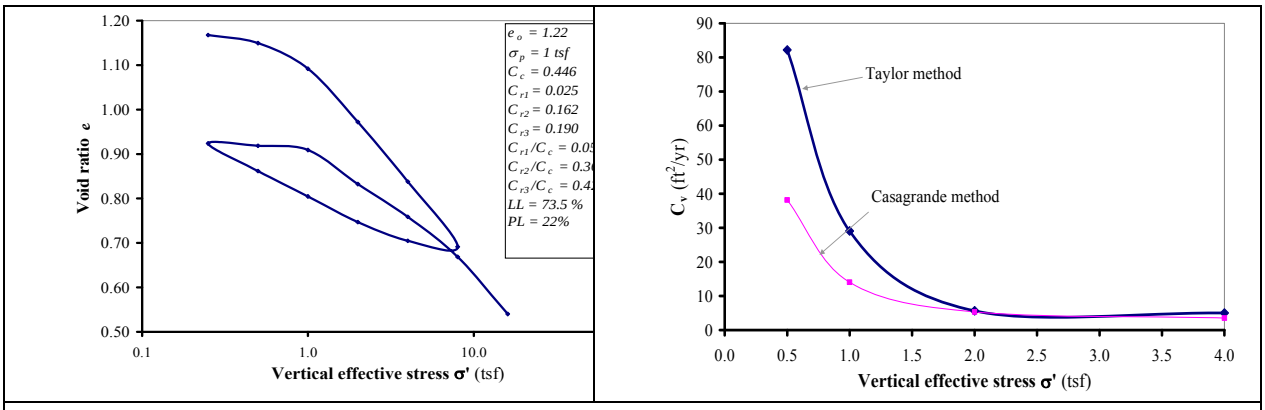

c) SH3 B2 16 – 18 ft (CH)

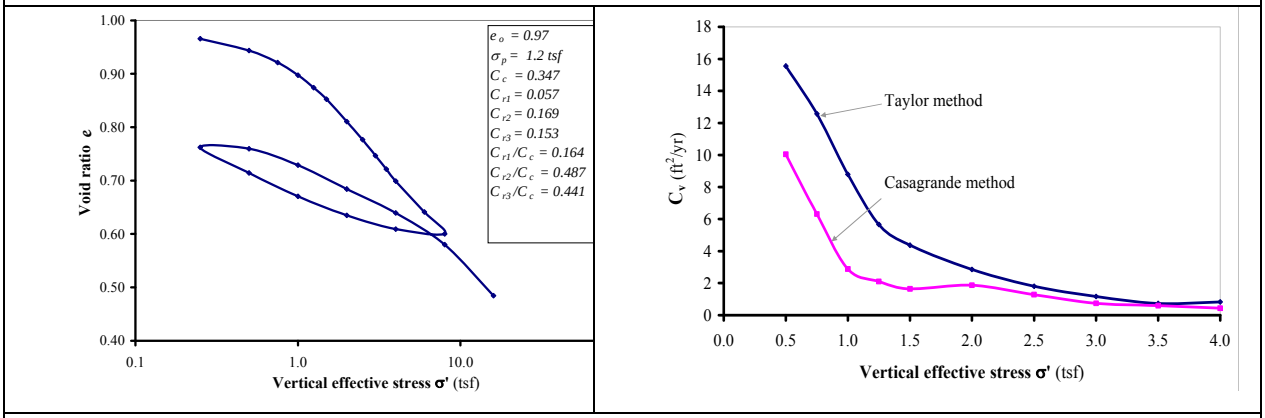

d) SH3 B2 18 – 20 ft (CH)

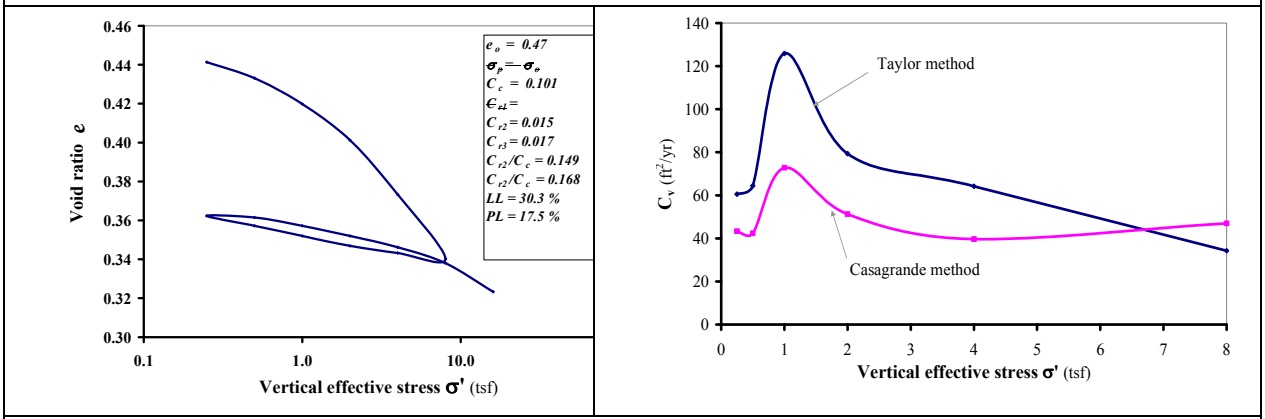

e) SH3 B1 24 – 26 ft (CL)

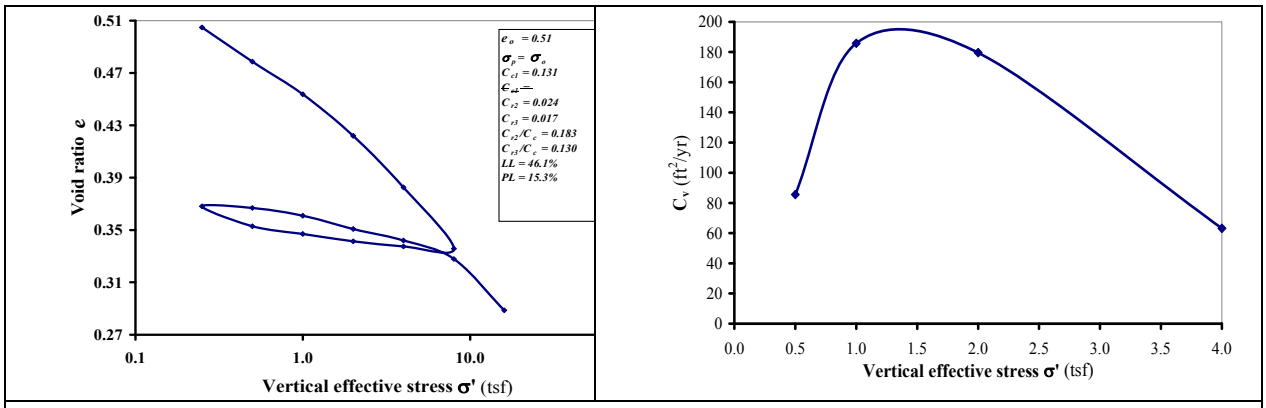

f) SH3 B1 28 – 30 ft (CL)

Fig. 4.24. e – log σ' Curve of a Houston Clay from SH3 and Their Respective C_v – σ' Curve.

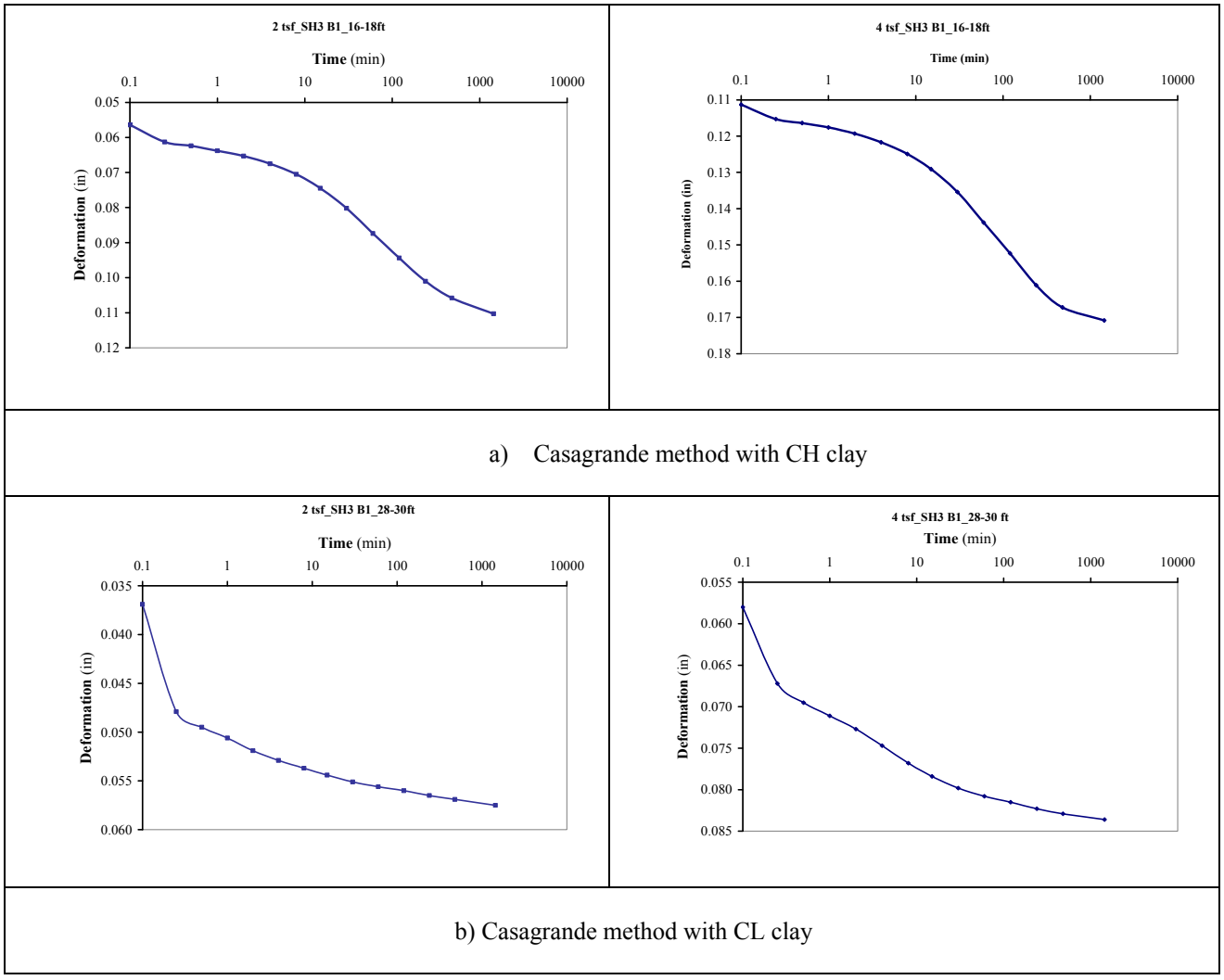

Fig. 4.25. Deformation vs. Time at log Scale Curve of Casagrande T_{50} (a) CH Clay and (b) CL Clay.

4.8. Constant Rate of Strain (CRS) Test (ASTM D 4186-86)

The Constant Rate of Strain (CRS) consolidation test is a faster test to determine the consolidation properties of clay soils than the standard incremental load (IL) consolidation test. The test can be completed, in some cases, in less than 24 hours, and it provides very similar e - log σ' since it is not a function of the applied strain rate (Wissa et al. 1971), as proven using the Houston CH clay (Fig. 4.26).

4.8.1. Strain rate effect on ε- log σ'relationship

The CRS tests were performed at different strain rates (ε) on three specimens from the same Shelby tube sample recovered from the SH3 bridge at Clear Creek Borehole B2 at a depth of 18 – 20 ft. The average strain rate was 0.16%/hr during the IL test.

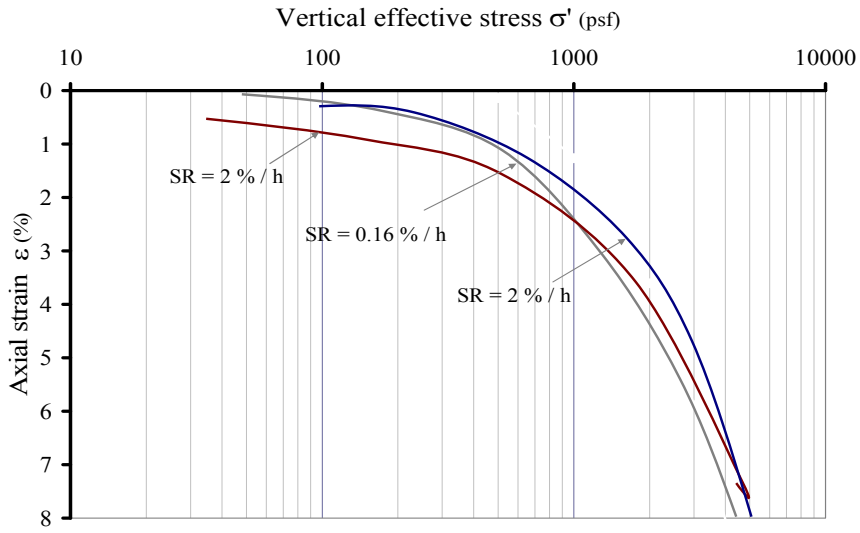

Fig. 4.26. Three ε- log σ' of CRS Tests Performed on Three Specimens from the Same Shelby Tube Sample at Different Strain Rates.

The strain rate was increased from 0.16%/hr to 2%/hr (Fig. 4.26), a rate increase of 12.5 time. The ε- log σ' relationships were very similar as shown in Fig. 4.26.

Consequently, the CRS test can be used for an accurate determination of the preconsolidation pressure, σ_p- compression index, C_c- recompression index, C_r from the obtained ε –log σ' or e –log σ' curve (Fig. 4.27). At the strain rate of 0.025/ hr, the CRS test was completed in less than 24 hrs, but the IL test was completed within 18 days.

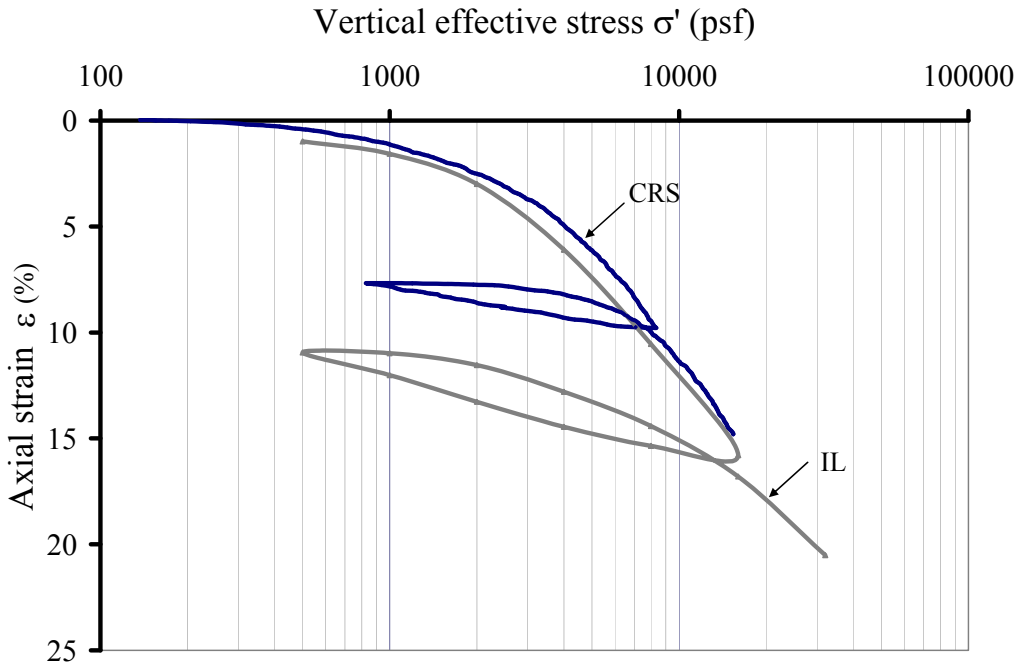

Fig. 4.27. Comparison of CRS Test (ε= *0.025/hr*) and IL Test ε – log σ' Relationship (Test Performed on Two Different Specimens from the Same Shelby Tube Sample Recovered from SH3 at Clear Creek, Borehole B5 at 10 – 12 ft Depth).

4.8.2. Strain rate effect for C_v

The concern with the CRS consolidation test is the determination of a reliable coefficient of consolidation C_v since it depends on the strain rate of the test (Fig. 4.28). The approach of Wissa et al. (1971) and of ASTM D 4186-86 is the specification of the range of the pore water pressure ratio with the effective stress ($\Delta u/\sigma'$) so that the obtained values can comply with the ones obtained from the IL test. As was observed on Fig. 4.29(a) even if the ε – log σ' curve from the CRS and IL test matched, their respective C_v – σ did not match, and the pressure ratio (Fig. 4.29(a)) did not comply with the ASTM preferable values of 3% to 30%.

The coefficient of consolidation is defined as follows (Chapter 2)

$$c_v = -\frac{H^2 \log\left[\frac{\sigma_{v2}}{\sigma_{v1}}\right]}{2\Delta t \log\left[1-\frac{u_b}{\sigma_v}\right]} \qquad 4\text{-}12$$

where:

σ_{v1} = applied axial stress at time t_1

σ_{v2} = applied axial stress at time t_2

H = average specimen height between t_1 and t_2

Δt = elapsed time between t_1 and t_2

u_b = average excess pore pressure between t_2 and t_1, and

σ_v = average total applied axial stress between t_2 and t_1.

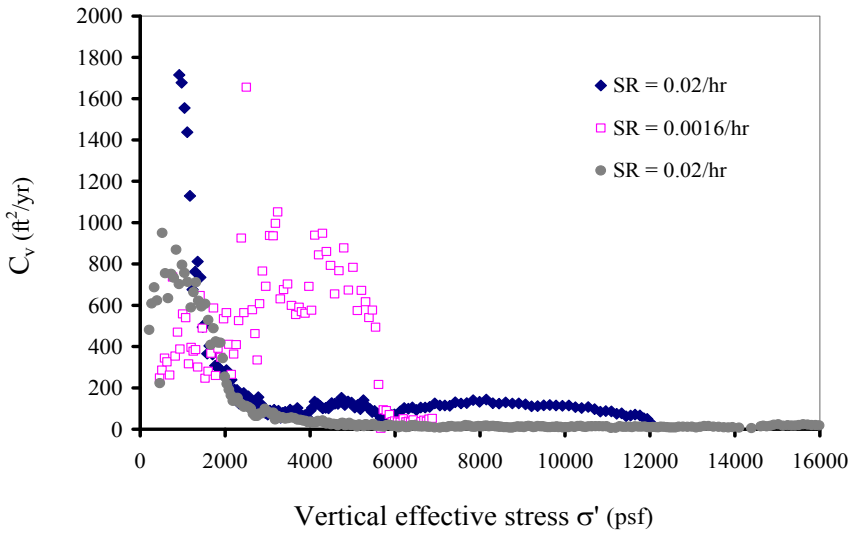

Fig. 4.28. Three C_v- σ' of CRS Tests Performed on Three Specimens (CH Clay) from the Same Shelby Tube Sample at Different Strain Rates.

Since the strain rate cannot be modified during the CRS consolidation test to fit the required pressure ratio, a correlation needs to be developed for each type of soft clay

to define the convenient strain ε, as presented by Dobak (2003). This needs to be done for the Houston clay.

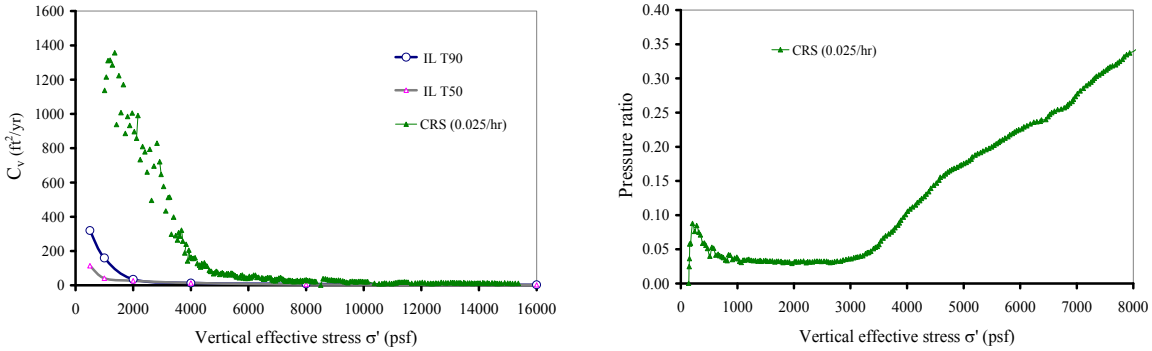

a.) b.)

Fig. 4.29. (a) Comparison of CRS Test (ε= *0.025/hr*) and IL Test C_v– σ' Curve (Test Performed on Two Different Specimens from the Same Shelby Tube Sample Recovered from SH3 at Clear Creek, Borehole 5 at 10 – 12 ft Depth); and (b) Pressure Ratio vs. Vertical Effective Stress Corresponding to the CRS Test.

4.9. Summary

Over 40 consolidation tests and 50 unconfined compression tests were performed to characterize the soils for SH3 and NASA Rd. 1 sites. The soil deposits are deltaic and some properties had notable differences between the new (current study) and old data (TxDOT reports).

Based on the laboratory study the following can be concluded:

(1) Since the increase in the in-situ stresses due to the embankment are relatively small (generally less than the preconsolidation pressure), using the proper recompression index is import. Since there is a large hysteresis loop during the unloading-reloading of the soft CH clays, three recompression indices (C_{r1}, C_{r2}, C_{r3}) have been identified. Review of the TxDOT design indicates that there is no

standard procedure to select the recompression index. It is recommended to use recompression index, C_{r1}, to determine the settlement up to the preconsolidation pressure.

(2) The consolidation parameters (C_c, C_r, C_v) are all stress dependent. Hence, when selecting representative parameters for determining the total and rate of settlement, expected stress increases in the ground should be considered. In estimating C_v, the Casagrande's T_{50} gives a lower value than T_{90}. C_v is relatively high before the preconsolidation pressure and notable reduction was observed thereafter.

(3) The Constant Rate of Strain (CRS) test can be used to determine the consolidation properties of clay soils. The rate used in the test influenced the coefficient of consolidation.

(4) Linear and nonlinear relationships have been developed to represent the compression index (C_c) in terms of moisture content and unit weight.

5. FIELD STUDY

5.1. Introduction

In order to verify the applicability of the conventional 1-D consolidation theory to predict the total and rate of settlement of embankments on soft clays, it was necessary to monitor the settlement of embankments in the field. Based on the current condition and accessibility, two embankments were selected. The selected locations are as follows:

(a) SH3 bridge embankment at Clear Creek (Project 3)

SH3 is a four-lane north-south highway (parallel to Interstate I45). The retaining wall at Clear Creek on the east side showed tremendous distress with multiple cracked panels and displaced joints. The embankment, about 14 years in service and sitting on very soft clay, was bulging on the east side of SH3.

(b) NASA Rd. 1 at Taylor Lake (Project 4)

This is a six-lane east-west highway (perpendicular to Interstate I45) with the three lanes supported on an embankment and the other three supported on piles across the Taylor Lake. The pavement supported on the embankment has settled about 2.5 in. over the years. This embankment has been in service for over seven years.

The field investigation for both sites included the following:

- site investigation
- field instrumentation and monitoring
- analyses of the data and comparing it to conventional consolidation theory.

It should be mentioned that in both locations there were no permanent reference points to determine how much the embankments have settled over their service life.

Hence, all the reported displacements (vertical and lateral displacements) are relative to the new set references at the starting date of the monitoring.

As field monitoring devices, the following instruments were used:

- 30 to 40 ft long extensometers to measure vertical settlements
- inclinometer for lateral displacements
- piezometers for measuring the pore water pressure
- demec points for retaining wall movements
- retaining wall rotation monitoring marks
- tensiometer for measurement of suction pressure.

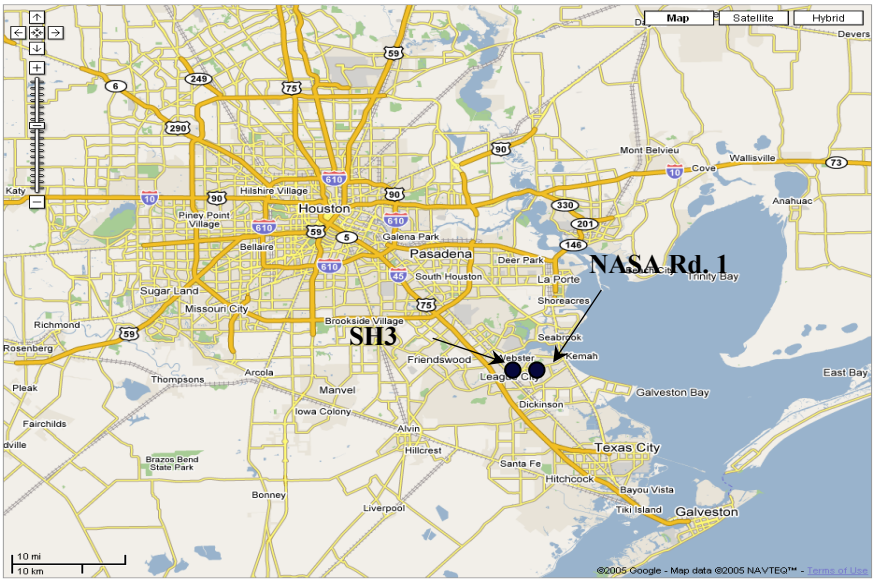

Fig. 5.1. Location of the Instrumented Embankment Sites.

5.2. Site History and Previous Site Investigation

5.2.1. SH3 at Clear Creek Bridge and Clear Creek Relief Bridge (Project 3)

For widening the roadway and the bridges over Clear Creek and Clear Creek Relief in 1971, seven soil borings were completed between September and October

1965. In February, March, and September of 1984, seven new borings were completed for the widening and elevating of the North Bridge (NB) roadway, for the construction of retaining walls at the NB roadway and bridge approaches. Finally, one boring was completed in November 1991 for the removal and replacement of the South Bridge (SB) and for the construction of retaining walls at the SB Clear Creek Relief bridge approaches in December 1993. A site visit in October 2006 showed that the retaining wall panels have developed multiple cracks and the some of the panel joints are misaligned indicating some form of ground movement.

Fig. 5.2. Sampling and Instrumenting at the SH3 Site (January 2007).

5.2.2. NASA Road 1 embankment at Taylor Lake

NASA Road 1 between Annapolis and Taylor Lake St. is a combination of a bridge on piles and a roadway on an embankment (Fig. 5.3). Both the bridge and roadway were built in 2000, and from the report of TxDOT, the roadway supported on embankment has settled more than 2.5 in. since then.

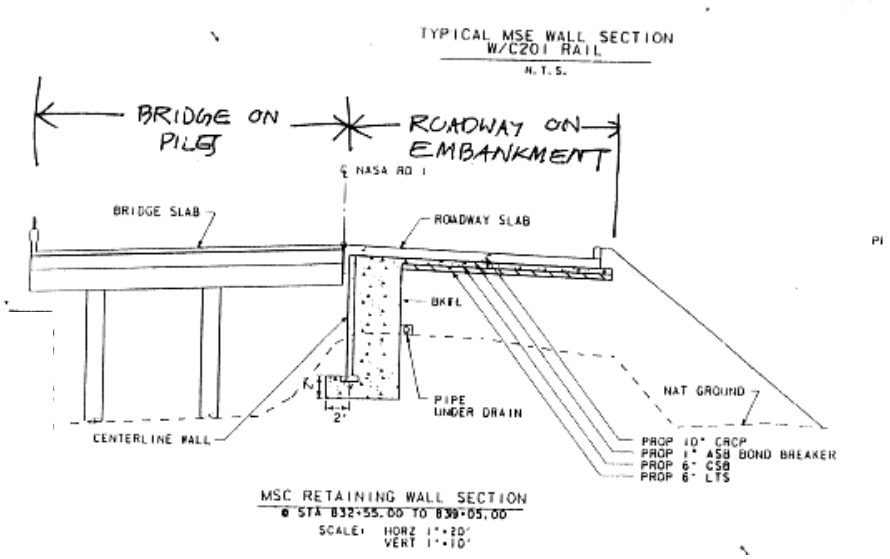

Fig. 5.3. Cross Section of the NASA Road 1 Embankment (Project 4).

5.3. Instrumentation

5.3.1. Extensometer

The vertical settlement devices were developed and built at the University of Houston. The devices measure the total settlement in the layer of height H (Fig.5.4).

When $\Delta\delta = \delta_1^{final} - \delta_1^{initial} < 0$ (-) the soft soil layer is settling.

When $\Delta\delta = \delta_1^{final} - \delta_1^{initial} > 0$ (+) the soft soil layer is expanding.

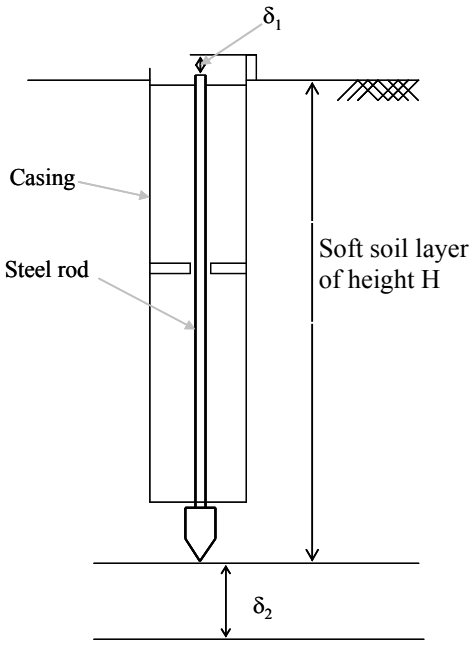

Fig. 5.4. Schematic of the Extensometer.

5.3.2. Operating principles of the inclinometer

Inclinometers are used to measure ground movement in unstable slopes and the lateral movement of ground around ongoing excavations. Inclinometers also monitor the stability of embankments, slurry walls, the disposition and deviation of driven piles or drilled boreholes, and the settlement of ground in fills, embankments, and beneath storage tanks. In this case, an inclinometer was used to monitor the lateral movement of Boreholes B2 and B4. The movement is a reflection of the embankment stability.

An inclinometer casing was installed in the ground and grouted. The inclinometer casing had four orthogonal grooves inside the casing (Fig 5.5(b)) designed to fit the wheels of a portable inclinometer probe (Fig 5.5(a)). This probe, suspended on the end of a cable connected to a readout device, was used to survey the inclination of the casing with respect to vertical (or horizontal), and in this way to detect any changes in inclination caused by ground movements.

The inclinometer probe is composed of two accelerometers with their axes oriented at 90° to each other. The A axis is in line with the wheels with the B axis orthogonal to it. Thus, during the survey, as the A+, A- readings were obtained; the B+, B- readings were also recorded. The inclinometer probe used in this study was manufactured by GEOKON Company. The readout box from the same company was used to collect the data.

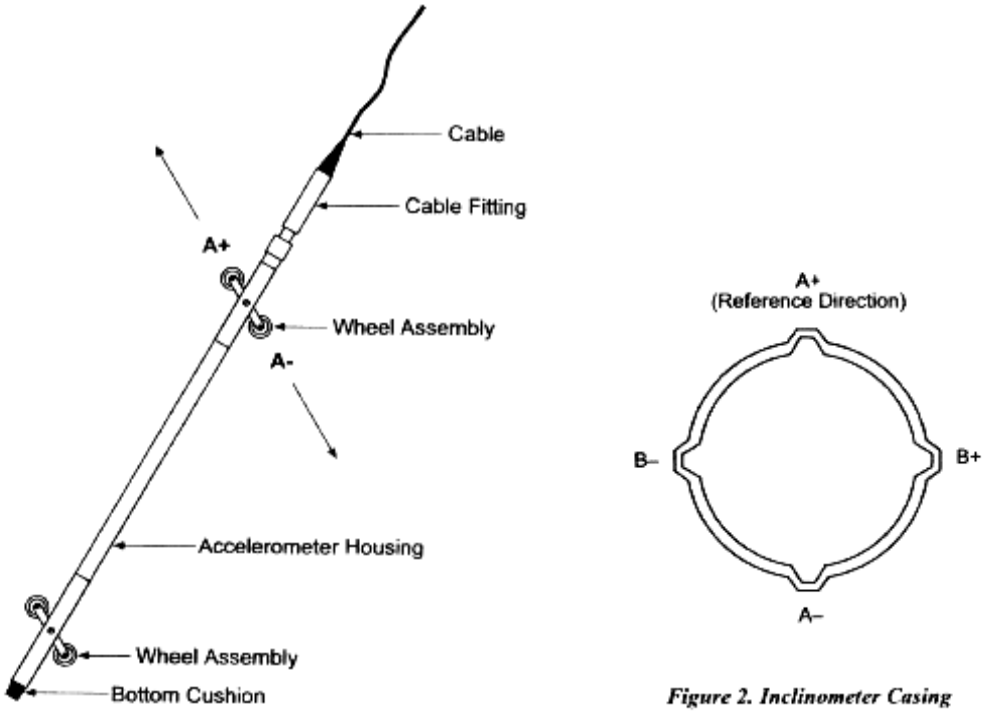

Figure 2. Inclinometer Casing

a) b)

Fig. 5.5. (a) Inclinometer Probe (Geokon Inc 2007) and (b) Inclinometer Casing.

5.3.3. Principles of the demec points

Demec points are fixed metallic discs glued on any surface in different configurations around a crack to monitor its movement (Fig. 5.6). In this study, demec

points were placed around the cracks on the retaining walls on SH3 to monitor their movements.

Fig. 5.6. Demec on the Embankment Retaining Wall (Project 3).

5.3.4. Tensiometer

Direct measurement of matric suction in a borehole can be made by using a tensiometer. A tensiometer consists of a tube with a porous ceramic tip on the bottom, a vacuum gauge near the top and a sealing cap. When tensiometer is filled with water and inserted into the soil, water can move into and out of the tensiometer through the connecting pores in the tip. As the soil dries and water moves out of the tensiometer, it creates a vacuum inside the tensiometer, which is indicated on the gauge. When the vacuum created just equals the 'Soil Suction,' water stops flowing out of the tensiometer. The dial gauge reading is then a direct measure of the force required for removing water from the soil. If the soil dries further, additional water moves out until a higher vacuum level is reached. Because water can move back and forth through the pores in the porous ceramic tip, the gauge reading is always in balance with the soil suction.

5.4. NASA Road 1 Embankment Instrumentation

The NASA Road 1 roadway between Annapolis and Taylor Lake St embankment was instrumented in April 2007. A total of four borings were performed (UH1, UH2, UH3, and UH4) and instrumented:

- Boreholes UH1 and UH3 were instrumented with sondex settlement devices.
- Boreholes UH2 and UH4 were each instrumented with a piezometer and an extensometer.

5.5. SH3 Embankment Instrumentation and Results

The SH3 embankment at Clear Creek was instrumented in January 2007 and was been monitored for 18 months.

5.5.1. Site instrumentation

In January 2007, the field was (Fig. 5.7) instrumented as follows:

- Boreholes B2 and B4 were instrumented with inclinometer casings, up to 30 ft deep, to monitor any lateral displacement of the embankment. Borings B2 and B4 were drilled, 5'4'' and 5'6'', respectively, from the embankment retaining wall.
- Boreholes B1, B3, and B5 were instrumented with extensometers made at the University of Houston and piezometers, up to 30, 20, and 20 ft, respectively. Boreholes B1, B3, and B5 were drilled at 5'1'', 5'3'', and 5'9'', respectively, from the retaining wall.
- Section 1 to 2 of 80 ft on the retaining wall (Fig. 5.7) had a number of cracks and the main section was instrumented with demec points. Figure 5.8 shows the schematic view of the instruments used.

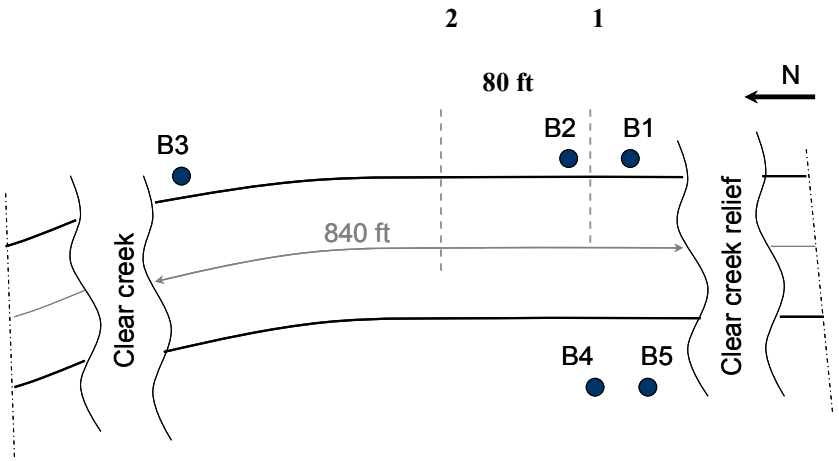

Fig. 5.7. Plan View of SH3 at Clear Creek with the New Boring Locations.

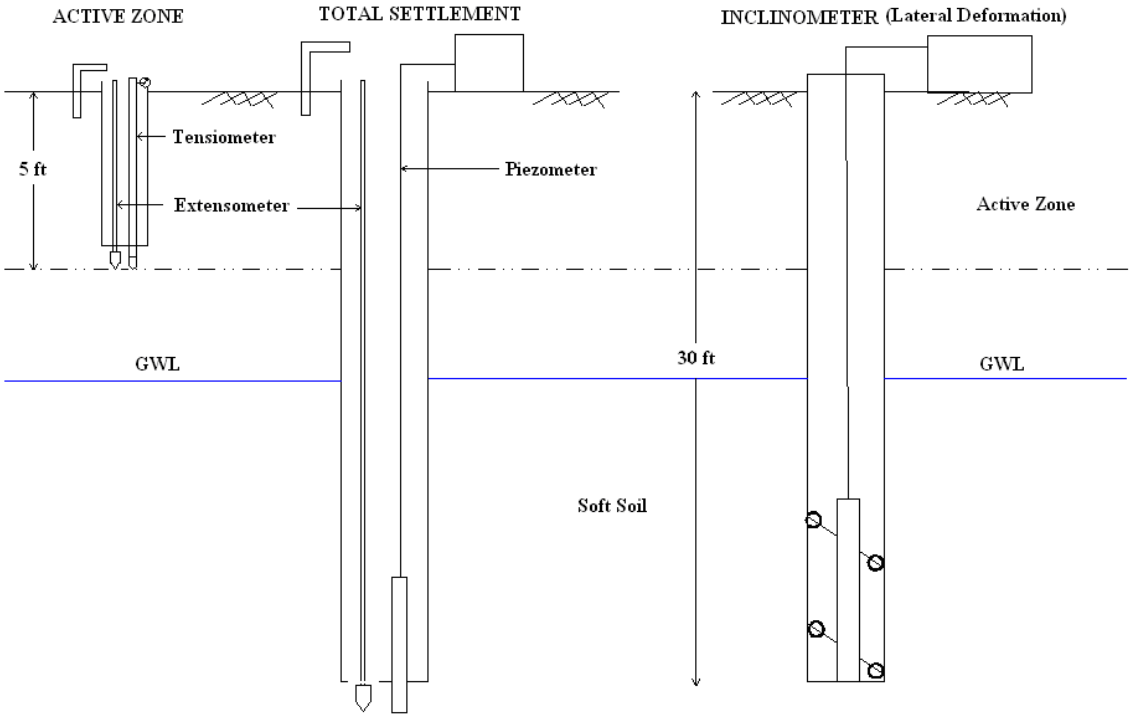

Fig. 5.8. Schematic View of Instruments Used in SH3.

5.5.2. Monitoring results

East Side of SH3

- **Groundwater Level**

The groundwater level varied during the monitoring period as shown in Fig. 5.9. It was influenced by the weather and the water level in Clear Creek. The ground water level fluctuated by 20 in. (equivalent to 0.72 psi) over the monitoring period.

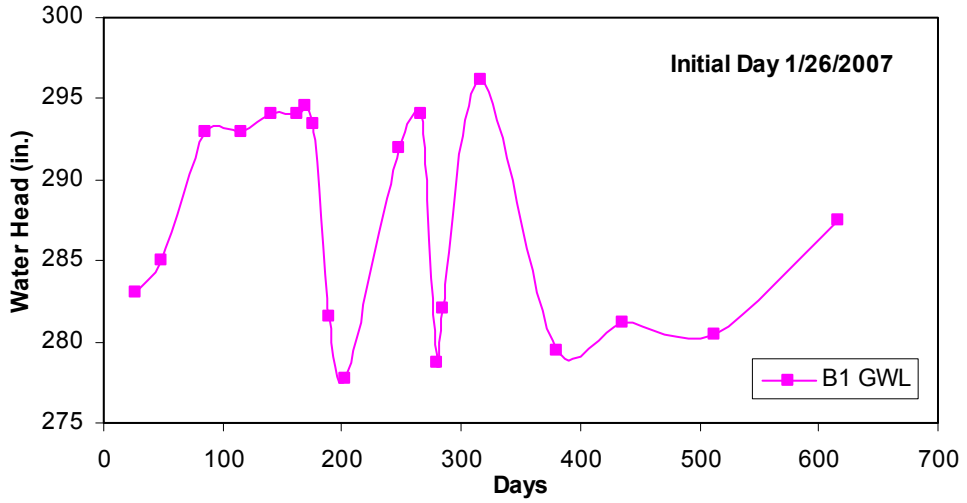

Fig. 5.9. Groundwater Table Variation with Time (Reference is the Bottom of the Casing at 30 ft Deep as Reference at Boring B1).

- **Inclinometer**

In the presentation of the embankment lateral movement from the inclinometers reading (Fig. 5.10), the Y-axis is the origin (Day 0 reading). The inclinometer reading had accuracy of $6x10^{-4}$ in.

From the Boring B2 reading, lateral displacement from Day 0 (installation day) to Day 24 due to the installation and the cement grout setting time. (The cement grout reached its optimum setting in 28 days). Inclinometer surveys were intermittently taken for 490 days after setting of the grout. Figure 5.11 shows the lateral movement in the

Borehole B2. From Fig. 5.10, it was determined that the soil moved laterally away from the wall by about 0.4 in. in the top 5 ft and the lateral movement substantially diminished below the 5 ft level to about 0.1 in. A displacement of 0.02 in. was recorded at a depth of 28 ft (Fig. 5.10).

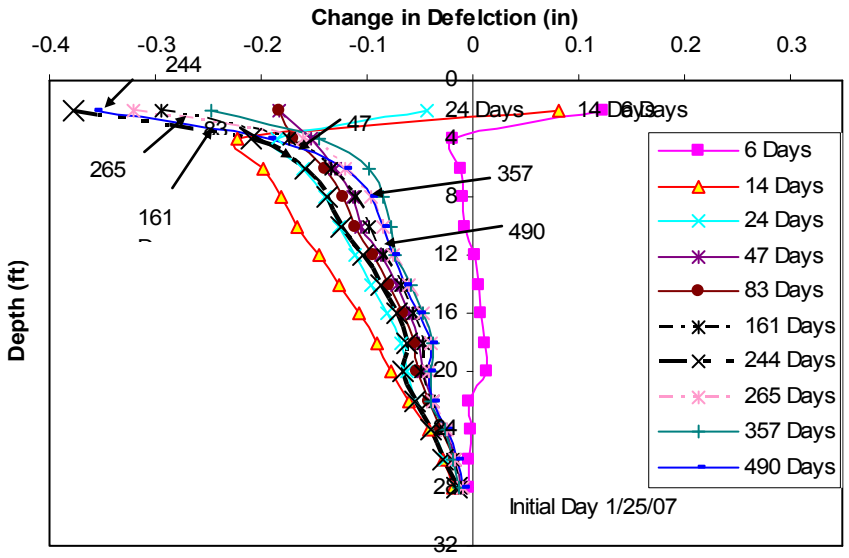

Fig. 5.10. Inclinometer Reading at Boring B2 (SH3).

- **Extensometer Response**

It must be noted that the extensometer will record the movement in the ground (Active Zone and consolidation included) over a height of 30 ft. At Boring B1, the ground initially expanded to 0.10 in. between the installation day and three months thereafter. Then the ground settled to 1.0 in. (Fig. 5.11). After 300 days, the trend was reversed. Over the period of measurement the extensometer readings were cyclic (heave and settlement). A similar pattern of ground movement was measured in Borehole B3 (Fig. 5.12). The components of the settlements must be separated to better interpret the results. The accuracy of the Vernier caliper used for the measurement was 0.004 in.

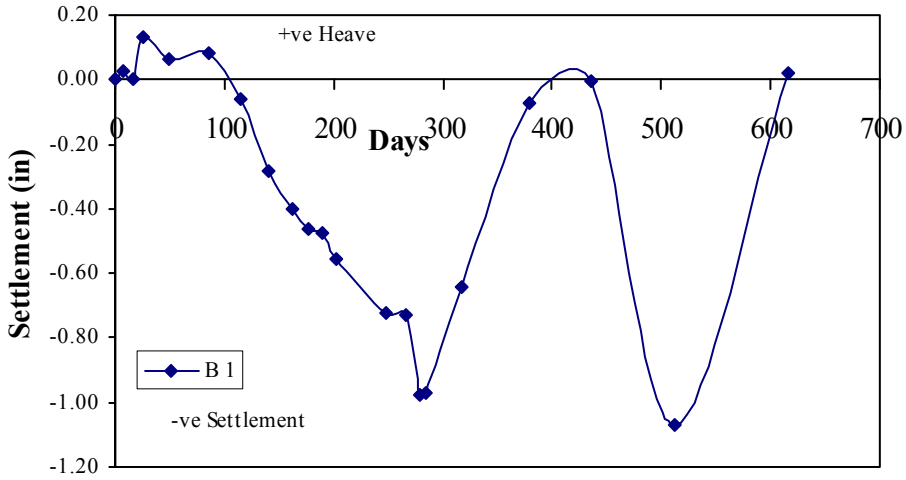

Fig. 5.11. Measured Relative Displacement with Time at Boring B1.

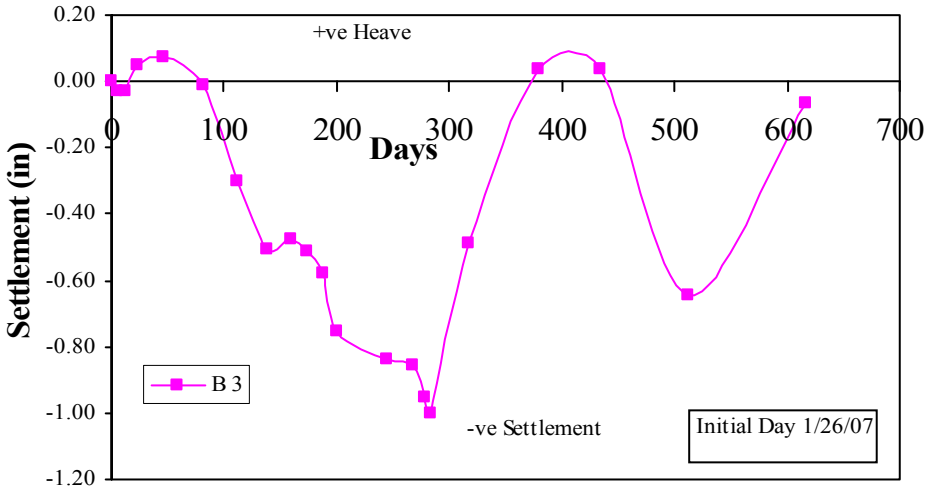

Fig. 5.12. Measurement of Vertical Displacement with Time at Boring B3.

- **Pore Water Pressure**

The initial pore water pressure was 9.8 psi in Borehole B1, and it slightly increased and decreased over 600 days of monitoring. The minimum and maximum pore water pressures measured were 9.5 psi and 10.5 psi, respectively. It must be noted that the hydrostatic pressure measured from the height of the water table was slightly higher

than the pore water pressure in the soil (Fig. 5.13). If the soil is consolidating the trend should have been reversed.

Based on 1-D consolidation theory, the excess pore water pressure (u_i) at a depth of 30 ft is equal to $0.676\Delta\sigma'$ where $\Delta\sigma'$ is 475 psf (Table 3.16). Hence the excess pore water pressure in the soil should be about 2.23 psi higher than the surrounding hydrostatic pressure; but this was not the case and the pore water pressure measurement did not indicate consolidation because the pore water pressure transducer was located in the CL soil close to the bottom drainage. The accuracy of the piezometers was 0.002 psi.

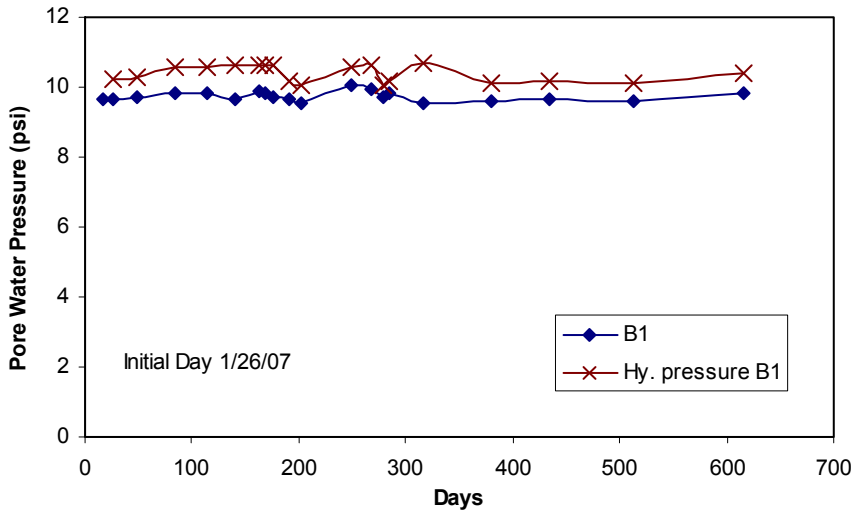

Fig. 5.13. Pore Water Pressure Variation with Time at Boring B1 (Project 3).

The initial pore water pressure was 6.15 psi in Borehole B3, and it slightly increased and decreased over 600 days of monitoring. The minimum and maximum pore water pressures measured were 5.8 psi and 6.5 psi, respectively. As measured in Borehole B1, the hydrostatic pressure measured in Borehole B3 from the height of the water table was slightly higher than the pore water pressure in the soil (Fig. 5.14). This may be due to

the fact that the pore water pressure transducer was located in the CL soil close to the bottom drainage.

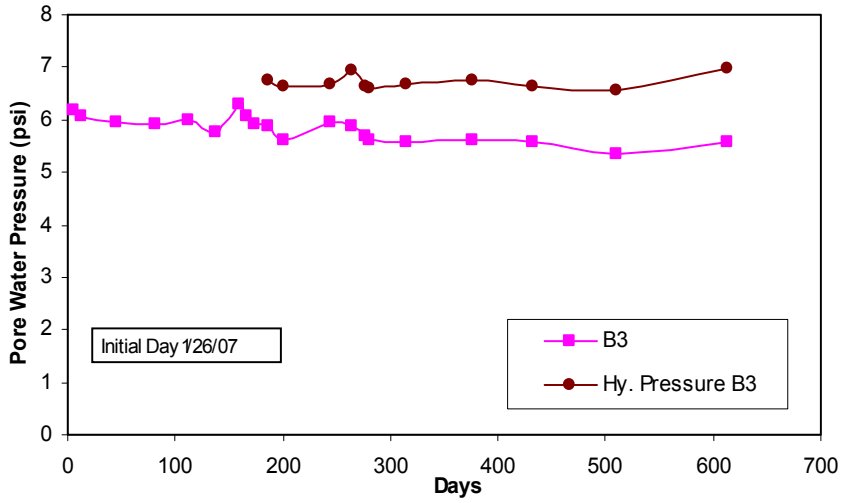

Fig. 5.14. Pore Water Pressure Variation with Time at Boring B3.

West Side of SH3

- **Groundwater Level**

The groundwater level varied during the monitoring period as shown in Fig. 5.15. It was influenced by the weather and the water level in Clear Creek. The ground water level fluctuated by 23 in. (equivalent to 0.83 psi) over the monitoring period.

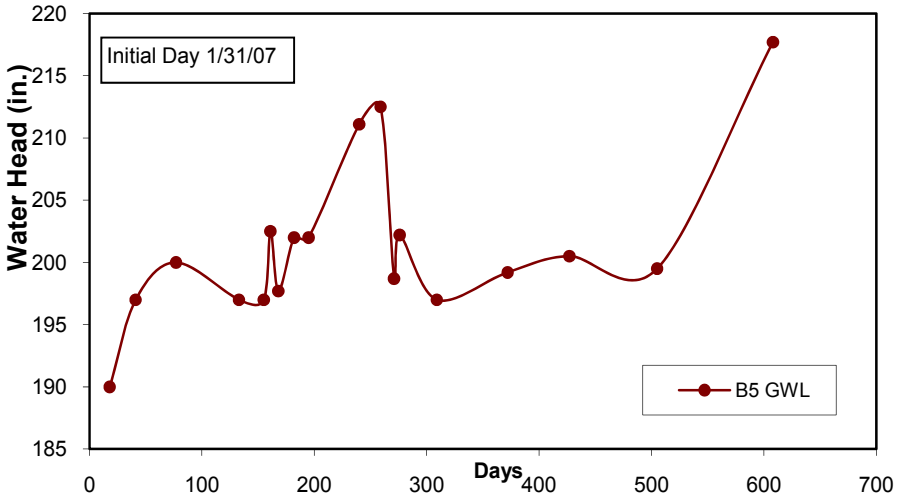

Fig. 5.15. Water Table Variation with Time (Bottom of the Casing at 20 ft Deep as Reference in Boring B5) (Project 3).

- **Inclinometer**

From the Boring B4 reading, the inclinometer casing had a lateral displacement from Day 0 (installation day) to Day 23 due to the installation and the cement grout setting time (the cement grout reaches its optimum setting in 28 days). A total lateral displacement of 0.3 in. towards the embankment was recorded near the ground surface. A relatively large lateral movement was observed in the top 5 ft as seen in Borehole B2. The bottom of the casing, at 28 ft depth, can be considered static (Fig. 5.16). Very small lateral movements in the soft soil region indicate no slope stability failure potential of the embankment. This rules out the possibility of any failure that could also add to the settlement of the embankment.

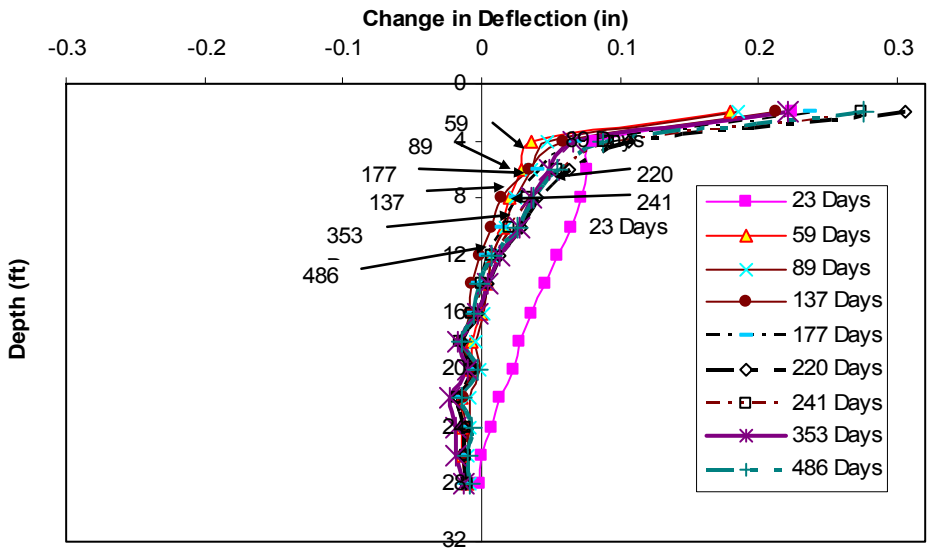

Fig. 5.16. Inclinometer Reading at Boring B4 (SH3).

- **Extensometer Response**

It must be noted that the extensometer will record the movement in the ground (Active Zone and consolidation included) over a height of 20 ft. At Boring B5, the soil settled 0.06 in. three months after installation (Fig. 5.17) and then expanded to less than 0.025 in. two months later. Over the period of measurement the extensometer readings were cyclic (heave and settlement). A similar pattern of ground movement was measured in Boreholes B1 and B3 (Fig. 5.11 and Fig. 5.12), but B5 had more fluctuation. The components of the settlements must be separated to better interpret the results.

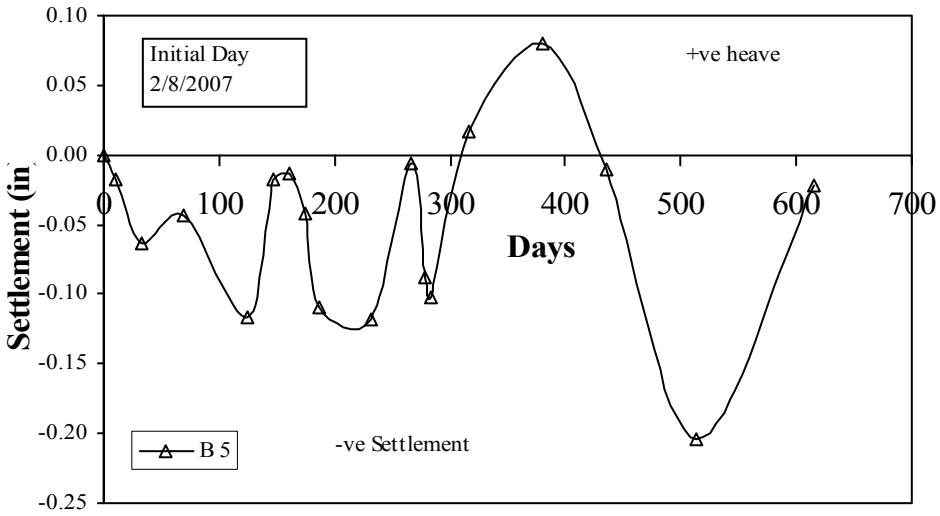

Fig. 5.17. Measured Relative Displacement with Time at Boring B5.

- **Pore Water Pressure**

The initial pore water pressure was 6.7 psi in Borehole B5, and it slightly increased and decreased over 600 days of monitoring. The minimum and maximum pore water pressures measured were 6.5 psi and 7.0 psi, respectively. It must be noted that the hydrostatic pressure measured from the height of the water table was slightly higher than the pore water pressure in the soil (Fig. 5.18). If the soil is consolidating, the trend should have been reversed. This may be due to the fact that the pore water pressure transducer would have been located close to the bottom drainage.

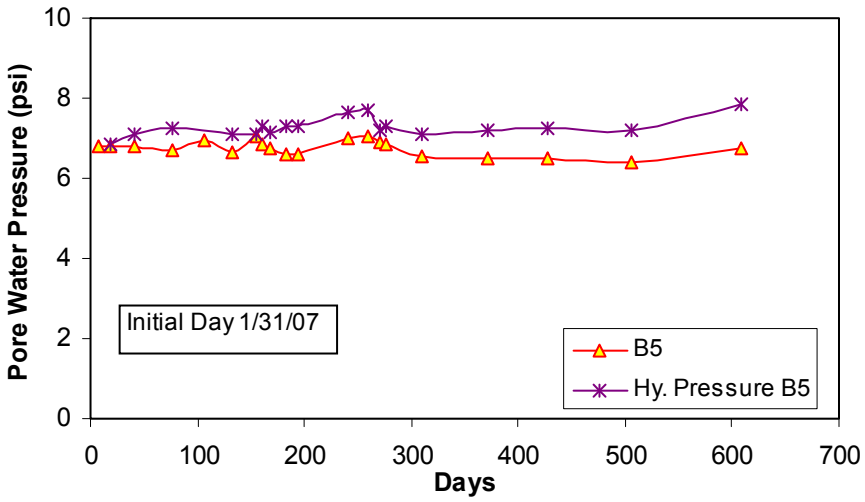

Fig. 5.18. Pore Pressure Variation with Time at Boring B5.

- **Tensiometer**

Two tensiometers with extensometers were installed to a depth of 5 ft to measure the matric suction and the settlement in the Active Zone near boreholes B2 and B3. Fig. 5.19 shows the suction pressure measured. Fig. 5.20 shows the settlement measured within the Active Zone.

During dry weather, the soil will shrink and the suction pressure will increase, the ground will settle and the extensometer reading will be negative. During wet conditions, suction pressure will decrease, the ground will swell and the extensometer reading will be positive. The maximum suction measured during dry and wet weather conditions were 77 kPa and 10 kPa, respectively. The corresponding vertical settlement and swelling in the soil measured by the extensometer were -0.2 in. (settlement) and 0.8 in. (ground heave), respectively.

In order to understand the drying and wetting phenomena in the soil, the measured data of rainfall and temperature are shown in the Fig. 5.21. The maximum average

rainfall occurred during the months of January to March with average monthly precipitation from 3 to 8 in. (75 mm to 200 mm). The 8-inch (200 mm) rainfall was reported during Hurricane Ike. This was reflected in the reduced suction pressure and swelling of the ground due to the increased moisture content. There was no extreme effect on the suction pressure and swelling due to Hurricane Ike. The maximum temperature was recorded during the months of May and June with temperatures of 84.7 ^{o}F and 79.5 ^{o}F, respectively. High temperature results in reduced ground moisture, higher suction pressure, and settlement (Figs. 5.19 and 5.20).

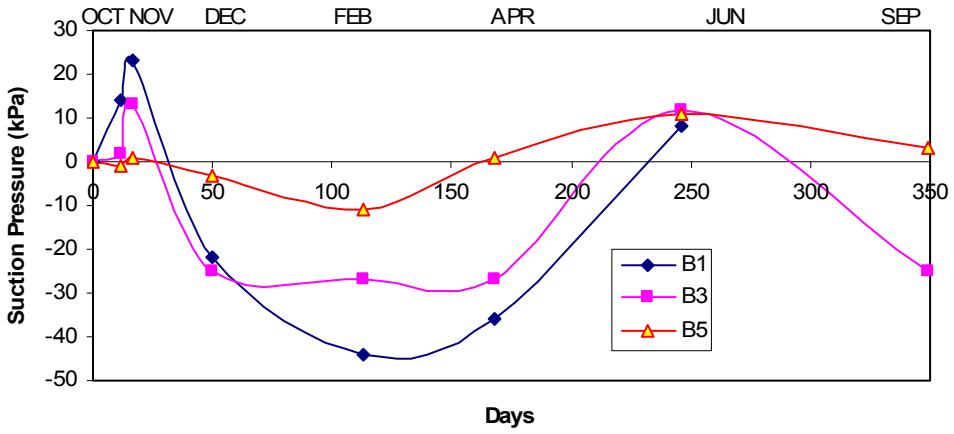

Fig. 5.19. Change in Suction Pressure.

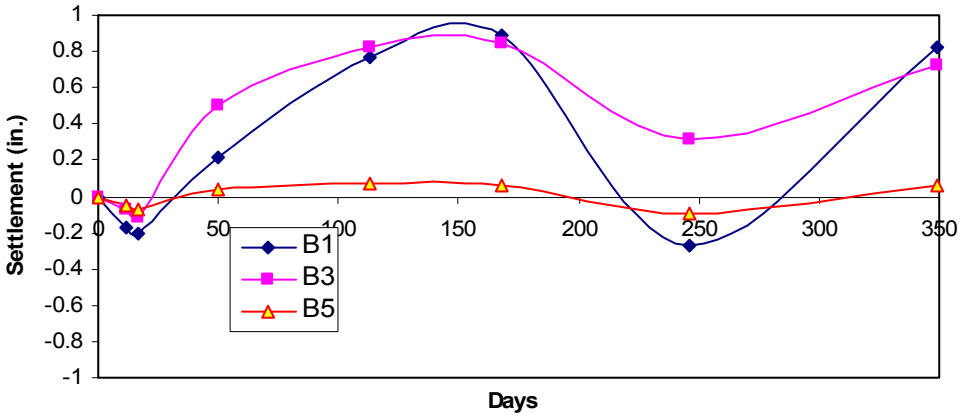

Fig. 5.20. Variation in Settlement in Active Zone.

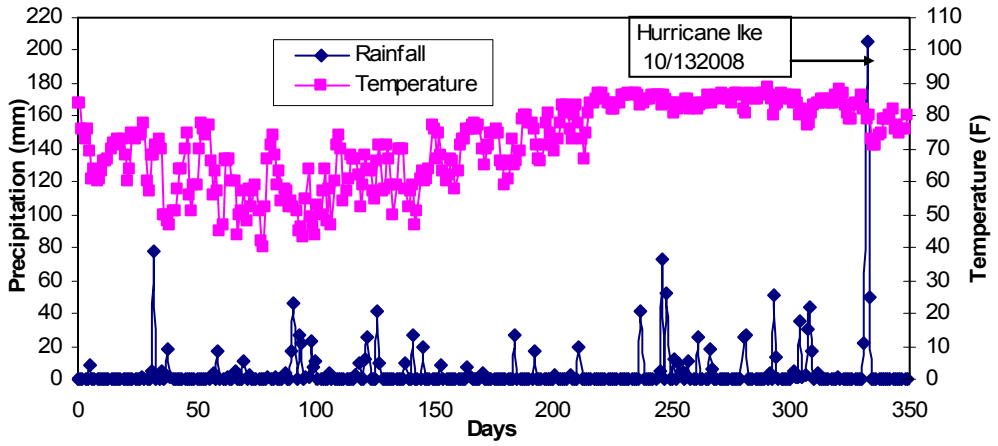

Fig. 5.21. Measured Rainfall and Temperature for the Houston (www.weather.gov).

- **Consolidation Settlement**

As mentioned before total settlements were measured using the long extensometers in Boreholes B1, B3 and B5. The consolidation settlement was determined by subtracting the Active Zone movement from the total settlement. Figure 5.22 shows the measured consolidation settlement over a period of a year and the consolidation settlement varied from 0.06 to 0.10 in.

Conventional consolidation theory predicted continuous consolidation settlement at this site. This was observed at the SH3 at Clear Creek embankment. Consolidation settlement measured over a period of 12 months at the edge of the embankment at the Clear Creek Bridge at SH3 varied from 0.08 to 0.10 inches after making the correction for the Active Zone. Based on the conventional consolidation theory, the settlement between 14 and 15 years will be in the range of 0.02 in. to 0.03 in. (Chapter 3), which was close to what was measured in the field. The difference between the measured and predicted consolidation settlement could be partly due to the Active Zone correction.

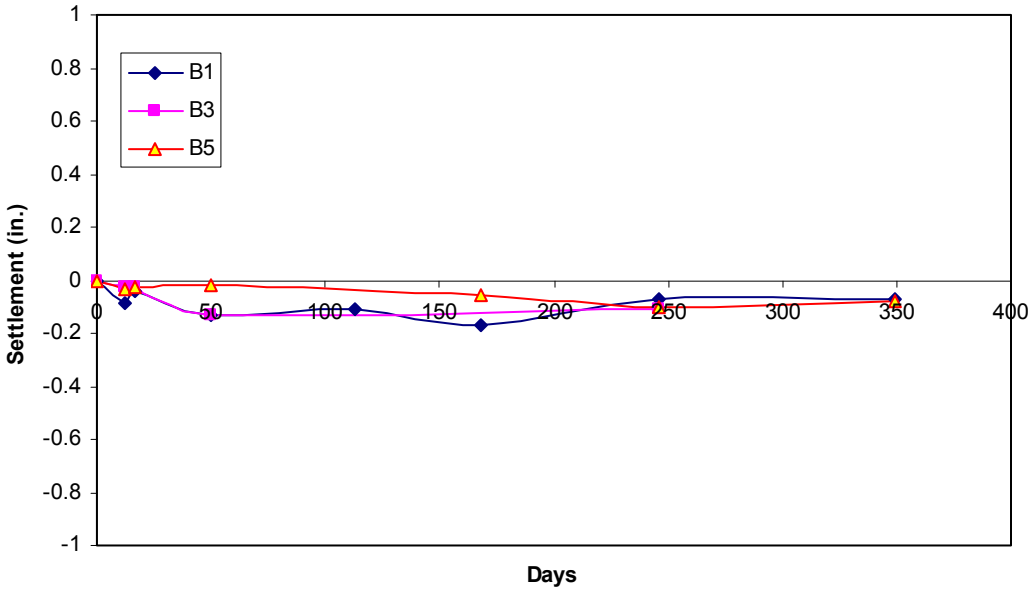

Fig. 5.22. Variation of Consolidation Settlement (Project 3).

- **Demec points**

Four of the configurations in Fig. 5.23(a) and 11 configurations 5.23(b) were installed. Eighteen months after the installation of the demec points on the retaining wall, particularly in Section 1-2 (Fig. 5.7), the measured changes in distance between the cracks and the retaining wall panels were between -0.08 in. and 0.12 in. (Fig. 5.24 and Fig. 5.25). The changes in the crack opening and closing over time can be related to the movement in the Active Zone. Compared to the Active Zone movement, the consolidation settlement is small and will have minimal effect on the panel cracking. The accuracy of the Vernier caliper used for measurement was 0.001 in.

a) b)

Fig. 5.23. Picture View of Demec Points on the Wall: a) for Wall Panel Displacement Monitoring and b) Crack Opening Monitoring (Project 3).

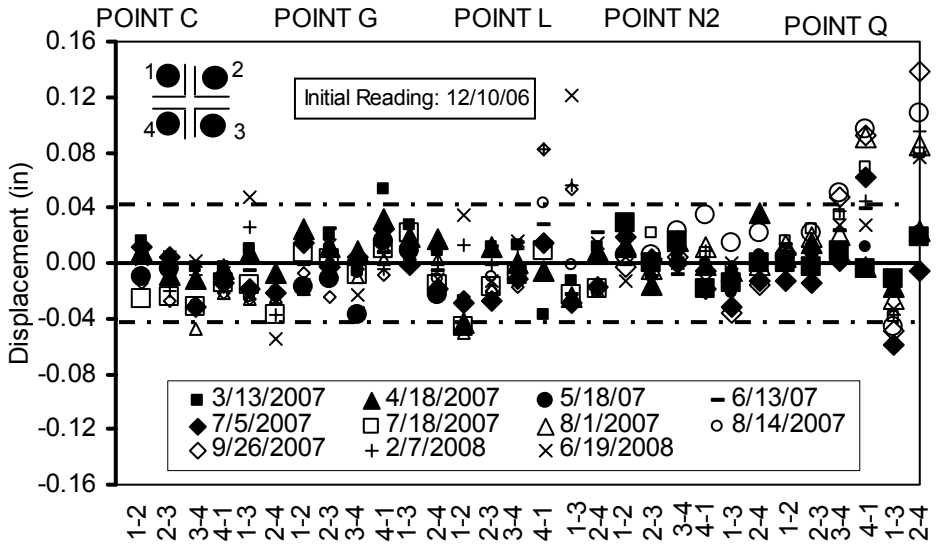

Fig. 5.24. Relative Displacements of the Wall Panels along the Embankment.

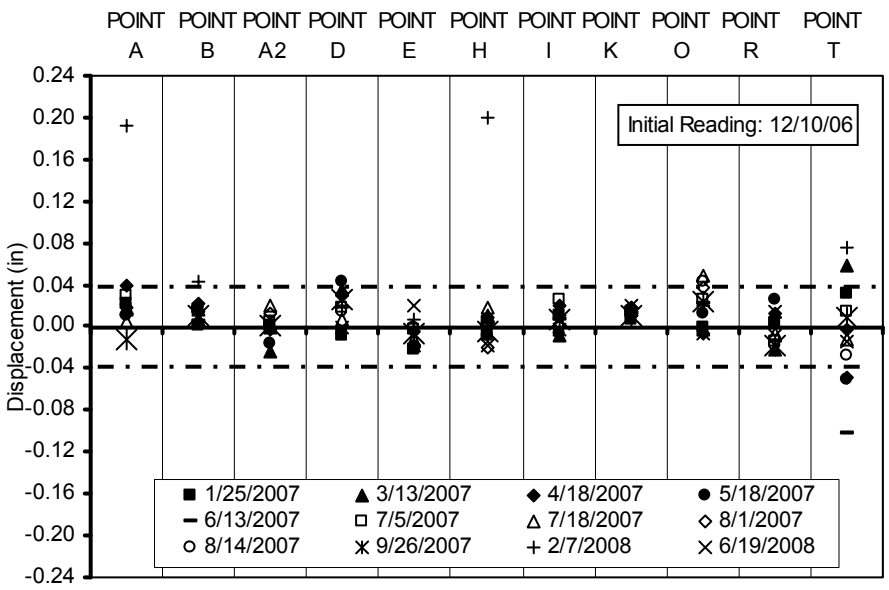

Fig. 5.25. Change in the Crack Opening along the Wall.

- **Wall rotation**

The wall was bulging at a few locations on the east side of SH3. The changes in the vertical alignment (rotation angle) of the panels were measured using a digital level. Eleven of the wall rotation monitoring marks were placed along the retaining wall (Figs. 5.26 and 5.27). The wall rotation at all 11 marks, within 550 days of monitoring varied between -1.0° and 1.0°, and the accuracy of the leveler was 0.1°. The wall panel rotations could be better related to the movements in the Active Zone.

Fig. 5.26. View of L2 Rotation Monitoring Mark Line on the Retaining Wall.

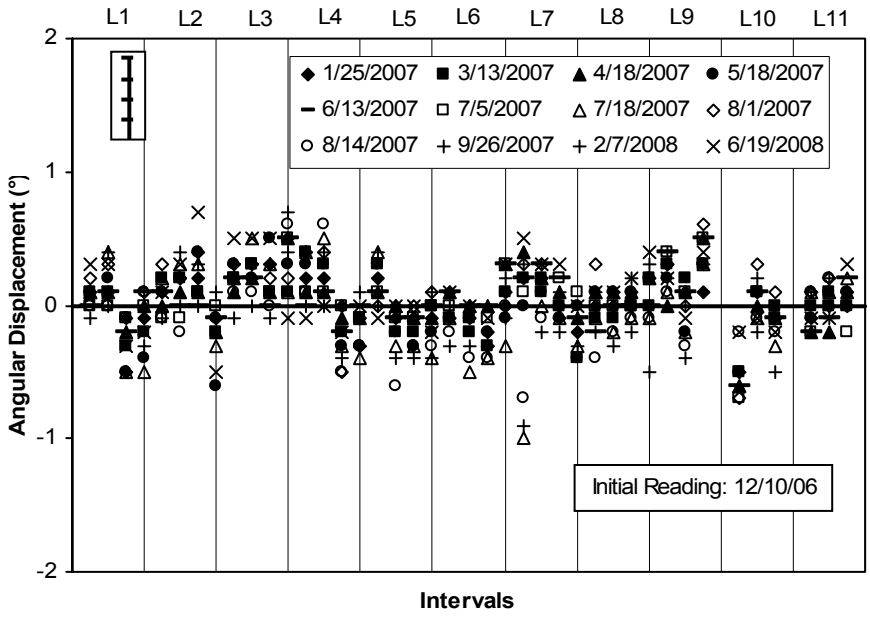

Fig. 5.27. Change in Wall Rotation Monitoring Mark Readings along the Retaining Wall.

5.6. NASA Road 1 (Project 4)

Piezometer and Ground Water Table Level Readings

Two piezometers were installed in Boreholes UH-2 and UH-4. The depth of UH-2 was 30 ft and Borehole UH-4 was 40 ft. At these boreholes, ground water levels were also monitored.

At Borehole UH-2, the initial pore pressure was 9.3 psi and it tended to fluctuate slightly over the monitoring period (Fig 5.28(a)). The minimum and maximum pore pressures measured were 8.5 and 9.5 psi, respectively. As observed before, the hydrostatic pressure was higher than the pore water pressure in the soil. The pore water pressure and hydrostatic trends were reversed at Borehole UH-4 (Fig 5.28(b)) and the difference was over 1.5 psi, representing the consolidation theory prediction.

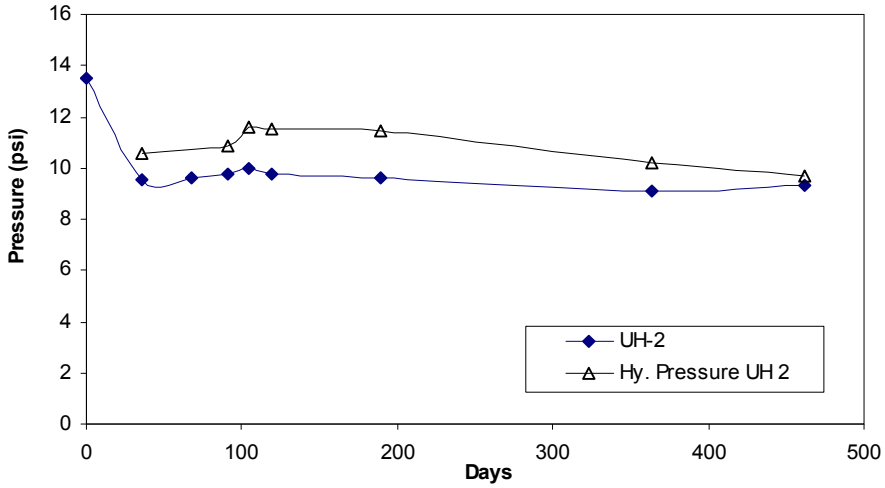

(a)

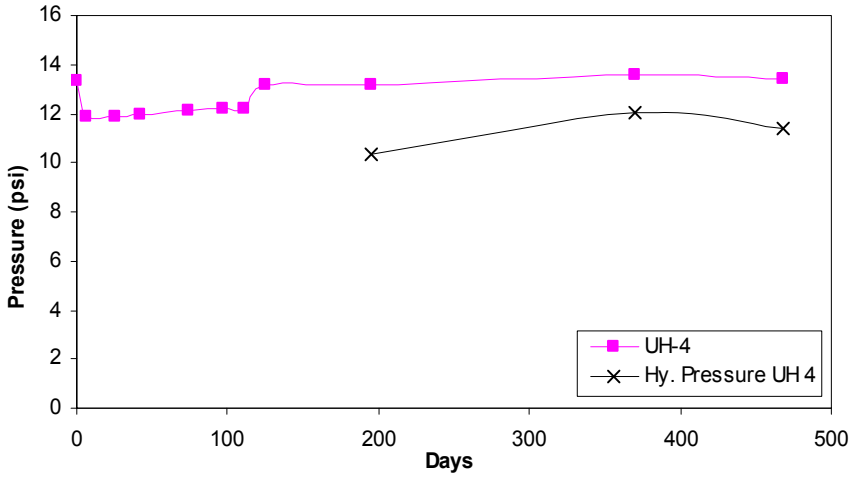

(b)

Fig. 5.28. Piezometer Readings at (a) Borehole UH-2 and (b) Borehole UH-4.

Extensometer Results

Extensometers were placed with the piezometers, at Boreholes UH-2 (20 ft embankment + 10 ft into the ground) and Borehole UH-4 (20 ft embankment + 20 ft into the ground). The Active Zone was not an issue as in the case of SH3 (Fig. 5.29). According to the final readings, 0.21-in. and 0.18-in. settlements were observed at Borehole UH-2 and Borehole UH-4, respectively.

Conventional consolidation theory predicted continuous consolidation settlement at this site. This was observed at this location. The consolidation settlement measured over a period of 12 months below the embankment at the Taylor Bridge at NASA Rd. 1 for a thickness of 20 ft (Borehole UH 4) was 0.18 in., and the predicted settlement using the 1-D consolidation theory was 0.21 in. (Chapter 3). For a thickness of 10 ft at Borehole UH 2, the consolidation settlement was 0.21 in., while the predicted settlement based on the consolidation theory (between 7 and 8 years) was 0.12 in. (Chapter 3). The agreement between measured and predicted consolidation settlements was good.

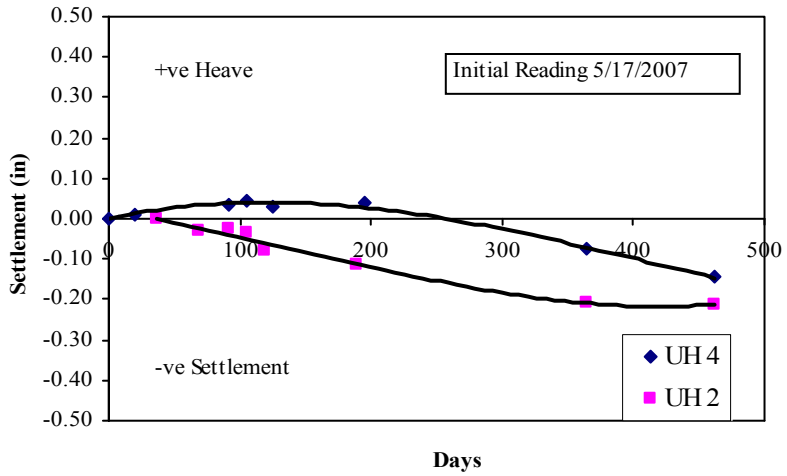

Fig. 5.29. University of Houston's Settlement Measurement Set-Up Readings.

5.7. Summary and Discussion

Two highway embankments that are in service were instrumented and monitored to determine the settlement due to consolidation of the soft clays supporting the embankments. The field instrumentation included extensometers, piezometers, inclinometers, demec points, and tensiometers. The embankments were monitored over period of 500 days. Since both of the embankments were next to a large body of water

(creek and lake), the changes in weather affected the ground water table height. During the study period, the water table fluctuated by as much as 35 in. At SH3 at Clear Creek, the embankment settlement was measured at the edges, and at NASA Road 1, it was measured under the embankment. Based on the field monitoring and analyses following conclusions are advanced:

(1) The maximum lateral movement recorded by the inclinometers was 0.4 in. near the ground surface. The lateral movement was less than 0.1 in. below a depth of 5 ft. Lateral measurements in the soft soils showed no sign of embankment stability failure.

(2) The largest vertical movements over time were measured in the top 5 ft of the Active Zone at SH3 at Clear creek. Changes in the Active Zone were monitored using a tensiometer (suction pressure) and an extensometer (vertical movements). During the period of monitoring, a maximum swelling of 0.8 in. and settlement of 0.2 in. were measured.

(3) Conventional consolidation theory predicted continuous consolidation settlement at these two sites. This was observed at both of the test locations. The consolidation settlement measured over a period of 12 months at the edge of the embankment at the Clear Creek Bridge at SH3 was between 0.08 and 0.10 in. after making the correction for the Active Zone. Based on the conventional consolidation theory, the settlement between 14 and 15 years will calculate to be 0.02 to 0.03 in., which was close to what was measured in the field. The consolidation settlement measured at the NASA Rd.1 bridge

site for the 20 ft thickness was 0.18 in. during the 12 month period. The magnitude of the consolidation settlement predicted for this site by the conventional theory, between 7 and 8 years, was about 0.21 in. The consolidation settlement measured at the NASA Rd.1 bridge site for the 10 ft thickness was 0.21 in. during the 12 month period. The magnitude of consolidation settlement predicted for this site by the conventional theory, between 7 and 8 years, was about 0.12 in. The 1-D consolidation theory predicted the settlement well.

(4) The piezometer readings, in three of the four cases, were below the surrounding hydrostatic pressure determined from the groundwater table height. During consolidation, piezometer readings should be higher than the surrounding hydrostatic pressure. This could be partly due to the fluctuation in the ground watertable.

6. CONCLUSIONS AND RECOMMENDATIONS

The prediction of consolidation settlement magnitudes and settlement rates is a challenging task, and it has been attracting the attention of numerous researchers since the inception of consolidation theory by Terzaghi in early 1920s. The challenges mainly come from the uncertainties about the subsurface conditions, soil disturbances during sampling and preparations of samples for laboratory testing, interpretations of laboratory test data, and assumptions made in the development of the 1-D consolidation theory (Duncan 1993; Olson 1997; Holtz and Kovacs 1981). Since the soft soil shear strength is low, the structures on the soft soils are generally designed so that the increase in the stress is relatively small and the total stress in the ground will be close to the preconsolidation pressure. Hence there was a need to investigate methods to better predict the settlement of embankments on soft soils.

There are several field and laboratory test parameters that are used in the settlement analysis and are very important in the prediction of consolidation settlement magnitudes and settlement rates. Determining the thickness of the in-situ soil that will be influenced by the new construction and estimating the increases in stresses are important. The laboratory test parameters such as compression index, C_c, recompression index (or swell index), C_r (or C_s), coefficient of consolidation, C_v, and preconsolidation pressure and their variability within the in-situ soils are important. In addition to engineering judgment used in determining some of these parameters, the geological nature of the soil deposits must be considered. Since the soils in the Texas Gulf Coast region are deltaic deposits, large variations in properties can be expected.

In this study, the procedure used by TxDOT to estimate the total and rate of settlement were reviewed. In order to verify the prediction methods, two highway embankments on soft clay with settlement problems were selected for detailed field investigation. Soil samples were collected from 9 boreholes for laboratory testing and over 40 consolidation tests and 50 unconfined compression tests were performed on the clay samples. The embankments were instrumented and monitored for 20 months to measure the vertical settlement, lateral movement, and changes in the pore water pressure. Based on this study the following can be concluded:

(1) The method currently used by TxDOT to determine the increase in in-situ stress is comparable to the Osterberg method and is acceptable. The approach used by the TxDOT to determine the preconsolidation pressure is acceptable (Casagrande Method).

(2) Total settlement has been estimated by TxDOT based on very limited consolidation tests. Since the increase in in-situ stresses due to the embankment is relatively small (generally less than the preconsolidation pressure), using the proper recompression index is import. Since there is a hysteresis loop during the unloading-reloading of the soft CH clays, three recompression indices (C_{r1}, C_{r2}, and C_{r3}) have been identified. Review of the TxDOT design indicates that there is no standard procedure to select the recompression index. It is being recommended to use recompression index C_{r1} to determine the settlement up to the preconsolidation pressure.

(3) The procedure used by TxDOT to determine the rate of settlement is not acceptable. In determining the rate of settlement, the thickness of the entire soil

mass must be used with the average soil properties and not the layering method. The layered approach will not satisfy the drainage conditions needed to use in the time factor formula and determine the appropriate coefficient of consolidation.

(4) The consolidation parameters (C_c, C_r, C_v) are all stress dependent. Hence, when selecting representative parameters for determining the total and rate of settlement, expected stress increases in the ground should be considered.

(5) The 1-D consolidation theory predicted continuous consolidation settlement in both the embankments investigated. The predicted consolidation settlements were comparable to the consolidation settlement measured in the field. The pore water pressure measurements in some cases did not indicate consolidation because they may have been located close to the bottom drainage. In one case, it indicated excess pore water pressure and hence consolidation was in progress.

(6) The Active Zone influenced the movements in the edge of the embankments. Movements in the Active Zone influenced the crack movements in the retaining wall panels.

(7) Constant Rate of Strain (CRS) test can be used to determine the consolidation properties of clay soils. The rate used in the test influenced the coefficient of consolidation.

Based on this study, the following recommendations are advanced:

(1) The thickness of the soil mass that is influenced by the embankment construction must be determined based on in-situ stress increase and the consistency of the soil below the embankment. The TCP and undrained shear strength should be used to determine the consistency of the soil.

(2) Since relatively large variations in the properties can be expected in the deltaic deposits, soil samples must be obtained for an adequate and representative number of boreholes to determine the consolidation properties.

(3) Determining the rate of settlement approach must be corrected.

(4) Based on only two already existing embankment settlements monitoring in the field, 1-D consolidation theory can be used to determine the total and rate of consolidation.

(5) Active Zone effects must be considered in designing the edge of the embankment including retaining walls.

(6) CRS must be considered as an alternative method to determine the consolidation properties.

(7) The number of consolidation tests used to determine the consolidation properties of the soils in each project must be increased. Due to the variability in the properties of deltaic deposited clay soils, it is recommended to use one consolidation test for each 5 ft within the soft soil layers for settlement analyses.

7. REFERENCES

ASTM International. (2002). "Annual Book of ASTM Standards," Edition 4, 2002, Vol. 04.08, Soil and Rock (I).

Azzouz, A.S., Krizek, R.J., and Corotis, R.B. (1976). "Regression analysis of soil compressibility." *Soil and Foundation*, *JSSMFE*, Vol. 16, No. 2, pp. 19-29.

Bjerrum, L. (1974). "Problems on Soil Mechanics and Construction on Soft Clays." *Norwegian Geotechnical Institute*, Publication No. 110. Oslo.

Boussinesq, J. (1883). "Application des Potentials à L'Etude de L'Equilibre e du Mouvement des Solides Elastiques", Gauthier-Villars, Paris.

Casagrande, A. and Fadum, R. E. (1940). "Notes on Soil Testing for Engineering Purposes," *Harvard University Graduate School of Engineering* Publication No. 8

Chung, S.G., Giao, P.H, Nagaraj, T.S. and Kwag, J.M. (2002). "Characterization of Estuarine Marine Clays for Coastal Reclamation in Pusan, Korea." *Marine Georesources and Geotechnology*, 2000, Vol. 20, pp. 237-254.

Cudny, M. (2003). "Simple multi-laminate model for soft soils incorporating structural anisotropy and destructuration," In P.A. Vermeer, H.F. Schweiger, M. Karstunen & M. Cudny (ed.), *Proc. Int. Workshop on Geotechnics of Soft Soils : Theory and Practice*, *Noordwijkerhout.* VGE.

Das, B.M. (2006). "Principles of Geotechnical Engineering," Brooks/Cole Pub Co. 589 p.

Dobak, P. (2003) "Loading Velocity in Consolidation Analysis." *Geotechnical Quarterly*, 2003, Vol. 47, No. 1, pp. 13-20.

Duncan, J.M. (1993). "Limitations of conventional analysis of consolidation settlement," *Journal of Geotechnical Engineering ASCE,* 119(9): 1333-1359.

Ganstine, D. (1971). "Statistical Correlations of the Engineering Properties of the Beaumont Clays." *University of Houston*, Thesis 1971.G36, 183 p.

GEOTAC (2006). "CRS – Instruction Manual." Trautwein Soil Testing Equipment Company, 63 p.

Gorman, C. T., Hopkins, T. C., Deen R. C., and Drnevich, V. P. (1978). ''Constant Rate of Strain and Controlled Gradient Consolidation Testing,'' *Geotechnical Testing Journal,* Vol. 1, No. 1, pp. 3–15.

Holtz, R.D. and Kovacs, W.D. (1981). "An introduction to geotechnical engineering." *Prentice-Hall Civil Engineering and Engineering Mechanics series*, Editors: N. M. Newmark and W.J. Hall, 733 p.

Ladd, C.C., Whittle, A.J., and Legaspi, D.E. Jr. (1994). "Stress-Deformation Behavior of an Embankment on Boston Blue Clay." ASCE Geotechnical Special Publication No. 40, *Conference on Vertical and Horizontal Deformations of Foundations and Embankments*, Proc. of Settlement '94, College Station, Texas, June, 1994, Vol. 2, pp. 1730-1759.

Leroueil, S., Magnan, J. and Tevenas, F. (1990). "Embankments on soft clays." New York, Ellis Horwood, 360 p.

Leroueil, S. and Vaughn, P. R. (1990). "The general and congruent effects of structure in natural soils and weak rocks." *Géotechnique* 40, No. 3, pp. 467-488.

Leroueil, S. (1994). "Compressibility of Clays: Fundamental and Practical Aspects." ASCE Geotechnical Special Publication No. 40, *Conference on Vertical and Horizontal Deformations of Foundations and Embankments*, Proc. of Settlement '94, College Station, Texas, June, 1994, Vol. 1, pp. 57-76.

Lowe, J., Jonas, E., and Obrician, V. (1969). "Controlled Gradient Consolidation Test," ASCE, *Journal of Soil Mechanics and Foundation Division*, Vol. 95, No. 1, pp. 77–97.

Mesri, G. (1988). "A Reevaluation of $S_{u(mob)}=0.22\sigma_p$' using Laboratory Shear Tests." *Can. Geotech. J.*, Vol.26, pp.162-164.

Nagaraj, T.S. and Miura, N. (2001). "Soft Clay Behaviour Analysis and Assessment." A.A. Balkema, Rotterdam, ISBN 9058093298.

Nash, D.F.T., Powell, J.J.M. and Lloyd, I.M. (1992). "Initial investigations of the soft clay test site at Bothkennar." Géotechnique 42, No. 2, pp. 163-181.

Nash, D.F.T., Sills, G.C. and Davison, L.R. (1992). "One-dimensional consolidation testing of soft clay from Bothkennar." *Géotechnique* 42, No. 2, pp. 241-256.

Olson, R, E. (1998). "Settlement of embankments on soft clays." *Journal of Geotechnical and Geoenvironmental Engineering*, ASCE, 124(8):659–669, 1998. The Thirty–First Terzaghi Lecture.

O'Neill, M.W. and Yoon, G. (1995). "Engineering Properties of Overconsolidated Pleistocene Soils of Texas Gulf Coast." *Transportation Research Record* 1479, TRB, National Research Council, Washington D.C., pp. 8-88.

Sallfors, G. (1975). ''Preconsolidation Pressure of Soft, Highly Plastic Clays,'' *Chalmers University of Technology*, Goteburg, Sweden.

Schlosser, F., Magnan, J.P. and Holtz, R.D., (1985). "Geotechnical construction". General Report, *Proc.11th International Conference on Soil Mechanics and Foundation Engineering*, San Francisco, Vol. 1, pp. 211-254.

Şenol, A. and Sağlamer, A. (2000). "Determination of Pre-consolidation Pressure with a

New, “Strain Energy-Log Stress” Method” *EJGE Paper* 0015. [http://www.ejge.com/2000/Ppr0015/Ppr0015.htm].

Smith, R. E. and Wahls, H. E. (1969). ‘‘Consolidation Under Constant Rates of Strain,’’ *Journal of the Soil Mechanics and Foundation Division*, ASCE, Vol. 95, No. SM2, pp. 519–539.

Shibuya, S. and Tamrakar, S.B. (1999). “In-situ and laboratory investigations into engineering properties of Bangkok clay.” *In Characterization of Soft Marine Clays*, Tsuchida & Nakase (1999) Balkema, Rotterdam, ISBN 90 5809 104 X, pp. 107-132.

Taylor, D. W. (1942). “Research on Consolidation of Clays,” *Serial No. 82*, Department of Civil and Sanitary Engineering, Massachusetts Institute of Technology, Cambridge, Mass

Terzaghi, K. and Peck, R.B. (1967). “*Soil Mechanics in Engineering practice*.” 2nd Edition, Wiley, New York, 729 p.

Terzaghi, K. (1925). “Erdbaumechanik auf Bodenphysikkalischer Grundlager.” Deuticke, Vienna, 399 p.

Vipulanandan, C., Ahossin Guezo, Y.J., and Bilgin, Ö. (2007). “Geotechnical Properties of Marine and Deltaic Soft Clays.” *CD Proceedings, GSP 173*, *ASCE, Geo Denver 2007*, Denver, CO.

Vipulanandan, C., Kim, M. and Sivram, H. (2007). “Microstructure and Geotechnical Properties of Houston-Galveston Soft Soils.” *CD Proceedings, GSP 173, ASCE, Geo Denver 2007*, Denver, CO.

Vipulanandan, C., Ahossin Guezo, Y.J., Bilgin, Ö, Yin, S. and Khan, M. (2008). "Recompression Index (C_r) for Overconsolidated Soft Clays." *ASCE Proceedings, GSP 178, Geo Congress 2008*, New Orleans, LA.

Whittle A.J. and Kavvadas M. (1994). "MIT-E3 A constitutive model for overconsolidated clays." *J Geotech Eng*, ASCE, 120(1):173–98.

Wissa, A.E.Z., Christian, J.T., Davis, E.H. and Heiberg, S. (1971). "Consolidation at Constant Rate of Strain." *Journal of the Soil Mechanics and Foundations Division*, ASCE, Vol. 97, No. SM10, Proc. Paper 8447, Oct., 1971, pp.1383-1413.